

HBRC Journal

Volume 1, Number 2, July 2005
ISSN: 1687-4048
DEP: 12479/2004

Contents

The Influence of Masonry Infill Walls on the Seismic Capacity of Reinforced Concrete Frames, a Probabilistic Study: M.M. ElAttar, M.O. Elseify, A.M. Ragab, and O.A. Hodhod	1
Air Curing Self-Compacting Concrete: H.E. Seleem	11
Utilization of Some Ceramic Industrial Wastes for Making Clay-Building Bricks: N.G. Abd El-Ghafour, H.S. Hassan, and H.H. Assal	23
Feasibility of Utilizing Waste GFRP Pipes as Lateral Reinforcement for Rectangular Reinforced Concrete Short Columns: M. S. Sayed	35
Statistical Assessment of Strength Acceptance Criteria in the Egyptian Code of Practice: M. M. El Attar, H. H. Abo Ghanima, and O. A. Hodhod	51
Torsional Capacity of Reinforced Concrete Columns: Y. M. Hussein	67
Effect of Web Inclination on the Behavior of Cold Formed Steel C-Purlins: A. M. Fadel	81
An Integrated Software for The Design of Beam-To-Column Rigid Connections: H. I. Hassanain	93
Post-Suburbia Arabia: W. Eirik Heintz	105
Urban Planning in Hermoupolis - A New View on the Conservation and Enhancement of Historic Settlements: J. Stefanou, and R. Mitoula	113
Evaluation of Cooling System's Design for Rural Development in Upper Egypt: A. M. Fahim	123
<i>Technical Note</i>	
Computation of Concrete Mix Ingredients on an Internet Platform: A. M. Ghaly, and L. G. Almstead	131

Vol. 1 No. 2
July 2005
ISSN: 1687-4048
DEP: 12479/2004

HBRC Journal

87 El-Tahrir St. Dokki 11511 P.O.BOX 1770 Cairo, EGYPT
Phone: 00202-7617062 Fax.: 00202-3367179
www.hbrc.edu.eg, journal@hbrc.edu.eg



Housing & Building National Research Center

The Influence of Masonry Infill Walls on the Seismic Capacity of Reinforced Concrete Frames, a Probabilistic Study

M. M. El-Attar¹
A. M. Ragab¹

M. O. ElSeify²
O. A. Hodhod¹

¹ Structural Engineering Department, Faculty of Engineering, Cairo University

² Civil Engineering Department, Faculty of Engineering, University of Calgary, Calgary, Canada

ABSTRACT

Many buildings are constructed with masonry infill walls. However, because of the absence of a realistic yet simple analytical model, the contribution of masonry infill panels having full contact with the R.C. frame members is often neglected in evaluating the seismic capacity. For many years the infill walls formed an integral part of buildings; however their distribution, size and material are totally based on architectural requirements. Neglecting the existence of infill panels as structural elements in determining seismic performance of buildings will result in inaccurate estimation of lateral stiffness, strength, ductility and seismic capacity of buildings.

Models used for infill panels can be divided into macro models and micro models. In macro models, the infill panel is replaced by one or two diagonal struts (Holmes [1], Chrysotomou et al. [2] and Stafford Smith [3]). Properties of the struts are determined based on experimental data or micro model (finite element) investigations. Macro models are computationally efficient and suitable to study the overall structural response of the building.

The objective of this research is to conduct a probabilistic study in order to numerically assess the effect of infill panels on the performance of buildings when subjected to earthquakes. Effect of infill panel distribution, thickness and strength are considered in this study. Moreover, the effect of openings in infill panels is also considered.

KEYWORDS: MASONRY, INFILL, SEISMIC, CAPACITY, PROBABILISTIC

ANALYSIS PROCEDURE

The performance of the structure is evaluated in terms of inter-story drift and damage index. To predict the nonlinear dynamic structural response, the computer program IDARC2D Version 4.0 developed by Valles et al. [4] is used. The state of damage in the structure is predicted with the use of a damage index procedure. The Park and Ang damage index which is already implemented in the program is used in this study. Park and Ang's damage index evaluates damage in terms of energy dissipated and maximum drift. Value of the damage index is calibrated using damage states from recent earthquakes. Table (1) shows the relation between value of damage index and various damage states. In the probabilistic analysis, an artificially generated ground motion was used to evaluate the response of the structure. It would have been preferable to use actual ground motion records. However, the number of usable free field records is small for this type of probabilistic analysis. Moreover, concrete compressive strength and reinforcing bars yield strength are also treated as random variables.

Ground Motion Generation

The Clough-Penzien [5] power spectral density function for the ground acceleration is used to generate ground motion. The power spectral density function is defined as:

$$S_g(\omega) = S_0 \frac{1 + 4Z_g^2 \left(\frac{\omega}{\omega_g}\right)^2}{\left[1 - \left(\frac{\omega}{\omega_g}\right)^2\right]^2 + 4Z_g^2 \left(\frac{\omega}{\omega_g}\right)^2} \frac{\left(\frac{\omega}{\omega_f}\right)^2}{\left[1 - \left(\frac{\omega}{\omega_f}\right)^2\right]^2 + 4Z_f^2 \left(\frac{\omega}{\omega_f}\right)^2} \quad (1)$$

Where S_0 is the amplitude of the white noise bedrock excitation; ω_g and ω_f are the frequencies of the first and second filters, respectively. Finally, Z_g and Z_f are the damping of the first and second filters, respectively. The value of ω_g represents predominant frequency of ground motion. Based on the study of 118 soil-site records, Lai [6] proposed a mean value for $\omega_g = 3.04$ Hz with a coefficient of variation of 0.425 and a mean value of Z_g equals to 0.32 with a coefficient of variation of 0.426. Value of ω_f is considered equal to 0.1 ω_g and Z_f is considered equal to Z_g . Creating the artificial ground motion records is based on generating random numbers representing ω_g and Z_g using mean, standard deviation and probability distribution for each parameter. Using these sets of random numbers, power spectral density functions are generated using Eq. (1) then, the stationary acceleration time history is generated based on the work developed by Shinzouka [7], as he suggested that a stationary acceleration time history can be generated using the formula:

$$\ddot{u}_g(t) = \sum_{k=1}^n \sqrt{2S_g(\omega_k)\Delta\omega} [\sin(\omega_k t + \Phi_k)] \quad (2)$$

Finally, the time varying intensity of the earthquake is modeled by multiplying the stationary acceleration time history by a suitable envelope function as the one which had been proposed by Suez et al. [8]:

$$\begin{aligned} \Psi(t) &= \left(\frac{t}{t_1}\right)^2 && ; 0 \leq t \leq t_1 \\ &= 1 && ; t_1 \leq t \leq t_2 \\ &= e^{-c(t-t_2)} && ; t_2 \leq t \end{aligned} \quad (3)$$

Where:

t_1 and t_2 : The rise and decay times of the ground motion.

$t_2 - t_1$: The strong ground motion duration.

c : The decay parameter.

Uncertainties in Material Properties

The main sources of uncertainties in member capacity are variation between specified strength and actual material strength. According to Mirza et al. [9], the concrete compressive strength can be modeled by a normal distribution with a mean value of concrete compressive strength (f_m) given by:

$$f_m = 0.675 f_c' + 7.59 \leq 1.15 f_c' \quad (MPa) \quad (4)$$

Where f_c' is the nominal value of concrete compressive strength. The coefficient of variation of concrete compressive strength is considered equal to 0.15 to represent average quality control. The variability of steel yield strength is modeled by a lognormal distribution with a mean value equal to 1.22 times the specified yield strength and a coefficient of variation equal to 0.107.

Building Design

A twelve story building is selected for this analysis as a sample for high-rise buildings. The Building is 20 x 25 m in plan with columns and beams spaced every 5 meters. A typical frame in the building is designed according to the provisions of the Egyptian Code for design and construction of concrete structures (2001). Concrete strength considered is 300 kg/cm² and steel yield strength is 4000 kg/cm². Four various cases are considered with respect to distribution of infill panels in the frame under consideration. The cases considered are frame (F1) with no infill panels, frame (F2) with infill panels in all bays (Total Infill), frame (F3) with infill panels in the outer bays only (Partial Infill) and frame (F4) with door openings and total infill. The configurations of various buildings considered in this study are shown in Figure 1.

Modeling of Infill Panels

The infill panel is represented using two diagonal masonry compression struts. The stress-strain relationship for masonry is idealized in compression by Mander et al. [10] using an increasing polynomial function until the peak stress is reached. Then, stress is dropped suddenly with increasing the strain, representing the brittle behaviour of masonry, until the stress reaches a small value at which it remains constant with the increase in the strain as shown in Fig. (2). Since the tensile strength of masonry is negligible, the individual masonry struts are considered to be ineffective if subjected to tensile forces. However, the use of two diagonal struts provides a lateral load resisting mechanism for opposite direction of loadings. Detailed formulation of the model is presented by Saneinejad et al. [11]

Summary of Analysis Procedure

The analysis procedure conducted in this study (ElSeify, M.O. [12]) is based on generating a large number of ground acceleration time histories (one thousand) using the procedure described earlier. The ground acceleration time histories are scaled to different values of peak ground acceleration (PGA) 0.1g, 0.2g & 0.3g. Similarly random values of concrete strength and steel yield strength are generated representing statistical characteristics for each variable. Each frame (F1, F2, F3 & F4) is subjected to the different generated earthquakes scaled to various PGA considering in the same time the various values of concrete compressive strength and steel yield strength. Results are presented in terms of the damage index and the maximum inter-story drift.

ANALYSIS RESULTS

Results of Probabilistic Analysis

The performance of the structure is evaluated in terms of inter-story drift and damage index. Values of maximum inter-story drift in each frame are shown in Table 2. This table shows that the highest inter-story drift corresponds to frame F1 (no infill panels) while the lowest inter-story drift corresponds to frame F2 (total infill). For example, for a peak ground acceleration of 0.2 g, the maximum inter-story drift for frame F1 equals to 4.4%, while it equals to 1.7% for frame F2 with a percentage decreases of 61%. Frames F3 and F4 corresponding to partial infill and total infill with openings, respectively resulted in intermediate values of inter-story drift.

Figures 3a to 3d show the probability of various damage categories of the four frames when being subjected to ground motion records scaled to a peak ground motion of 0.2g. These figures show that probabilities of collapse for frames F1 and F2 are 4% and zero, respectively. The probabilities of severe failure for frames F1 and F2 are 6% and 3%, respectively. On the other hand, the probabilities of slight damage for frames F1 and F2 are 4% and 70%, respectively. Frames F3 and F4 corresponding to partial infill and total infill with openings, resulted in intermediate values of damage between those of frames F1 and F2.

For peak ground acceleration of 0.2g, Comparing frame F1 (frame with no infill panels) which is the traditional method for modeling with frame F4 (frame with infill panels with openings) which represents the actual condition shows a reduction in maximum inter-story drift from 4.4% to 2%. For the same two frames frame F4 shows reduction in collapse cases and moderate damage state with an increase in minor damage state.

Effect of Infill Panel Parameters

The previous analysis had been conducted for a thickness of infill panel equal to 25 cm and compressive strength equal to 100 kg/cm². A sensitivity analysis is conducted to investigate the effect of reducing wall thickness from 25 cm to 12 cm and reducing infill strength from 100 kg/cm² to 50 kg/cm² on the damage index and the maximum inter-story drift. Frame F2 with total infill is considered in this study. Results of the analysis of the infill walls with reduced various thickness are presented in Table 3. The results show that reducing wall thickness or infill strength results in an increase in damage index and maximum inter-story drift. For example at peak ground acceleration equal to 0.3 g, reducing wall thickness from 25 cm to 12 cm resulted in an increase in damage index from 0.48 to 0.58 and an increase in maximum inter-story drift from 3% to 3.55%. Similar observations were observed when the compressive strength of infill wall was reduced.

CONCLUSIONS

A probabilistic study is conducted to investigate the effect of infill walls on response of reinforced concrete frames to earthquake ground motion. Cases of total infill in all panels, partial infill and infill with openings are considered in the analysis. Results show that considering existence of infill walls results in a decrease in the maximum inter-story drift and a decrease in the damage index. The effect of reduction in wall thickness is also considered in the analysis and it was found that wall thickness has a considerable effect on the damage index and the inter-story drift.

REFERENCES

1. Holmes, M., "Steel Frames with Brick Work and Concrete Infilling", Proceedings of Institute of Civil Engineers, London, England, Part 2, 1961, Vol. 73, pp. 473-478.
2. Chrysotomou, C.Z. et al., "Non Linear Seismic Response of Infilled Steel Frames", Proc.10th World Conference on Earthquake Engineering, Madrid, 1992.
3. Stafford Smith, B., "Behaviour of Square Infilled Frames", Journal of Structural Eng., ASCE, 1996, Vol. 92, pp.381-403.
4. Valles, R.E., Reinhorn, A.M., Kunath, S.K., Li, C. and Madan, A., "IDARC2 Version 4.0: A Computer Program for the Inelastic Analysis of Buildings", Technical Report NCEER-96-0010, 1996, State University of New York at Buffalo, N.Y.
5. Clough, R.W. and Penzien, J., "Dynamics of Structures", McGraw-Hill, 1975, New York.
6. Lai, S.-S.P., "Statistical Characterization of Strong Ground Motion Using Power Spectral Density Function", Bulletin Seismol. Society, 1982, Am 72, pp. 259-274.
7. Shinzouka, M., "Digital Simulation of Random Process in Engineering Mechanisms With Aids of FFT Technique", in Stochastic Problems in Mechanics, Eds. S.T., Ariaratnam and H.E.E. Liepholz, 1974, University of Waterloo press, Waterloo, Canada

8. Suez, R.H., Wen, Y.K. and Ang, A.H.S., "Stochastic Evaluation of Seismic Structural Performance", Journal of Structural Engineering, ASCE, 1985, Vol. 111, No. 4, pp. 1204-1218.
9. Mirza, S.A., Hatzinikolas, M., McGregor, J.G., "Statistical Descriptions of Strength of Concrete", Journal of Structural Engineering, ASCE, 1979, Vol. 105, pp. 1021-1036.
10. Mander, J.B., Priestly, M.J.N. and Park, R., "Theoretical Stress-Strain Behaviour of Confined Concrete", Journal of Structural Division, ASCE, August, 1988, Vol. 114, No. 8, pp. 1827- 1849.
11. Saneinjad, A. and Hobbs, B., "Inelastic Design of Infilled Frames", Journal of Structural Engineering, April, 1995, Vol. 121, No. 4, pp. 634-650.
12. ElSeify, M.O., "Seismic Analysis of Infilled Frames", Thesis submitted in partial fulfillment of the requirements for a Master of Science in civil engineering, Cairo University, 2003.

Table 1 Relation between Park and Ang Damage Index and Various Damage States

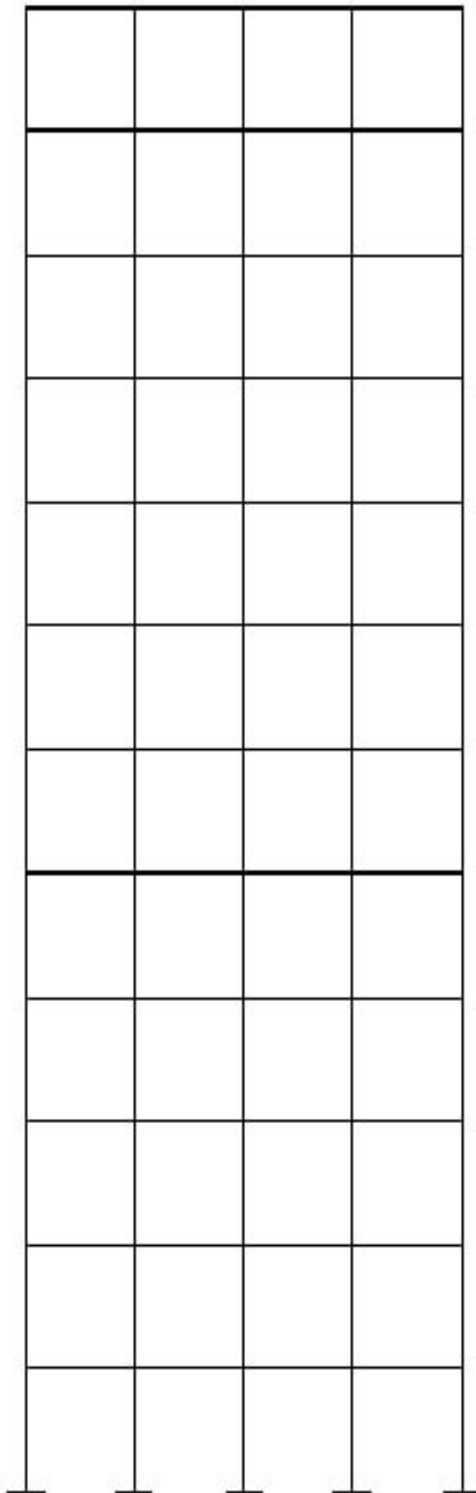
Range of Damage Index	Damage State	Appearance
0.0	No Damage	Undeformed / Uncracked
0.0 – 0.2	Slight Damage	Moderate Cracking
0.2 – 0.5	Minor Damage	Severe Cracking
0.5 – 0.6	Moderate Damage	Spalling of Concrete Cover
0.6 – 1.0	Severe Damage	Buckled Bars – Exposed Core
> 1.0	Collapse	Loss of Shear / Axial Capacity

Table 2 Relation between Peak Ground Acceleration (PGA) and Maximum Inter-story Drift for Different Frames

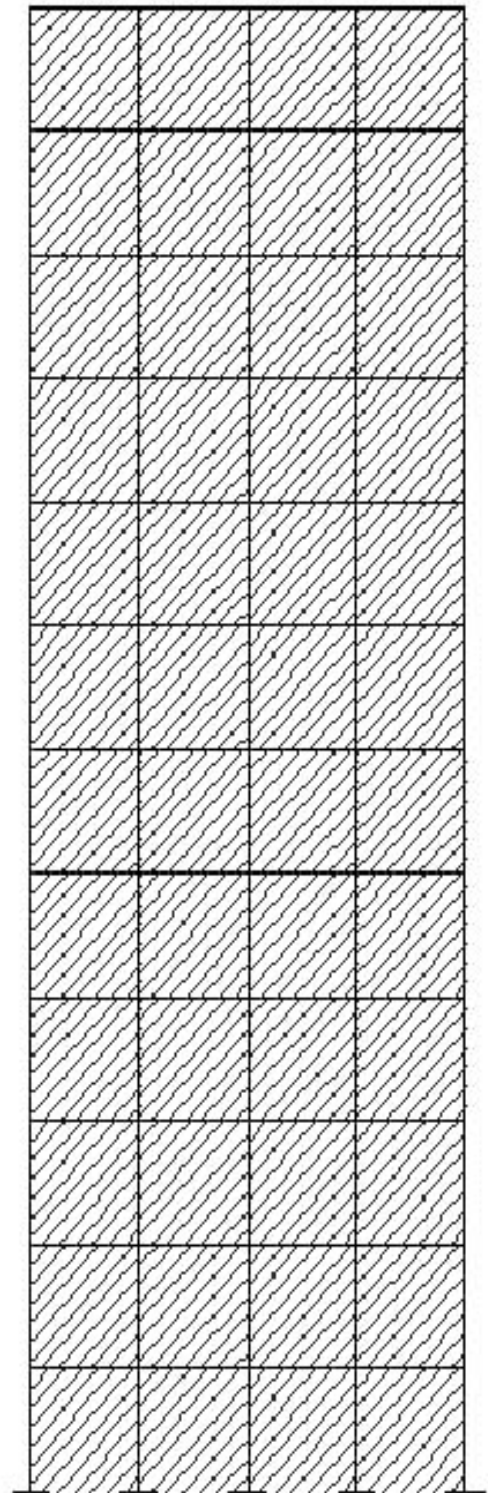
PGA (g)	Maximum Inter-Story Drift (%)			
	F1	F2	F3	F4
0.1	2.0	0.7	1.2	1.0
0.2	4.4	1.7	2.8	2.0
0.3	9.8	3.0	5.8	3.6

Table 3 Damage Index and Maximum Inter-story Drift for Various Infill Thicknesses for Frame (F2)

PGA (g)	Damage Index		Maximum Inter-story Drift (%)	
	t = 25 cm	t = 12 cm	t = 25 cm	t = 12 cm
0.1	0.12	0.14	0.7	0.8
0.2	0.25	0.30	1.7	2.0
0.3	0.48	0.58	3.0	3.55

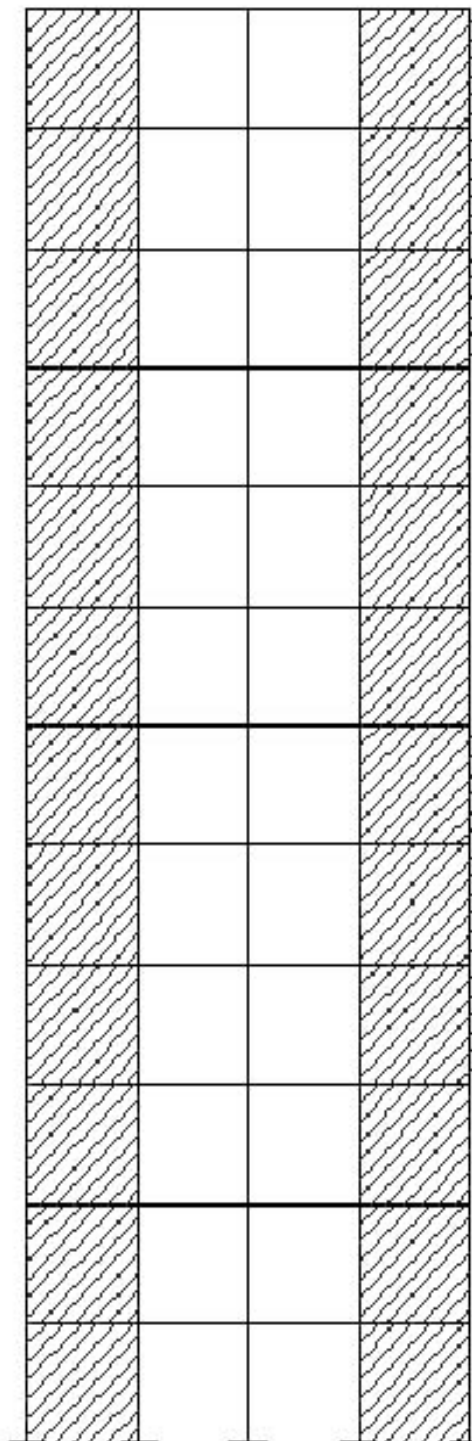


Frame (F1)

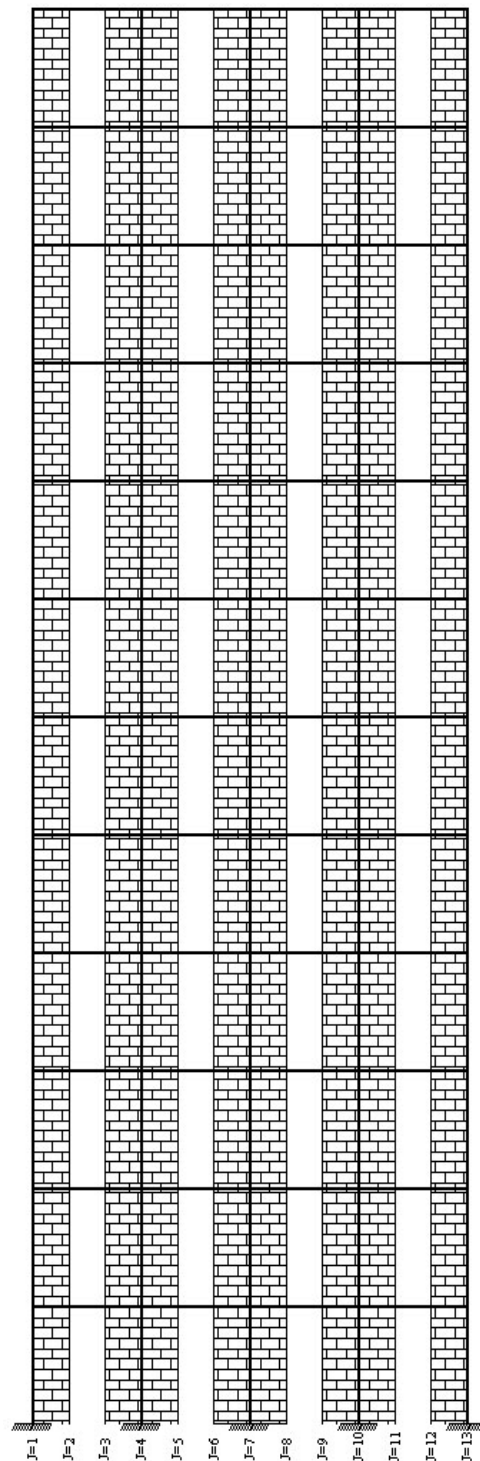


Frame (F2)

Fig.1: Various Building Configurations Used in the Analysis



Frame (F3)



Frame (F4)

Fig.1: Various Building Configurations Used in the Analysis (continue)

Masonry Stress

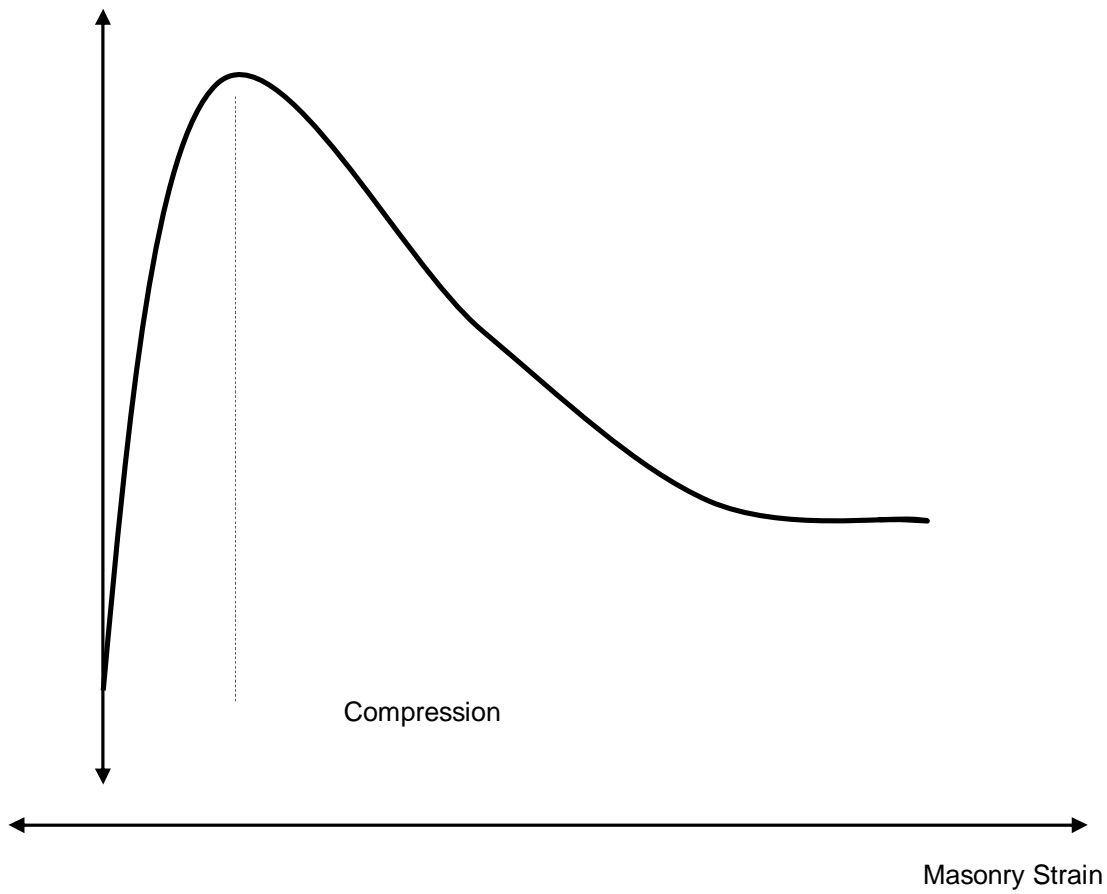


Fig. 2: Constitutive Model for Masonry (Mander et al. [10])

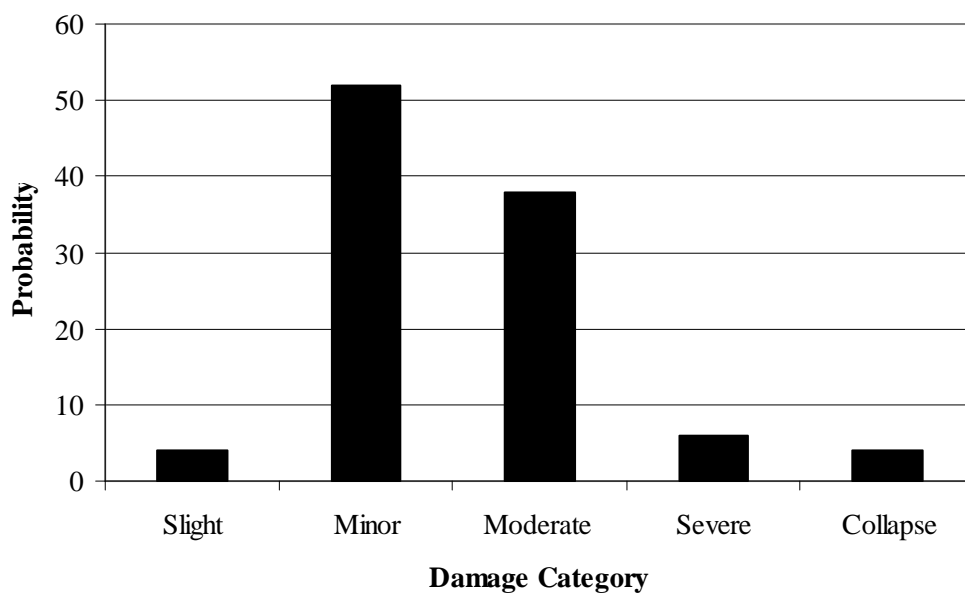


Fig. 3a: Probability of Various Damage Categories for Building F1

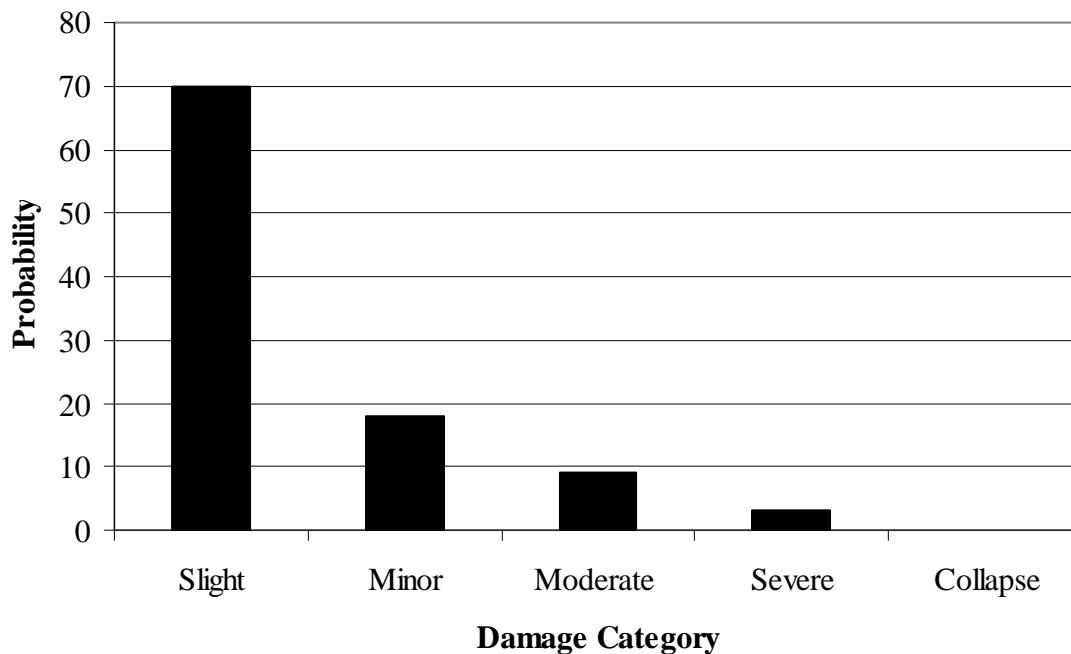


Fig. 3b: Probability of Various Damage Categories for Building F2

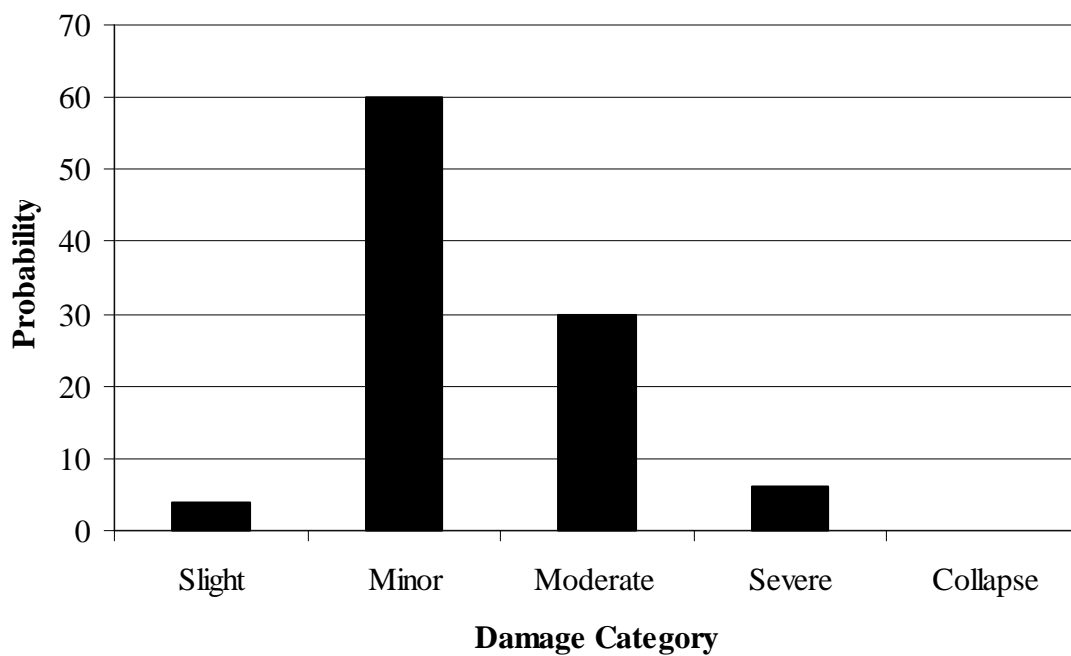


Fig. 3c: Probability of Various Damage Categories for Building F3

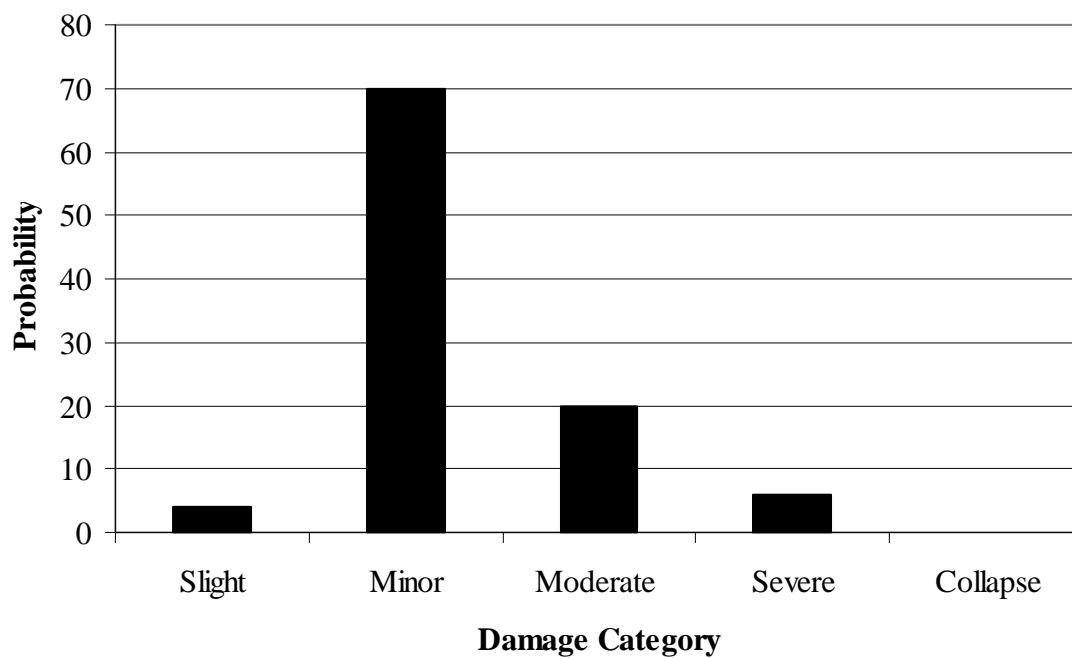


Fig. 3d: Probability of Various Damage Categories for Building

Air CURING SELF-COMPACTING CONCRETE

H. E. SELEEM

*Strength of materials Dept., Housing & Building National Research Center, Cairo.
Dokki Giza 11511, P.O. Box 1770 Cairo, EGYPT*

ABSTRACT

The present experimental program extended over three main stages to explore the possibility of dispensing water curing by means of Latex addition to the self-compacting concrete (SCC) mixtures constituents. Two latex dosages, based on the latex solid part, were employed in the first stage of work, namely 3%, and 5%. The validity of this approach was evaluated through compressive strength results of cube specimens having different curing regimes. Through the remaining stages, the minimum dosage was adopted as suitable for the purpose of this work from the technical and economical viewpoints. Further enhancement of the Latex modified concrete (LMC) mixture by fibers addition to the mixtures was thoroughly investigated in the second stage of work in terms of the performance criteria of the generated SCC mixes. It is generally agreed that the fibers have a pronounced contribution to the hardened concrete mechanical strengths, but its adverse effect on the fresh concrete workability is very often disadvantage. It was found here that owing to the increased viscosities of the mixtures incorporating Latex, it is possible to utilize the fibers benefits in the hardened state without significantly impairing the sought performance criteria in the fresh state. The durability aspects were the concern of the last stage of work. Test results proved that the LMC has a superior quality over the other kinds of concrete regarding permeability to liquids. Also, the ability of the LMC mixtures to resist sulfate attack in terms of surface scaling and strength retrogression is better than or the ordinary concrete mixture and it was comparable to it for the SCC without Latex.

KEYWORDS: Latex: Latex modified concrete: curing compounds

INTRODUCTION

Self compacting concrete (SCC) as outlined in many articles is a great development in concrete industry. That is because it has the features of high flowability to fill all of the formworks without the need of compaction, and relatively high viscosity to the extent that offsets segregation during transporting, placing, and finishing. Therefore, satisfactory degree of uniformity is attained that is not dependent on labor's skills. Despite all these advantages, many developments are still needed; like dispensing or at least shortening the water curing period. Curing is a concern, especially in circumstances where there is a lack of water. Curing compounds may be used at these circumstances, but their application requires skilled labor. Using latex polymers provide better solution for this challenge. The concept of polymer-hydraulic cement concrete is not new, it has been patented since about 80 years¹. Special type of polymer, referred to as Latex, is added to the concrete as a modifier, hence Latex Modified Concrete (LMC). Latexes are liquids (typically aqueous) in which microscopic polymer particles are dispersed. They are formed by the polymerization of monomer emulsions.

In the present work, it was tried to produce SCC mixes that satisfy the performance criteria and in the same time are not significantly affected by rareness of damp or water curing. It was also tried to further enhance the LMC mixtures by adding steel or polypropylene fibers. The LMC was also tested for some selected durability aspects. Test results were satisfactory regarding the possibility of adopting this approach, i.e. Latex modification to overcome the need to water curing.

EXPERIMENTAL PROGRAM

In the present work, it was tried to produce SCC mixtures that are not significantly affected by water curing. Two main SCC mixtures were adopted for this purpose, shown in Table 1. The performance criteria of these mixtures were assigned experimentally and accepted as suitable SCC mixtures. For each of them, two latex contents were employed. Hence four LMC mixtures were produced altogether with two control SCC mixtures and an ordinary mixture having the same cement content as the other mixtures, Table 1. The investigation proceeded through three main stages:

- exploring the validity of using Latex to overcome the sensitivity to water curing, and the proper latex dosage to be used.
- Enhancing the LMC by adding fibers to the mixtures. That will eventually lead to increasing tensile strength and many other mechanical properties of concrete, and also offset the surface tensile cracks that may develop during rapid loss of water (shrinkage).
- Evaluating some of the durability aspects that might affect the concrete during its service life.

Materials

Ordinary Portland cement of Blaine surface area $3200 \text{ cm}^2/\text{gm}$ that complying with the Egyptian Standard Specification 373-1991, and silica fume containing about 95% SiO_2 were used throughout this investigation. The aggregates were well-graded natural siliceous sand with a fineness modulus of 2.6, and siliceous gravel with nominal maximum size 19 mm. Limestone powder passing sieve no. 200 (75 micron) was employed. High range water reducer (superplasticizer) commercially known as addicrete BVF was used at a dosage of 3.0% from binders weight to accomplish high flowability.

The employed Latex polymer is styrene butadiene rubber, used in a liquid form. Its solid part content (assigned experimentally) is 40% of the total Latex weight. Two latex dosages were employed - on the basis of Latex solid part - as a ratio of cement weight, i.e. (p/ c) of 3%, and 5%. The first dosage is relatively low as compared to the advised^{2,3} minimum (p/ c) ratio of 5%. Tracing the effects of fibers' type and content was accomplished via employing two different types with two dosages for each of them. The first one is steel fibers commercially known as (Geos). These fibers are plain, smooth and waved in shape, having circular cross-section diameter 1, and length 25mm. The second one is polypropylene fibrillated fibers 18 mm length.

Experimental Plan

First stage; The main objective of this stage is to assign the minimum Latex content which could be employed to achieve the concern of air curing. It is well known that LMC has markedly water retention properties, i.e. reduced water evaporation due to the sealing effect of the impermeable polymer films formed. Two main SCC mixtures were adopted as control ones, and for each of them two Latex contents were used on the basis of (p/ c) ratio. Another ordinary concrete mixture was cast for comparison purpose. A cement content of 400 kg/m^3 was used through all mixtures. Details of the mixtures' constituents are presented in Table 1.

Verification of the minimum effective content of Latex was based on evaluating the results of the compressive strength at 7 and 28 days and the splitting tensile strength at 28 days for the adopted different curing regimes, which were as follows:

- Air curing
 - One day water curing, then air curing.
 - Two days water curing, then air curing.
 - Water curing till the age of testing.
- It is worth to mention that air curing was done outdoor in a shaded area.

Second stage; At this stage, it was tried to enhance the LMC mixtures by fiber inclusion. The adopted latex content was chosen from the preceding stage of work, (p/ c) ratio of .03 as appropriate for the air curing purpose. The two SCC mixes MSC1 and MSC2, and the two LMC mixes MLC1 and MLC3, shown in Table 1, were chosen as control mixes for this stage of work. Polypropylene and steel fibers are introduced within each of the two LMC mixes. The first fiber type was employed with two percentages, 0.1% and 0.2% of concrete volume, whereas the second fiber type with percentages 0.5% and 1.0%, as shown in Table 2. All of these mixes were tested for flowability, viscosity, and blocking behavior in the fresh state. The two SCC mixes MSC1 and MSC2 were cured in water till the age of testing, whereas the other 10 mixes incorporating Latex as a cement modifier were cured outdoor in air till the age of testing. The hardened concrete mechanical properties are presented and discussed elsewhere⁴.

Table 1: Concrete mixes for the first stage of work

Mix		Ordinary	SCC		LMC			
		Mc	MSC1	MSC2	MLC1	MLC2	MLC3	MLC4
(gravel/ sand) ratio		2 : 1	1.5 : 1	1.2 : 1	1.5 : 1	1.5 : 1	1.2 : 1	1.2 : 1
Ingredients, kg/m ³	cement	400	400	400	400	400	400	400
	silica fume	–	80	–	80	80	–	–
	powder	–	173	115	173	173	115	115
	w/ b ⁽¹⁾	0.5	0.395	0.39	0.395 ⁽⁴⁾	0.395 ⁽⁴⁾	0.37 ⁽⁴⁾	0.37 ⁽⁴⁾
	sp/ b ⁽²⁾	0.03	0.03	0.03	0.03	0.03	0.03	0.03
	p/ c ⁽³⁾	–	–	–	0.03	0.05	0.03	0.05

⁽¹⁾: water/ binder, ratio by weight

⁽²⁾: superplasticizer/ binder, ratio by weight

⁽³⁾: total solids of latex polymer/ cement, ratio by weight

⁽⁴⁾: total water content including the water in the polymer latex

Third stage; The prime concern of this stage is the durability in terms of sulfate attack and permeability. The ordinary and the SCC mixes Mc and MSC1 respectively, and the LMC mix MLC1, shown in Table 1, were adopted for the durability investigation.

Permeability is the major property which affects all other durability aspects. That is because it deals with the ability of aggressive media to ingress inside the concrete mass. For this test, 3 specimens (20*20*12) cm were cast corresponding to each of the investigated mixes. At the age of 28 days, they were subjected to water pressure: 1 bar for 48 hrs, 3 bars for 24 hrs, and lastly 7 bars for 24 hrs. This test was carried out in accordance to Din 10485. The resistance to sulfate attack is generally evaluated due to several attack mechanisms, like swelling due to the formation of the expansive compounds, surface scaling, and strength degradation. The last two mechanisms are the considered ones. For this purpose, 4 groups, each comprising 3 companion cubes (15*15*15), cm were cast for each of the three investigated mixtures. The first group was tested at 28 days age. The remaining groups were tested after exposure to 10% sodium sulfate solution for 2, 3, and 11 months.

RESULTS & DISCUSSION

First Stage

Compressive strength development; Here, the effect of different curing regimes on the strength development at different ages for the mixes incorporating Latex with different dosages as well as the ordinary and the SCC ones are investigated. Figs. 1, and 2 show the 7-day and the 28-day compressive strength for the above cited mixes and conditions, from which the following observations are drawn.

- The compressive strength of the mixes containing silica fume, i.e. with relatively dense microstructure, is not sensitive to varying the Latex content from 3% to 5%, as the corresponding variation in the 28-day strength does not exceed 2%. On the other hand, the mixes without silica fume were rather sensitive to changing the Latex content. For these mixes, increasing the Latex content from 3% to 5% caused an increase in the 28-day compressive strength up to 9%.
- Reasonable water curing period for about 2 days serves to enhance the strength development for all LMC mixes. The subsequent air curing is also essential for the polymerization effect. This finding is consistent with other published data⁶. Anyhow, the strength after only one day water curing is still higher than it for the corresponding SCC mixtures (without Latex) continuously cured. Even more, with air curing, i.e. no water curing at all, the strength of the LMC mixes is comparable to that of the SCC mixes water cured till the age of testing. Hence, it is possible by employing only small content of Latex, about 3%, to totally dispense water curing especially for mixes containing pozzolanic materials. It should be emphasized that whenever possible water curing for about 2 days or at least 1 day is always required to promote cement hydration.
- Adding Latex to the SCC mixes, even at small dosages causes a pronounced increase in the compressive strength amounted to 10%, and 7% at 28 days for the mixes with and without silica fume respectively, provided that the LMC mixes are properly cured. Apparently, the efficiency of Latex is more pronounced with the inclusion of the micro-filler silica fume. That is because the polymer Latex deposits on the surface of the fine grains and therefore the formed network structure is more closely linked.
- The effect of Latex on strength development is more recognized at early ages.
- Continuous water curing for SCC significantly enhance early strength development.

Table 2: Concrete mixes for the second stage of work

Mix	MPL1	MPL2	MPL3	MPL4	MSL1	MSL2	MSL3	MSL4	
(gravel/ sand) ratio	1.5 : 1	1.5 : 1	1.2 : 1	1.2 : 1	1.5 : 1	1.5 : 1	1.2 : 1	1.2 : 1	
cement	400	400	400	400	400	400	400	400	
	silica fume	80	80	–	–	80	80	–	–
	powder	173	173	115	115	173	173	115	115
	w/ b(1)	0.395	0.395	0.37	0.37	0.395	0.395	0.37	0.37
	sp/ b(2)	0.03	0.03	0.03	0.03	0.03	0.03	0.03	0.03
	p/ c(3)	0.03	0.03	0.03	0.03	0.03	0.03	0.03	0.03
fiber* %	polypropylene	0.1	0.2	0.1	0.2	–	–	–	–
	steel	–	–	–	–	0.5	1	0.5	1

(1): water/ binder, ratio by weight, including the water in the polymer latex

(2): superplasticizer/ binder, ratio by weight

(3): total solids of latex polymer / cement, ratio by weight

*: by volume

Second Stage

Fiber reinforced LMC mixes; As outlined before, 8 fiber reinforced LMC mixes, and 2 control LMC mixes without fiber and the corresponding SCC mixes were tested at this stage of work. All concrete mixes were tested for the fresh properties using an assembly of slump cone and J-ring, shown in Fig. 3.

The performance criteria which characterize SCC fresh properties are : the filling ability, segregation resistance, and passing ability. These properties were respectively evaluated by the following measures: flow diameter from the slump cone test, (T50) value which is the time the concrete assumes to reach 500 mm flow diameter, and the difference between the heights of concrete in-and outside the J-ring. Full details of these measurements are presented elsewhere⁷. In the hardened state, they were tested for compressive strength at 7 and 28 days age, and the splitting tensile strength at an age of 28 days. Thereby after fresh concrete testing has been completed, the concrete was poured into the oiled steel molds of 6 cubes of 15 cm side length and 3 cylinders (15*30) cm in dimensions. For each of these tests the results of three companion specimens were averaged for one test result.

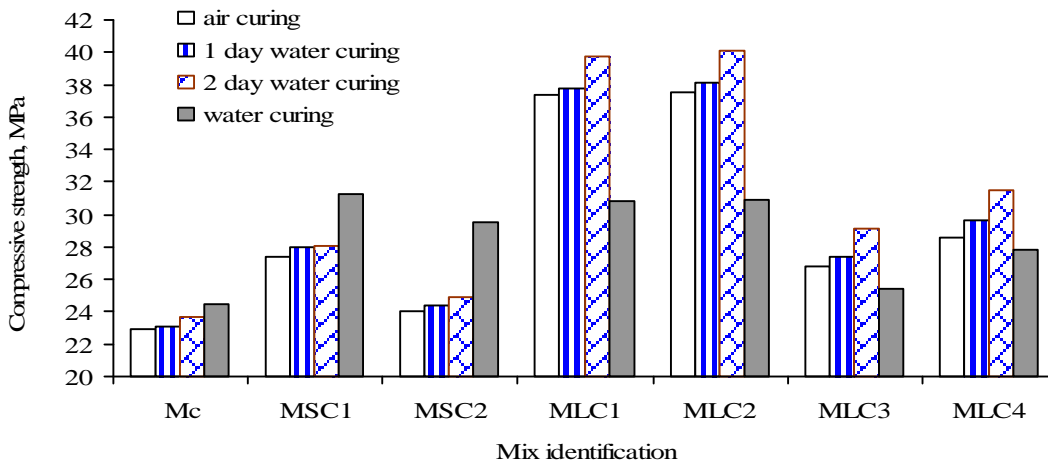


Fig.1: The Effect of Different Curing Regimes On The 7-Day Compressive Strength Of Different Kinds Of Concrete

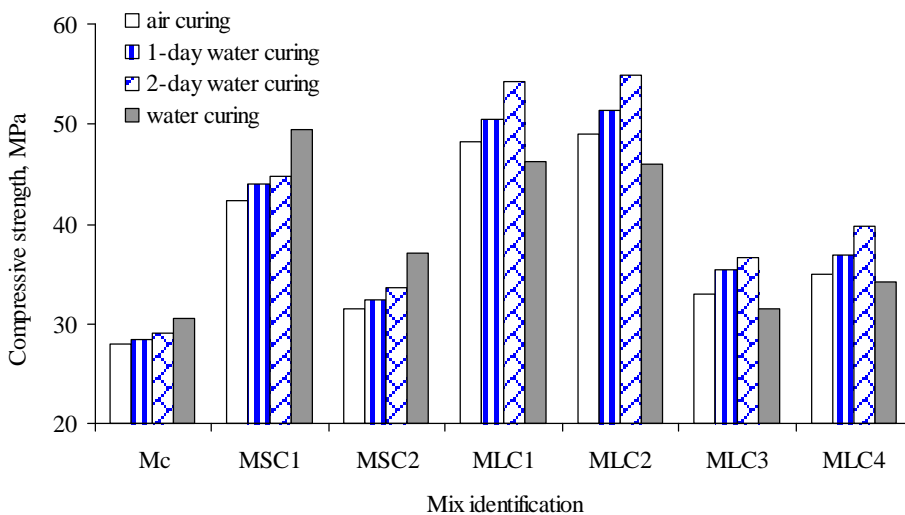


Fig.2: The Effect of Different Curing Regimes on the 28-Day Compressive Strength of Different Kinds of Concrete

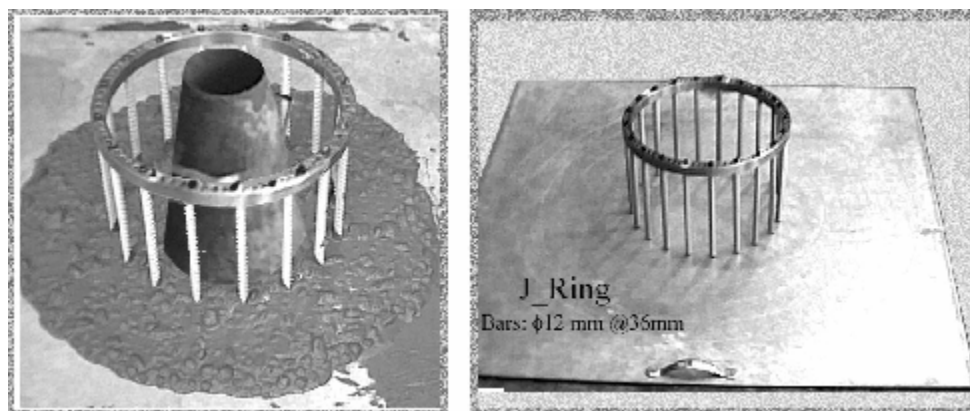


Fig.3: The Slump Cone- J-Ring Assembly

The effect of Latex on the performance of SCC mixes; It was reported that adding Latex to concrete mixtures has a remarkable effect on reducing the water content due to the dispersing effect of surfactant in the Latexes⁶. This fact was found true for the SCC mix without silica fume (MSC2), and the corresponding Latex mix (MLC3). Hence, the total water content of the Latex mix MLC3 was slightly reduced as compared to the SCC mix MSC2 for comparable slump flow values, as could be noticed from Table 1. On the other hand, that was not the case for the mix incorporating silica fume (MSC1). Latex addition to this mix considerably reduced its flowability, and consequently increased its viscosity as could be realized from Figs. 4, and 5 respectively. Thereby, the total water content must not be reduced beyond that of the corresponding SCC mix. Through this work, the total water content of the silica fume mixes incorporating Latex were slightly increased over the corresponding SCC mixes to maintain an appropriate level of flowability.

The filling ability of the fiber LMC mixes; As could be seen from Fig.4, the effect of fibers in reducing the flow diameter generated almost identical trends for both groups of mixes; with and without silica fume. The smooth texture steel fibers at a percentage of 0.5% did not affect the flow diameter of the LMC mixes. At the next employed percentage of 1.0%, there was a slight reduction in the flow diameter about 3.0% only. Obviously, the increased viscosity of the LMC mixes alleviated the fibers restricting effect and conveniently suspended it to eliminate concentration that might occur in some places. The polypropylene fibers although employed at much less percentages than the steel fibers, were more restricting to flow than the steel one. The reductions in the flow diameter of the Latex mixes due to employing the polypropylene fibers averaged about 1.5% at 0.1% fibers, and about 4.5% at 0.2% fibers.

The viscosity of the fiber LMC mixes; The importance of viscosity is generated from the fact that, increasing the viscosity maintain good suspension of coarse aggregate during deformation of the concrete. Thereby, it should be conveniently high to stabilize SCC with high flowability against segregation. The (plastic) viscosity of the SCC mixture could be conveniently expressed for by the (T50) value. That is the time for the concrete diameter to reach 500 mm in the slump flow test. It worth to mention that this measure is primarily indicative of the filling ability of concrete, which in the same time is greatly affected by the viscosity. Hence, it is customarily employed to assess the viscosity. Through this work, the viscosity was raised by increasing the content of fine materials (powder), and also by employing the polymer Latex. Fig. 5 lists the (T50) value for the two groups of mixes. Generally, the Latex mixtures with silica fume were of higher viscosities than those for the Latex mixtures without silica fume. Obviously, the fibers have some effect in restricting the concrete flow. Therefore, the (T50) values are increased with increasing the fibers content. That is not an evidence of increasing the viscosity, but due to the fibers' restricting effect as mentioned before. Anyhow, these results are still important in

evaluating the restricting effect and consequently the filling ability of the concrete mixtures. As shown in Fig.5, the (T50) value is more affected by the polypropylene fibers than by the steel fibers. Fortunately, the (T50) value for all fiber reinforced LMC mixes ranges from 3.3 sec to 4.5 sec, i.e. within the accepted range of values (2-5) seconds as suggested by the European Federation (EFNARC)⁸.

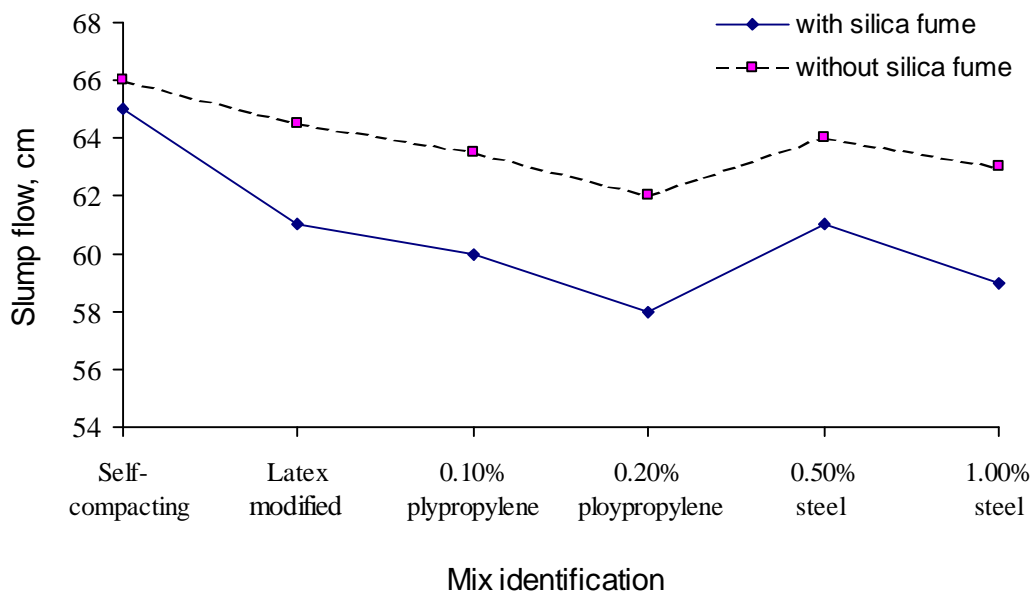


Fig.4: The Filling Ability of the Investigated Concrete Mixes

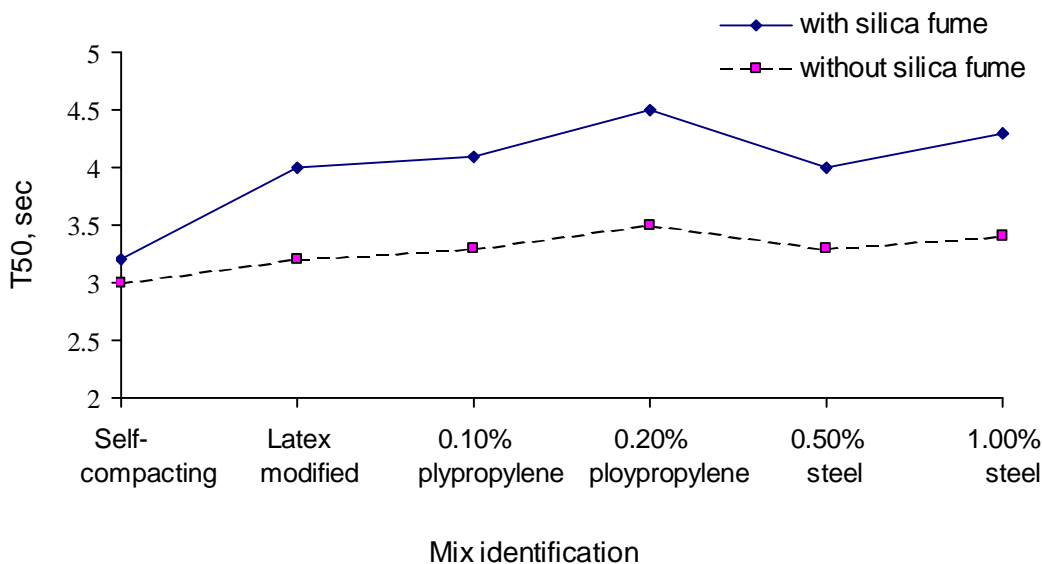


Fig.5: (T50) Value of the Investigated Concrete Mixes

The passing ability of the fiber LMC mixes; This term refers to the ability of SCC to flow through tight openings such as spaces between steel reinforcing bars without segregation or blocking. Thereby, the bar spacing is an important criterion in determining this ability. Through this work, the minimum bar spacing in the J-ring assembly was set to 36mm, then if necessary the spacing was increased by 12mm each time till the state of no blocking is reached. The blocking limit which is the difference between the concrete heights in-and outside the J-ring is suggested here to be equal to the NMS of coarse aggregate, i.e. 19mm. Table 3 lists the minimum bar spacing for no blocking corresponding to each of the tested mixes. For control mixes (without fibers), the minimum bar spacing is 36 mm, i.e. about twice the NMS of coarse aggregate. As could be realized from Tables 1 and 2, the control mixes are of different (gravel/sand) ratio, with or without silica fume, and the Latex is included only in the LMC mixes. Therefore, the above mentioned blocking limit is valid for a wide range of concrete mixes. From Table 3, according to the definition of blocking driven here, fiber inclusion seems to have a regular influence on the bar spacing requirements. The minimum bar spacing which should be employed with the steel fiber reinforced LMC mixtures is about 2 times the length of the fibers. On the other hand, the polypropylene fibers do not seem to affect the bar spacing requirement.

Table 3: Bar spacing for no blocking

Mix	MSC1	MSC2	MLC1	MLC3	MPL1	MPL2
Bar spacing, mm	36	36	36	36	36	36
Mix	MPL3	MPL4	MSL1	MSL2	MSL3	MSL4
Bar spacing, mm	36	36	48	48	48	48

Third Stage: Durability of the LMC

As mentioned before the permeability and the ability to withstand against sulfate attack of one of the LMC mixtures is investigated and compared to that of the corresponding SCC mixture and the ordinary mixture.

Permeability; For permeability evaluation, 3 companion specimens (20*20*12) cm corresponding to each of the investigated mixes were brought to the testing machine at 28 days age. Immediately after completing the water pressure exposing regime, the specimens were divided equally into two halves and the water penetration depth and pattern were recorded. Table 4 displays the 28-day permeability results of the investigated concrete mixtures. The results cited in the table show that:

- The ordinary concrete mixture (Mc) although has the same cement content as the SCC mixture (MSC1) and the LMC mixture (MLC1), but its permeability is much higher than both. The difference is attributed to the all of the mixture constituents as well.
- The LMC mixture MLC1 exhibited less penetration depth than the SCC mixture MSC1. Apparently, Latex inclusion helps to refine the pore structure of the resulting concrete.

The test results shown in Table 4, reveal the superiority of the LMC as water tight and almost impermeable to liquids, which would further affect all other durability aspects.

Table 4: Average water penetration depth

Mixture	Ordinary	SCC	LMC
	Mc	MSC1	MLC1
Average penetration depth, mm	26.5	5	2.8

Surface scaling and expansion potentiality; Surface scaling is a typical damage mechanism in concrete that may not occur in mortar. Surface scaling occurs when the mortar on the surface of a concrete breaks away from the coarse aggregate as the mortar expands or deteriorate. Evaluating this phenomenon was carried out in terms of mass changes of the specimens after soaking in a 10% sodium sulfate solution for about one year. In circumstances where there is cover spalling, the overall weight will be reduced. If the spalling doesn't take effect, the cubes' weight might be increased as a result of the formation of the expansive compounds which are highly water absorbent. Anyhow, the formation of hydration products is also a possible reason of weight increase (autogenous increase). The changes in the two cases are indicative to the extent of sulfate attack. The LMC specimens, as mentioned before, were air cured whereas those of the SCC and ordinary mixtures were cured in water. It was necessary to bring them all to the same moisture condition before exposure to the sulfate solution. Therefore, the LMC specimens were immersed in tap water for 24 hrs before sulfate exposure. Results of weight variations over about one year are presented in Fig. 6 for the LMC mixture, the SCC mixture, and the ordinary one.

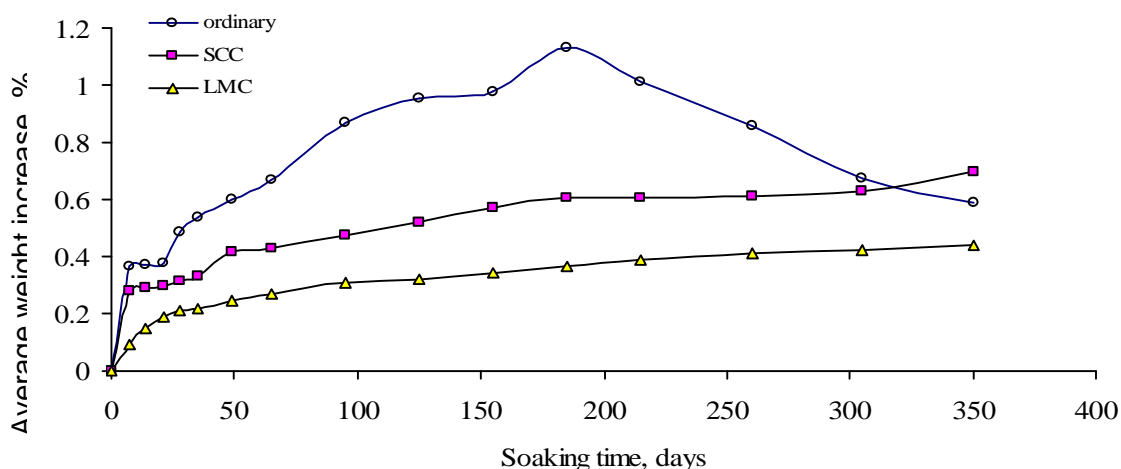


Fig.6: Weight Changes of Concrete Cubes due to Soaking in 10% Sodium Sulfate Solution up to One Year

As could be seen, the LMC specimens were the least affected by the 10% sodium sulfate solution. At about 6 months, the monitored weight increases were about 1.13% for the ordinary concrete, 0.6% for the SCC, and 0.37% for the LMC. Starting from this age, signs of deterioration started to form on the surface of the ordinary concrete specimens and their weights decreased continuously as a result of surface scaling and break down of the cubes' edges. On the other hand, no signs of deterioration or weight loss were noticed for the specimens of the SCC mixture, as well as the LMC mixture. It is worth to mention that the LMC has a poor water resistance such that its strength is decreased when exposed to water. This phenomenon is attributed to the partial re-emulsification of the formed polymer film⁹. Nevertheless, its sulfate resistance in terms of weight changes or surface scaling is superior to that of the other kinds of concrete.

Compressive strength variations over time due to sulfate exposure; Fig.7 shows the strengths of the investigated mixtures at periods extended over about one year for different exposure conditions. Till about 3 months of sulfate exposure, all kinds of concrete responded almost equally. At this time the concrete strengths were not appreciably affected by sulfates, probably as a result of richness in cement. After about 11 months of sulfate exposure, i.e. at one year age, the difference between the different kinds of concrete regarding strength retrogression became apparent. Defining the retained strength as the strength ratio of that after a certain period of sulfate exposure to that of the continuously cured specimens to the same

period. The retained strengths of the employed mixtures; Mc, MSC, and MLC after about one year are 80.5%, 94.2%, and 92% respectively. The ordinary concrete (Mc) specimens were the most affected, while those of the SCC specimens were the least in this effect. It is interesting to note that although the one year strengths were impaired due to sulfate exposure as compared to the strengths of the continuously cured specimens, nevertheless they were higher than the strengths after initial curing (28 days). Apparently the relatively high cement content, and the good mix design enhanced the mixtures ability to withstand sulfate attack.

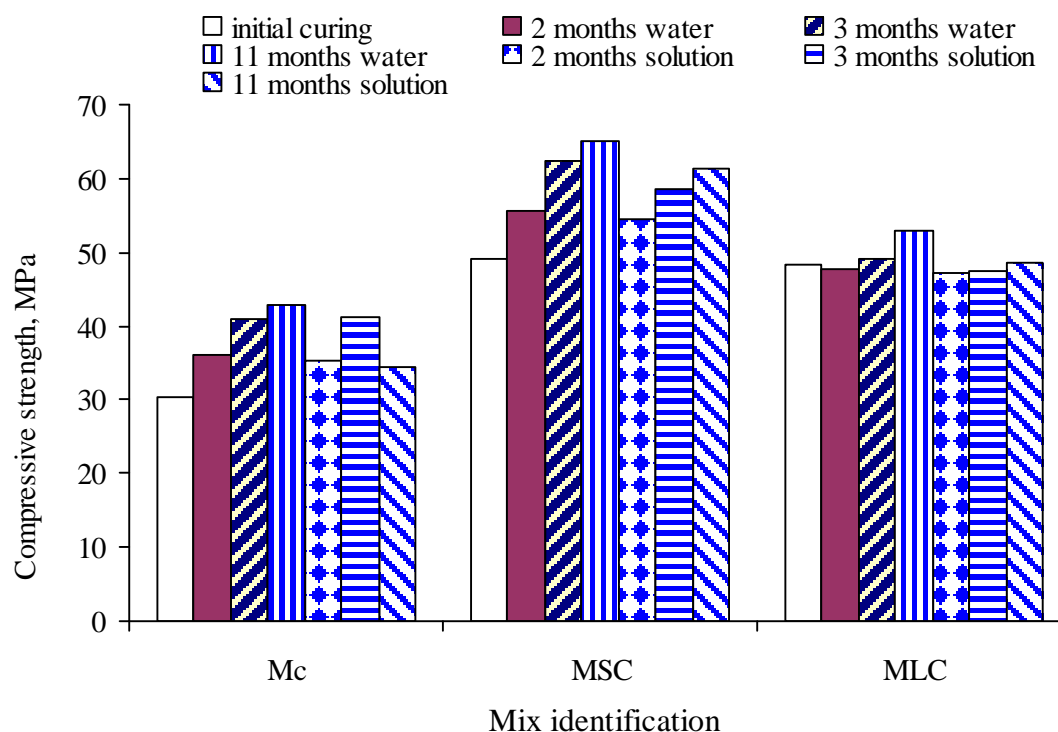


Fig.7: The Effect Of 10% Sodium Sulfate Solution On Concrete Compressive Strength Up To One Year

CONCLUSIONS

Test results reveal that Latex addition to the SCC mixtures even at a low dosage (3% of cement weight) is a powerful tool to produce concrete that is not significantly affected by water curing, especially when silica fume is included within the mixture constituents. Moreover, it serves to enhance the mixture viscosity to the extent that fibers addition doesn't induce any problem to the workability requirements. The generated mixtures due to Latex addition are as durable as the SCC ones but their water impermeability is more evident than for the other kinds of concrete.

REFERENCES

1. Amr S. El-Dieb, "Latex-Modified Concrete, Process Technology and Properties", Dar El-Hakeem, Egypt 2001.
2. Ohama, Y., "Principle of Latex Modification and Some Typical Properties of Latex-Modified Mortars and Concrete", ACI Materials Journal, Vol. 84, No. 6, 1987.
3. Su, Z., Bijen, J., and Larbi, J., "The Influence of Polymer Modification on the Adhesion of Cement Paste to Aggregate", Cement and Concrete Research, Vol. 21, No. 1, 1991.
4. Seleem, H.E.H., and Nofal, N., "The Effect of Steel Fibers on the Fresh and Hardened SCC Properties", International Conference on Future Vision and Challenges for Urban Development, Dec. 2004, Housing & Building Research Center, Cairo, Egypt.
5. DIN 1048, part 1, "Test Methods for Concrete", December 1987.
6. ACI 548.3R-95, "State-of-the-Art Report on Polymer-Modified Concrete", ACI Committee 548, ACI Manual of Concrete Practice, Part 5, 1999.
7. Seleem, H.E.H., and Nofal, N., "Optimization of Water Content of Ordinary and Self-Compacting Cementitious Mixtures", International Symposium of Advances in Concrete Through Science and Engineering, Evanston, U.S.A., March 2004.
8. "Specification and Guidelines for Self-Compacting Concrete", European Federation of National Trade Associations Representing Producers and Applicators (EFNARC), SCC Technical Committee, Feb. 2002.
9. Popovics, S., "Strength Losses of Polymer-Modified Concretes Under Wet Conditions", Polymer Modified Concrete, ACI SP-99, Vol.1, pp. 165-189, 1987.

UTILIZATION OF SOME CERAMIC INDUSTRIAL WASTES FOR MAKING CLAY-BUILDING BRICKS

N.G. Abd El-Ghafour, H.S. Hassan, and H.H. Assal

*Housing and Building National Research Center, Dokki, Giza, Egypt.
Department of Raw Materials & their Processing, email: hbrc@hbrc.edu.eg*

ABSTRACT

The clay deposits at Kom Osheem area, Fayoum Governorate, Egypt, were previously investigated. These clays are silty to silty mud with a mineralogical composition of montmorillonite, montmorillonite - illite, kaolinite and illite clay minerals in addition to, quartz, feldspar and calcite as the non-clay minerals. Chemically, these clays contain low Al_2O_3 , high SiO_2 and low soluble salts. The ceramic properties of Kom Osheem clays show that they are highly plastic and very sensitive upon drying. Ceramic tiles industry produces a lot of wastes such as ceramic sludge, broken under quality tiles and the accumulated dust. These wastes comprise a great pollution problem on the surrounded environment. In this work each of 15,25 and 50% ceramic sludge additives were mixed with the studied clayey raw material for making building bricks. The mix contains 15% sludge and 85% clay shows a lower plasticity coefficient and an insensitive behavior upon drying in addition to suitable physico-mechanical properties for the fired clay articles. This suggested mix was applied within a common brick fabric in Fayoum Governorate for studying the possibility of its industrial application.

Keywords: Montmorillonite, Ceramic sludge, Clay bricks, Physico-mechanical, Kom Osheem clays.

INTRODUCTION

In the last few years, many researchers were interested in studying the problem of industrial wastes. Building material industries continuously produce various types of wastes. Accumulation of such wastes could be considered as one of the main sources for the environmental pollution. Ceramic tiles industry produces different kinds of wastes, such as dust collected by the filters of chimneys; broken tiles which may be refused through the quality control process and finally, the sludge which is produced during recycling of water through special pressed water filters. Sludge is a type of ceramic tiles industry wastes which represents a terrible problem inside the factory due to its daily accumulation and disability for its recycling in the ceramic tiles industry. Also, this sludge causes a serious problem outside the factory; since transferring it away certainly leads to an environmental pollution. This work aims to study the possible utilization of ceramic waste sludge in the clay building bricks industry. Kom Osheem clays, Fayoum Governorate, Egypt, were previously investigated by many authors. For instance, Abd El-Ghafour¹ studied textural, chemical and mineralogical composition of Kom Osheem clays. Utilization of ceramic sludge in building clay bricks could be investigated by mixing the clayey raw material with various percentages of sludge. These mixes were moulded, dried, and fired at ranges of temperatures suitable for making building bricks. The fired articles were evaluated through their physical and mechanical properties. Finally, the most suitable mix could be utilized on an industrial scale within one of a widespread Egyptian brick fabric.

MATERIALS AND METHODOLOGY

The materials used in this work were clays from Kom Osheem area (El-Fayoum Governorate, Egypt) and a ceramic sludge as a waste product from a ceramic factory lies near to the studied clayey material.

The mineralogical composition of the studied raw materials was examined using a Philips PW 1050/70 X-ray diffractometer. The powder X-ray diffraction method was used for the identification of non clay minerals. The oriented aggregates of the <2 μ fraction method was used for the identification of clay minerals through untreating, glycerol solvating and heating at 550°C for 2 hrs. The identification of clay and non-clay minerals was based on the mineral powder diffraction file data book². The semi-quantitative estimation of the separated clay minerals was calculated according to the method of Johns et al.³. Philips PW-1400 X-ray fluorescence spectrometer and traditional chemical analysis method were applied for studying the chemical composition of the clay samples.

To evaluate the suitability of the clay/ceramic sludge mixes for making building bricks, each of clay and ceramic sludge samples were dried, ground and sieved through 1-mm sieve. Four clay/ceramic sludge mixes with 0, 15, 25 & 50% ceramic sludge additives were prepared. The ceramic properties in terms of plasticity as well as drying and firing behaviour were determined. The plasticity measurements were carried out adopting the method of Pfefferkorn⁴, based on deformation caused by the action of a piston on clay cylinders of different water contents. Water content corresponding to a compressibility = 3.3 is considered as plasticity coefficient (PC) i.e. water of plasticity. On the other hand, the drying behaviour was calculated according to ASTM⁵. The obtained data were used for drawing Bigote's curves⁶ from which the drying sensitivity coefficients (D.S.C.) were calculated for each mix. Physical and mechanical properties were studied after firing the dried articles at 800, 850 and 900°C with 1 °C/min interval of firing and 2hrs soaking time.

Results and Discussion

Kom Osheem clays, Fayoum Governorate, Egypt, were previously investigated. These clays contain clay > silt > sand particles. They had a grain size distribution ranged from silty clay, clayey mud to silty mud according to the classification of Picard⁷. On the other side, the ceramic sludge has a random size distribution with a nearly trimodal classes, (Fig. 1).

Kom Osheem powder clay sample (non-clay fraction) is composed of quartz, feldspar, gypsum and calcite. The clay fraction of Kom Osheem clays is composed of montmorillonite, kaolinite, montmorillonite – illite and illite minerals in a descending order of abundance, (Abd El – Ghafour¹). On the other hand, the mineralogical composition of the dried powder ceramic sludge is composed mainly of quartz and albite in addition to kaolinite and illite, (Fig. 2).

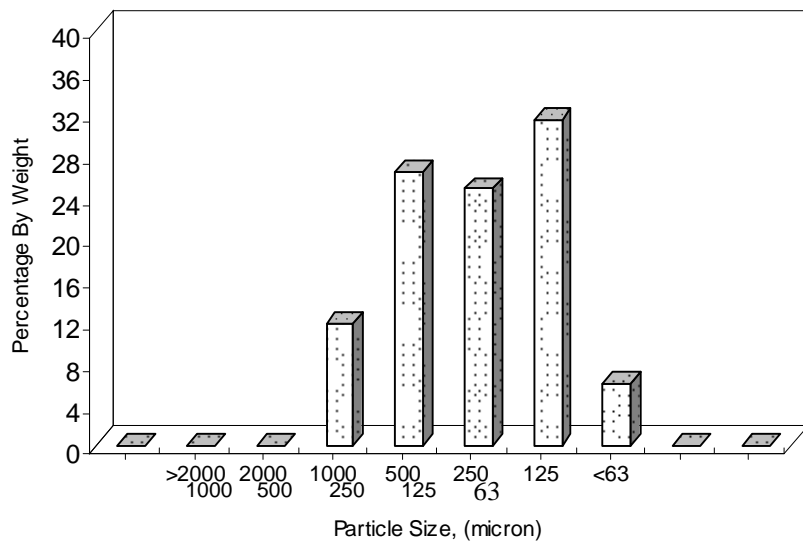


Fig. 1: Histogram shows the particle size distribution of the studied Waste ceramic sludge

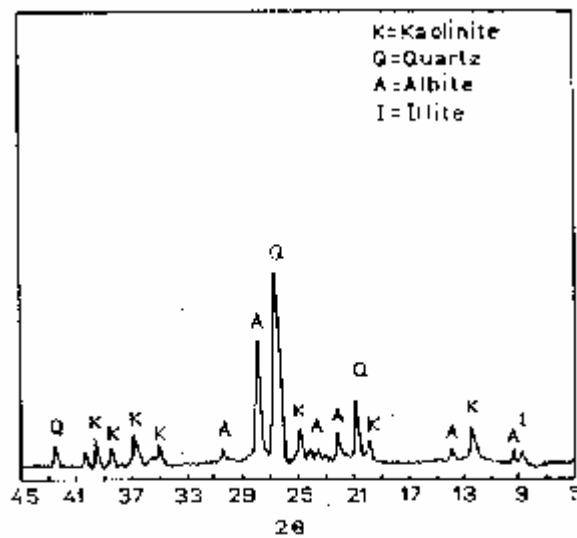


Fig. 2: X-ray Diffraction Pattern of the Studied Ceramic Waste

The data of chemical analysis (Table 1) indicates that Kom Osheem clays contain high SiO₂ (54.51%) and low Al₂O₃ content (19.64%). These values could be attributed to the presence of clay minerals, feldspars and quartz. It is obvious that, the chemical composition of Kom Osheem clay sample is in agreement with its mineralogical composition.

Table 1: Average Chemical Analysis Data of the Clay and Ceramic Waste Sludge Materials.

Oxides Content,%	Kom Osheem Clay	Ceramic Sludge
SiO ₂	54.51	61.43
Al ₂ O ₃	19.64	19.13
Fe ₂ O ₃	4.18	3.29
TiO ₂	1.33	0.96
CaO	5.78	4.78
MgO	1.28	1.22
Na ₂ O	1.14	2.17
K ₂ O	1.40	1.04
SO ₃	0.60	0.14
L.O.I.	10.10	5.76
Total Soluble Salts	100.00	99.92
Cl ⁻	0.71	0.05
SO ₄ ⁻	0.24	1.81
Na ⁺	0.66	0.97
K ⁺	0.14	0.35

Such clay can be utilized successfully in brick making. The chemical composition of the studied ceramic sludge reveals its enrichment in SiO₂ (61.43%), CaO (4.78%), and Na₂O (2.17%). The percentage of Al₂O₃ in the sludge is nearly similar to that in Kom Osheem clay. Generally, the more or less close chemical relationship between the studied clay and ceramic sludge has encouraged designing different mixes between them.

The type of clay minerals and its particle size distribution are the principal factors affecting the plasticity of clays, (Platen & winkler)⁸. According to Pffeferkorn's technique⁴, Figure, (3) shows that, Kom Osheem clay is characterized by a high plasticity coefficient (P.C = 32.5). This can be attributed to the high content of montmorillonitic clay minerals as well as the high clay fraction. These results coincide with the mineralogical and textural composition of such clay. It was observed that, as the ceramic sludge additives are increased, the PC is gradually decreased to 28.7 with 50% ceramic sludge. It is also observed that, for a mixture of 85% clay, and 15% ceramic sludge, the P.C decreases to 31.7. This limited decrease in PC will not affect greatly the plastic behavior of the mix but may keep good ceramic properties for the end product. The presence of more plastic clays leads to good ceramic properties (Searle & Grimshaw⁹ and Abdel Ghafour¹⁰).

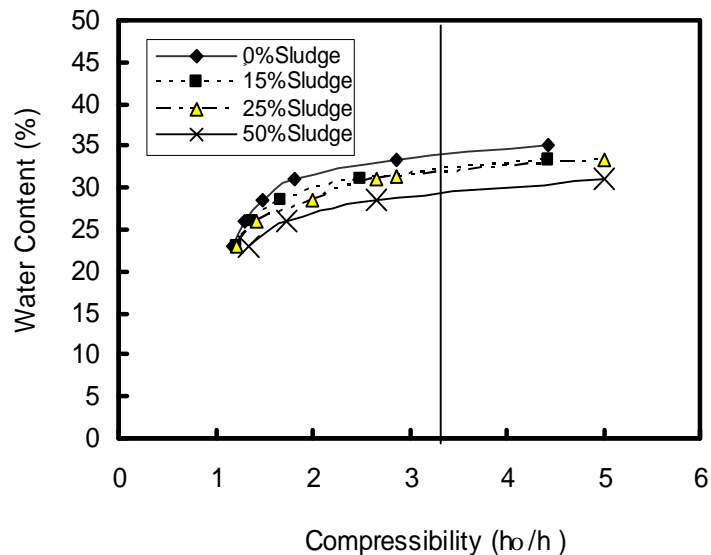


Fig.3: Plasticity Curves of The Studied Clays with Various Percentages of Ceramic Industry Waste Sludge.

Plastic pastes of Kom Osheem clay as well as their mixtures with ceramic sludge (0, 15, 25 & 50%), were hand molded into cubes of 5 cm side length. The percentage of the linear shrinkage during drying process was determined and plotted as a function of the percentage of water content (Bigot's curves, Fig.4). The drying sensitivity coefficient (D.S.C.) was calculated from these curves. The D.S.C. of Kom Osheem clay (2.18) indicates that such clay is sensitive upon drying (ASTM⁵) due to its high clay fraction and its montmorillonitic clay minerals. Generally, it should be noted that drying shrinkage of such low grade clay is also attributed to the amounts and the particle size of clay minerals. At the same time the amount of water lost during drying is directly proportional to, but not equal to, the percentage of shrinkage. The D.S.C. of clay / ceramic sludge mixtures decreases in the order $1.00 > 0.93 > 0.87$ against 15, 25 & 50% ceramic sludge additives, respectively.

This means that addition of 15-50% of ceramic sludge leads to a corresponding decrease in the D.S.C from very sensitive (2.18) to insensitive (0.87-1.00) mixes during the drying process. Such values declare insensitive and safe drying behavior without effect on the plastic and workable nature of the sludge-bearing mixes.

The dried green articles were fired in an electric furnace at temperatures between 800°-900°C. The data of physico-mechanical properties are listed in Table 2, and their graphical relationships are represented in Figures (5&6). Rising firing temperature increases firing shrinkage percentages and bulk density values of the fired clay articles. Addition of up to 50% ceramic sludge gradually decreases bulk density with increasing linear shrinkage at all firing temperatures. This means that the more addition of ceramic sludge the less firing shrinkage will be obtained. It should be recorded that, the amounts of silica and free quartz included or added to the clayey raw material with respect to the applied firing temperature are responsible to a great extent for the amount and type of firing shrinkage or expansion, (Abd El-Ghafour, 1995¹⁰). In this work it is noticed that, addition of 50% ceramic sludge partly fixed the increasing trend of firing shrinkage especially on firing at higher temperatures (850 o-900oC).

The water absorption values also decreases with increasing firing temperature. Generally, the increase of firing temperature decreases the volume of articles and accordingly decreases the pore spaces. The decrease of water absorption percentages and the increase of bulk density values by rising firing temperature indicate an increase in the formed glassy phase which fills some of the open pores of the fired clay articles due to the progressive vitrification in the clay body. The general decrease in water absorption percentage with increasing the firing

temperature indicates an increase in the glassy phases that fill some of the open pores of the fired articles (El-Mahallawy11).

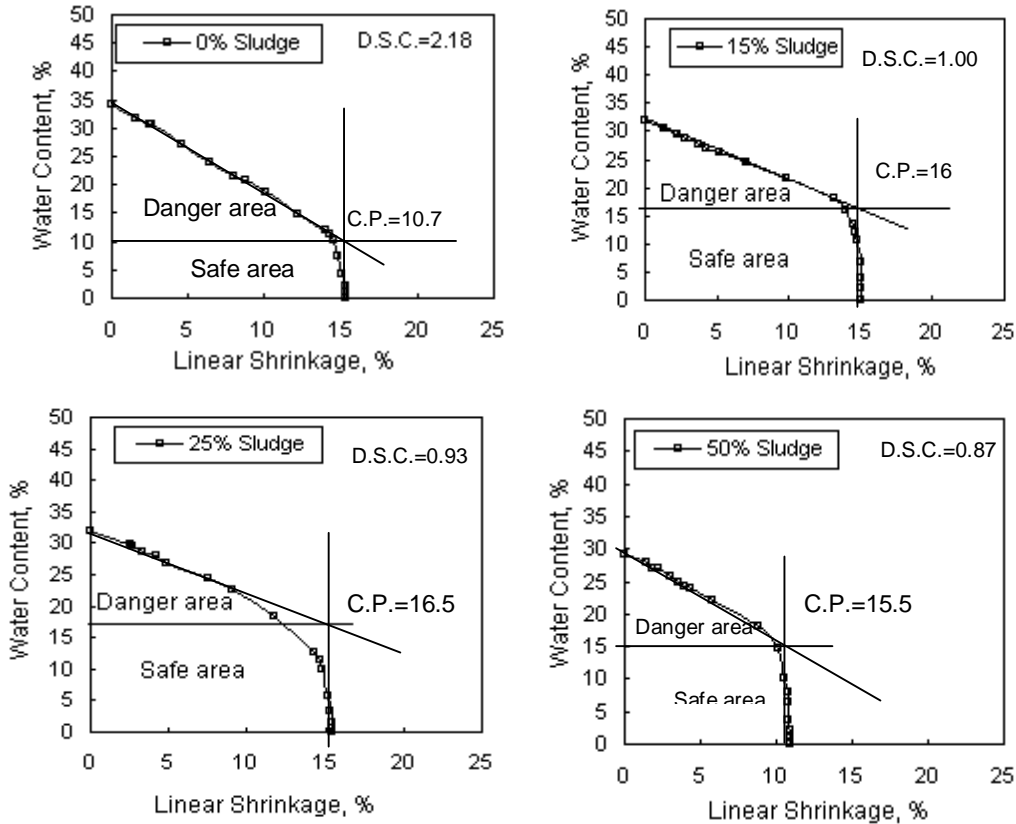


Fig. 4: Bigot’s Curves of the Studied Unfired Clay Articles.

Generally, the values of water absorption given by the fired articles could be considered as a direct reflection to the firing shrinkage and bulk density values.

It should be recorded that, the high content of CaCO_3 in the clayey material or in the added waste gives the fired articles more open pores during the release of CO_2 gas through the firing process. This behavior normally increases the porosity and consequently the water absorption values. On increasing the firing temperatures, the porosity and water absorption decrease due to filling of some pores by the formation of more glassy phase (Khalil and Kabesh¹² & Khalil and Korashy¹³). This may explain the abrupt decrease of water absorption values of the fired clay articles with 50% ceramic sludge from 800° up to 900°C.

Table 2: Data of Physical and Mechanical Properties of the Fired Clay Articles with Ceramic Sludge Additives

	Sludge (%)			
	0	15	25	50
Firing Volume Changes (%)				
800° C	33.50	33.00	32.43	24.88
850° C	35.18	33.92	33.70	25.29
900° C	39.84	39.01	37.69	25.80
Water Absorption (%)				
800° C	14.11	14.56	15.80	17.38
850° C	10.47	13.41	15.38	16.09
900° C	10.06	11.60	13.89	15.79
Bulk Density (g/cm³)				
800° C	1.741	1.732	1.701	1.650
850° C	1.775	1.743	1.708	1.697
900° C	1.936	1.853	1.765	1.699
Dry Compressive Strength (Kg/cm²)				
800° C	225	183	164	123
850° C	235	221	217	199
900° C	271	237	235	229
Wet Compressive Strength (Kg/cm²)				
800° C	171	162	129	93
850° C	199	184	161	153
900° C	227	193	186	184

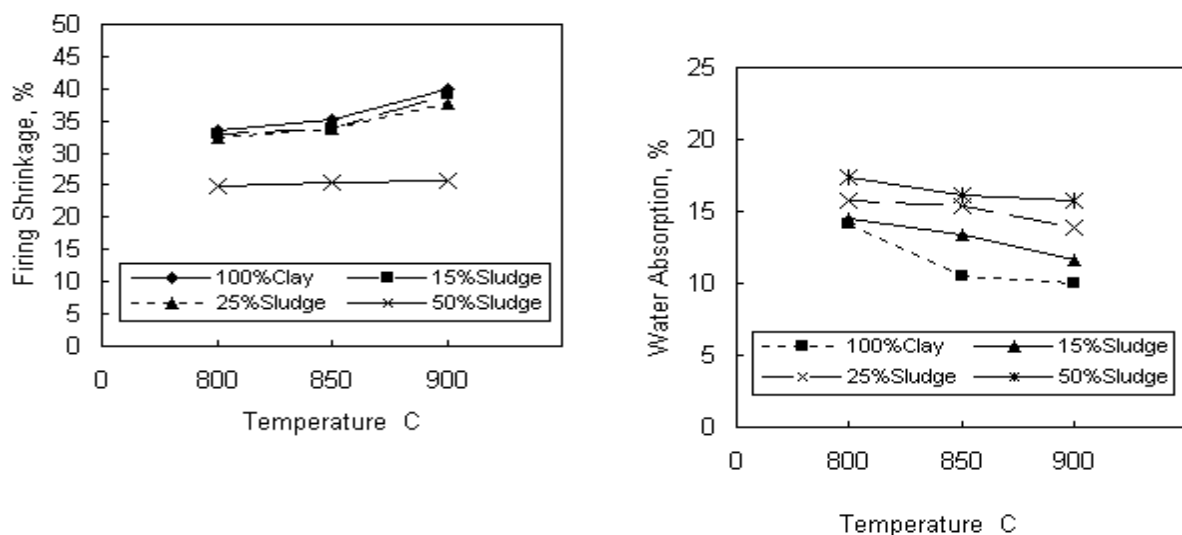


Fig. 5: Firing Shrinkage and Water Absorption of the Fired Clay/Ceramic Sludge Articles.

The dry & wet compressive strength values of the fired clay articles generally, increase with increasing firing temperature. For the fired articles, the compressive strength values indicate that phases produced upon firing act as binding materials after cooling. Therefore, these values are increased with increasing firing temperature. Kom Osheem fired clay articles have the highest dry and wet compressive strength since they have a vitrification temperature of about 910°C, which produces molten phases acting as strong binding materials after firing, (Abd El-Ghafour¹⁰). The compressive strength values of all fired articles are decreased by increasing the percentage of additives at the same firing temperature. Mix with 15% ceramic sludge achieved reasonable compressive strength values at all firing temperatures. It is well known that fluxes or impurities and vitrification of clays are dependent upon each other. Feldspars which are included in the clayey raw material and the sludge additives represent the main source of alkalis within the studied mixes. Such alkalis act as a fluxing agent leading to a high degree of vitrification in the clay body. Accordingly, the relative differences in the composition of the studied mixes, their impurities and fluxes may explain the differences in the obtained compressive strength values. Finally, mixes with various percentages of ceramic waste sludge more or less save the workable water, improve the drying sensitivity, in addition to the modification of some physical and mechanical properties of the fired articles into reasonable ones under a normal applied range of firing temperature (800-900°C).

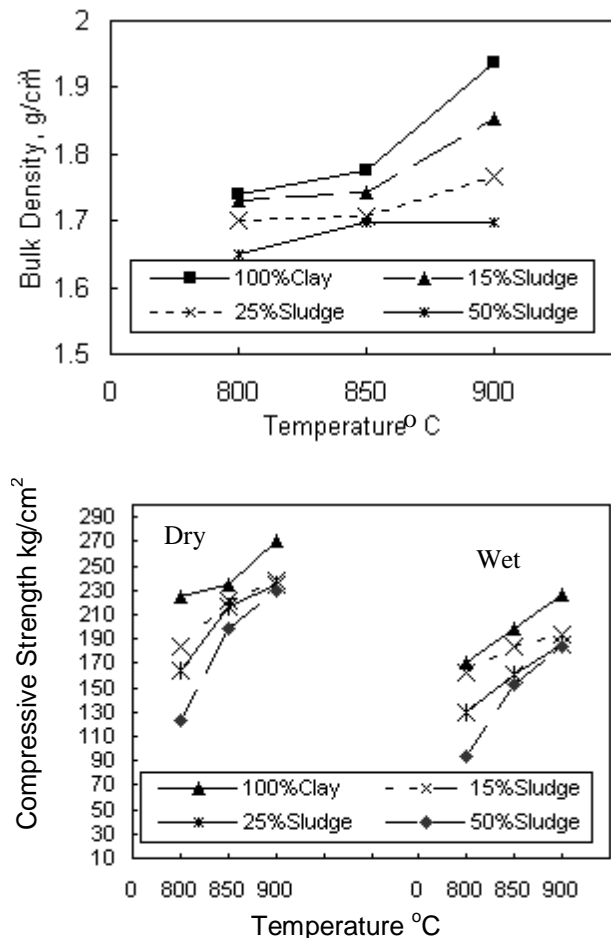


Fig. 6: Bulk Density and Compressive Strength of The Fired Clay/Ceramic Sludge Articles.

The mix with 15% ceramic sludge and 85% of Kom Osheem clay was applied in a clay brick fabric in Fayoum Governorate. The techniques of mixing , molding , drying and firing were

applied according to that followed in the ordinary Egyptian clay bricks fabrics which take the environmental protection in their consideration. Solid green clay bricks with average dimensions of 24.59 length, 12.97 width and 7.94 cm height were extruded and left for drying for two weeks. The green clay bricks were fired in a Hoffman furnace at about 800°C. Table (3) shows the physical and mechanical data of

Table 3: Data Of Physical and Mechanical Properties of the Fired Clay Bricks With 15% Ceramic Sludge Additives.

Sample No.	Dimensions cm.			Dry Weight Kg.	Water Abs. %	Bulk Density g/cm ³	Dry Compr. Strength Kg/cm ²	Wet Compr. Strength Kg/cm ²
	L	W	H					
1	21.0	10.0	7.0	2.591	8.59	1.76	133.57	117.13
2	20.9	10.1	6.9	2.382	9.25	1.64	155.59	109.77
3	21.0	9.9	6.9	2.612	9.09	1.82	144.73	122.66
4	21.0	10.0	7.0	2.542	9.33	1.73	123.86	114.69
5	21.0	10.1	7.0	2.474	9.02	1.67	126.48	117.13
6	21.0	10.0	6.8	2.403	8.79	1.68	138.43	116.38
7	21.0	10.1	6.9	2.719	8.59	1.86	140.91	121.67
8	20.9	10.0	6.5	2.412	8.43	1.78	129.33	124.72
9	20.9	10.0	7.0	2.471	8.55	1.69	143.48	118.40
10	21.0	10.1	6.8	2.561	8.42	1.78	140.91	118.66
Average	20.9	10.0	6.9	2.516	8.81	1.74	137.73	118.12

the fired clay/ceramic sludge building bricks. The average dimensions of the fired bricks show that those bricks were suffered from an average firing shrinkage equal to about 15%. The average bulk density value for the fired bricks was 1.74 g/cm³, while the average percentage of water absorption was 8.81%. The average percentages of dry and wet compressive strength for the studied fired bricks were 137.73 and 118.12 kg/cm², respectively. It should be recorded that, all the results of physical and mechanical properties, except firing shrinkage are completely agree with the limits of the Egyptian Standards¹⁴ and The Egyptian Code for Design and Construction of Buildings¹⁵. Accordingly, the industrial application of 15% ceramic waste sludge with a highly plastic clays produce suitable building clay bricks by firing at temperatures as low as 800°C. More over, the huge amounts of ceramic waste sludge can be recycled in the building bricks industry. Finally, a dual target could be achieved; first, an environmental protection against the pollution caused by the accumulation of ceramic waste sludge and second, saving a part of the clayey raw material needed urgently for building brick industry.

CONCLUSIONS

Kom Osheem clays are silty to silty mud with clay > silt > sand fractions. The identified clay mineral assemblage includes montmorillonite, montmorillonite-illite, kaolinite and illite in a descending order of abundance. They contain quartz, feldspars and calcite in addition to low Al_2O_3 and high SiO_2 contents. The mineralogical composition of the ceramic sludge includes mainly quartz and albite in addition to kaolinite and illite. Its chemical composition reveals the enrichment of SiO_2 , CaO and Na_2O . The percentage of Al_2O_3 in the sludge is nearly similar to that in Kom Osheem clays. It is concluded that:

1. Addition of ceramic sludge to Kom Osheem clay decreases its plasticity coefficient, but not affect greatly the plastic behaviour of the studied mixes.
2. Addition of ceramic sludge to the studied sensitive clay decreases its drying sensitivity coefficient (D.S.C.) from very sensitive to insensitive during the drying process.
3. The more addition of ceramic sludge, the less firing shrinkage and bulk density values in addition to the more water absorption values will be obtained.
4. The compressive strength values of Kom Osheem fired clay articles generally, increase with increasing firing temperature.
5. The mix with 15% ceramic sludge achieved reasonable compressive strength values at all firing temperatures. So, it was chosen for industrial application in a clay fabric in Fayoum Governorate.
6. All the physical and mechanical properties of the fired clay building bricks, except firing shrinkage are completely agree with the limits of The Egyptian Standards No.1756,(1989) and The Egyptian Code for Design and Construction of Buildings.
7. Ceramic waste sludge can be used in clay brick making with a suitable percentage (not more than 15%), and firing at 800°C .
8. Utilization of ceramic waste sludge in building clay bricks industry shares in the environmental protection against the pollution caused by the accumulation such solid waste, in addition to saving the great need of clayey raw material for making clay building bricks.

REFERENCES

1. Abd El-Ghafour, N.G., 2000 "Utilization of by-pass cement dust, sand and clay mixture for making building bricks" Egyptian Journal of Applied Sciences, V.15, No.1, pp.332-349.
2. Mineral Powder Diffraction File Data book, 1993, (Sets 1-42), ICDD, Pennsylvania, U.S.A.
3. Johns, W.D., R.E.Grim, and W.F.Bradley, 1954 " Quantitative estimation of clay minerals by diffraction methods" J.Sed.Petrol., V.24, pp.242-251.
4. Pfefferkorn, F., 1924 " Untersuchungen uber die Plastizitat und Thixotropie von Tonen", Sprechsaal, V.57, p.297.
5. ASTM, Standard C67-66, 1966 "Standard methods of sampling and testing bricks", pp.59-67.
6. Lach, V., 1965 " Rozhboru suovin pro silikatory prumysl", Testing of raw materials in silicate industry, SNTL, Prague.
7. Picard, M.D., 1971 "Classification of fine-grained sedimentary rocks", J. Sed.Petrol., V.41, pp.179-195.
8. Platen, H. and H.G.F.Winkler, 1958 " Plastizitat und thixotropie von fraktionierter tonmineralen, kolloidz, V.158, p.3.
9. Searle, A.B. and R.W., Grimshaw, 1959 " The chemistry and physics of clays and other ceramic materials", Ernst Ben Ltd., London.
10. Abd El-Ghafour, N.G., 1995 "Ceramic properties of some Egyptian clay deposits and the possibility of their modification", Ph.D. thesis, Fac.Sc.Cairo University.
11. El-Mahllawy, M.S., 2004 "The composition and ceramic properties of some Egyptian shale deposits and their possible utilization as building materials" ,Ph.D.thesis, Fac. Sc.Zagazig University.
12. Khalil, A.A. and A.M. Kabesh, 1981 " The use of Wadi Gharandel clay deposits for various ceramic products", III, Physical and mechanical properties of the prepared ceramic bodies, Sprechsaal 114, p.444.

- 13.Khalil, A.A. and S.A. El-Korashy, 1988 "Firing characteristics of Sinai calcareous clays"
Ceramic International, V.15, p.297.
- 14.Egyptian Standard Specification (ESS) No.1756, 1989 "Building units made from desert
clay", pp.19.
- 15.Egyptian Code for Design and Construction of Buildings, (under press).

FEASIBILITY OF UTILIZING WASTE GFRP PIPES AS LATERAL REINFORCEMENT FOR RECTANGULAR REINFORCED CONCRETE SHORT COLUMNS

M. S. SAYED

*Department of Strength of materials,
Housing and Building National Research Center, Giza, Egypt*

ABSTRACT

Since 1980, Egyptian government investment has been directed to the infrastructure projects. Water supply and water drainage networks are among those projects which are very costly, therefore they are designed with a life span of about one hundred years. There is a new trend towards the use of durable and maintenance free systems. The "GFRP" pipes are one of the economic solutions if the project life span is taken into consideration. A number of investors currently produce the "GFRP" pipes in the Egyptian market. They follow the latest technologies in their production lines, however they still suffer 2-5% deficiency of their produced pipes, which consequently regarded as rejected pipes. There was a successful attempt to use such pipes as transverse reinforcement for short circular columns, which was published by the author (M.Sayed 2005). The present paper focuses on the feasibility of applying the factory rejected "GFRP" pipes as transverse reinforcement for rectangular columns after sawing them into slices of intended width. The main parameters which control the use of such pipes were considered, including the slice width, spacing, and configuration. An experimental program consisting of nine short rectangular columns was designed to cover all the governing parameters. Although the experimental results showed that columns laterally reinforced by GFRP slices have a comparable behavior to conventionally reinforced concrete columns, An additional research efforts are needed to validate the use of the proposed system in the practical field.

Keywords: GFRP, Pipes, Recycling, Concrete, Rectangular Columns, Confinement.

INTRODUCTION

GFRP pipes are one of the most durable solutions for infrastructure applications. Due to the expensive cost of the system, their use still suffers a competition with the conventional systems. One of the reasons which increases the cost of "GFRP" pipes is the factory rejected pipes at the quality control stage. Most of the Egyptian producers suffer a 2-5% of their product as waste pipes. This percentage represents 900-2250 meter length of waste pipes per month if the factory produces 1.5 km of pipes per day. An effort has been done by the author to utilize the waste pipes as lateral confinement for circular column.

This study represents a research program that aims at spreading the uses of the factory-rejected pipes in structural applications. As the rectangular cross section are the most popular and convenient shape in construction of reinforced concrete columns, the challenge is to try to use the factory rejected pipes, after sawing them into slices, as lateral reinforcement for reinforced concrete columns of rectangular cross section.

The use of lateral reinforcement for columns greatly enhances the ductility of the confined concrete. This subject was a major field of research through the last decades from (Wang et. al. 1978) to (Sheikh and Toklucu 1993) and (Mossallam 1999). To the author knowledge, it was not easy to find research studies in the field of recycling of waste "GFRP" pipes for lateral

reinforcement of concrete columns however, there are some researches in the effect of confinement using interlocking spirals on behavior of axially loaded columns (Khaloo, et. al. 1999).

This study uses the idea of interlocking of lateral reinforcement to create a new technique, which may be adopted for the factory rejected "GFRP" pipes to be used as lateral reinforcement for columns of rectangular cross section. The study consists of an experimental program and theoretical study based on the Egyptian code for the design and construction of concrete structures (ECCS 203-2001). The experimental program consists of casting and testing of nine reinforced concrete columns carefully designed to represent the main factors, which may affect their behavior. The factors include the slice spacing, width, and horizontal alignment. The aim of the theoretical study is to compare the experimental results with the code provisions regarding concrete columns.

It was proved from the experimental results that using of the factory rejected "GFRP" pipes as lateral reinforcement for columns of rectangular cross section was feasible. In addition, the theoretical study showed that the formula of Egyptian code for the design and construction of concrete structures could be used with highly accepted factor of safety to predicate the ultimate load of those columns laterally reinforced by the "GFRP" slices.

FABRICATION OF "GFRP" PIPES

The filament winding process is adopted by most of "GFRP" producers as a production method to fabricate their pipes. As shown in Figure.(1), a mandrel of the intend diameter is rotated on its axis, and wound with a continuous filament of reinforcement. The fibers are passed through a resin bath immediately before contact with the laminate. According to manufacture information and fabrication process, the inner and outer surfaces of the pipes are lined and treated against the chemical attack of the adherent severe environment. A precise quality control system is applied on each pipe just before its delivery to the site. Due to unexpected human or machine errors, a percentage of the products are rejected. The rejected pipes not only have a negative environmental impact but also have an economical bad effect.

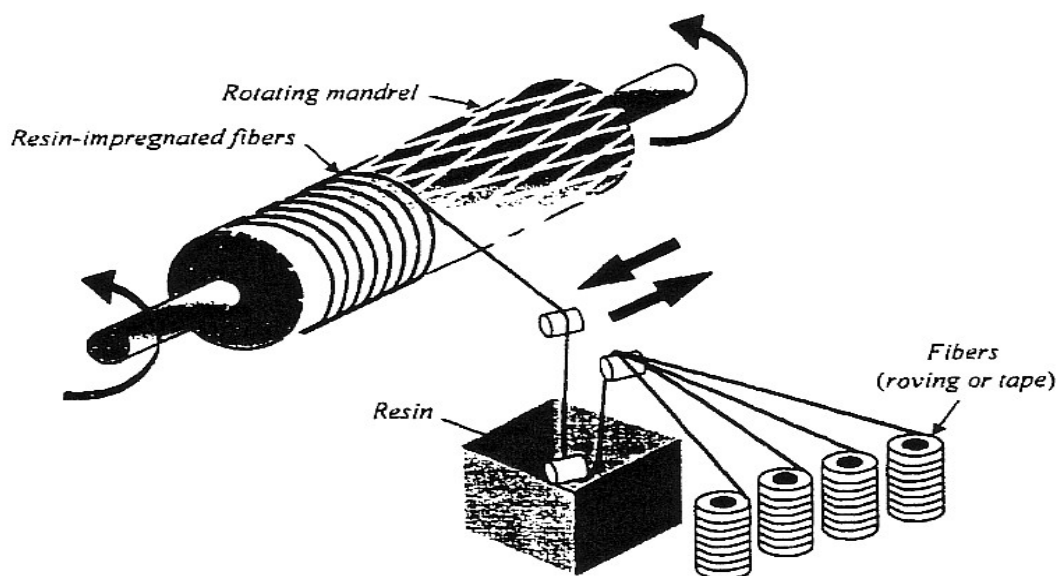


Fig.1: Scheme of the Filament Winding Process

EXPERIMENTAL PROGRAM

Configuration of Tested Columns

Nine short reinforced concrete columns were designed to study the feasibility of utilizing the factory rejected "GFRP" pipes as lateral reinforcement for columns of rectangular cross section. The cross section of the tested columns was 40.0 cm length and 20.0 cm width while the height was 140 cm. All columns were reinforced longitudinally by 6 rebars of 12 mm diameter high-grade steel (40/60). The tested columns were divided into two groups, **the first group** represents the **control columns** which were laterally reinforced by either separate hoops or by interlocking circular stirrups. Mild steel of 8 mm diameter was used as a lateral reinforcement for this group of columns. **The second group** was laterally reinforced by **"GFRP" slices**. The slices were interlocked together in a way to give the columns their rectangular shape, refer to Photo (1). This type of interlocking ensures the creation of three longitudinal confinement zones all over the height of the columns. In addition to the congested reinforcement at the upper and lower ends of the columns, prefabricated bolted steel jackets were used to avoid any kind of damage or cracks, which may affect the accuracy of the collected results.

The studied parameters were the slice spacing, slice width, and horizontal alignment (either staggered or stepped shape). Figure (2) shows the tested columns along with the description of the studied parameters, the upper third of the figure shows the control column while the middle and lower third of the figure show those column which were laterally reinforced by the "GFRP" slices. In addition, Table (1) shows the same information in a tabulated form.

The alphanumeric characters were used to identify the tested columns, (e.g., C1-HS20), the first two characters represent the column number while the second ones represent the type of lateral reinforcement either steel hoop or GFRP slices, followed by the pitch distance in (cm).

Table 1: Details of the tested columns

Group	Column Identification	Type of Lateral Reinforcement	Configuration of Lateral Reinforcement	Pitch (cm)	Slice Width (cm)	Remarks
(A) Steel Stirrups	C1-HS20	8 mm	Separate hoops	20.0	-	Control columns
	C2-HS10	8 mm	Separate hoops	10.0	-	
	C3-CS10	8 mm	Interlocking circular hoops	10.0	-	
(B) "GFRP" Slices	C4-GF20	10 bar	Interlocking slices	20.0	3.0	
	C5-GF20	10 bar		20.0	6.0	
	C6-GF20	10 bar		20.0	3.0	
	C7-GF10	10 bar		10.0	3.0	
	C8-GF10	10 bar		10.0	1.5	
	C9-GF10	10 bar		10.0	1.5	

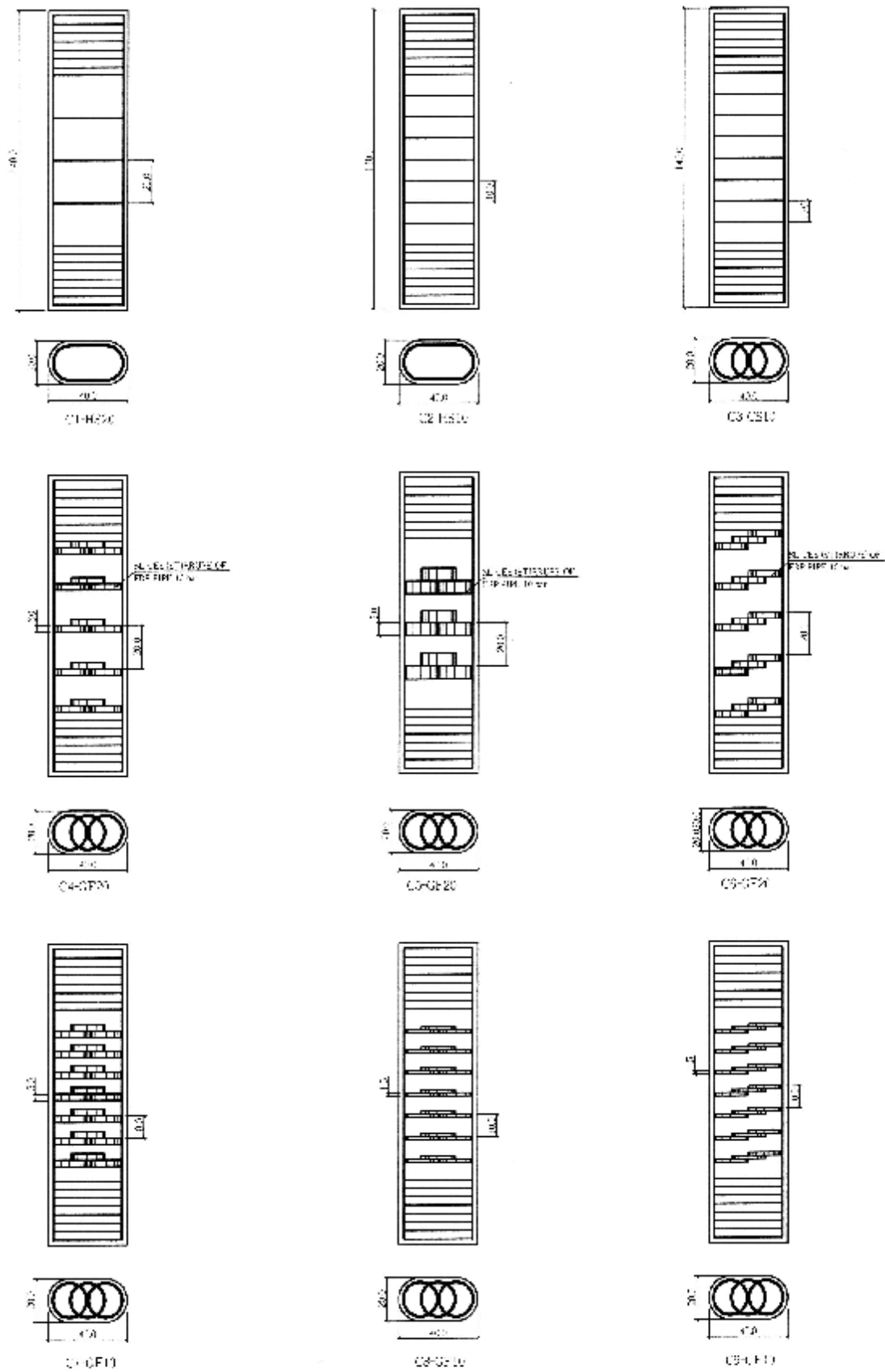


Fig. 2: Reinforcement Configuration of the Tested Columns



Photo.1 : Configuration of the Interlocking "GFRP" Slices Used as Lateral Confinement for Group (B)

Concrete Mix Constituents

Sand, crushed stone and ordinary Portland cement materials were used to produce concrete of target 28 days compressive strength of 250 kg/cm^2 . Table (2) represents the mix proportions of the designed concrete. Super-plasticizer type (F) was used to produce the concrete which was of 8 cm slump. This slump was intended to overcome any kind of honeycombing at the column's ends. Photo (2) shows the reinforcement cages of columns C7-GF10 and C3-CS10. All the tested columns were cast from the same concrete mix. Thirty-six standard cubes ($15 \times 15 \times 15 \text{ cm}$), in addition to the same quantity of standard cylinders ($15 \times 30 \text{ cm}$) were tested at the age of 28 days to get the specified concrete strength. All the columns were tested exactly at their 28 days age.

Table 2: Mix Proportions of the Designed Concrete Mix

Mix Number	Intended Strength (f_{cu})	Cement (kg)	Dolomite Crushed Stone (kg)	Sand (kg)	Water (liter)	Super-plasticizer Type (F)
1	250 kg/cm^2	350	1170	585	210	2.1 liter

The "GFRP" Pipes

A total of 10 bar "GFRP" waste pipes were used to fabricate the tested columns. The pipes outer diameter was 160 mm and the wall thickness was 8 mm. During the fabrication process of the pipes, the inner surface was lined to facilitate the removal of the pipes from the mandrel during fabrication. Hence, the inherent cohesion between the inner surface of the pipes and the concrete core can be neglected. Only the pipe confinement was trusted to develop the confinement effectiveness. All the rejected pipes were received in 300 cm length accompanied with full description and highlighting of the leakage points on the pipes. During the sawing of the pipes into slices the defected slices were thrown away and a direct tensile test was conducted according to ASTM D 2290-92 on circular rings cut from the pipes and tested as tension specimens to evaluate the tensile strength. The tensile strength of the used pipes was 1.43 t/cm^2 .



Photo 2. Reinforcement Configuration of Columns C7-GF10 and C3-CS10



Photo 3. Casting of Concrete Columns

Instrumentation and Testing Procedure

Three linear variable differential transducers (LVDT) were used to measure the vertical and horizontal strains. Two transducers were attached at the opposite sides of the column at a gauge distance of 60 cm while the third (LVDT) was mounted at the middle height of the columns at a distance of 20 cm. The data was collected using a data acquisition system. All transducers (LVDT) were mounted using pegs drilled inside the core of the columns to get the actual deformations of the concrete. Photo (4) shows one of the concrete columns during test. All columns were tested using a compressive testing machine of 500 ton capacity. The columns were tested up to failure which was recognized when a sudden drop in the applied load was reached. All necessary precautions were taken to ensure the concentric application of the applied load.



Photo 4: One of the Tested Columns During the Test

ANALYSIS OF EXPERIMENTAL RESULTS

Columns Laterally Reinforced by Either Single Hoops or Interlocking Circular Steel Stirrups (GROUP (A))

Column C1-HS20 and C2-HS10 were laterally reinforced by the common shape of stirrups used practically in the field, while column C3-CS10 was reinforced laterally by unusual shape of steel stirrups (interlocking circular stirrups) to be a good reference to those columns laterally reinforced by the "GFRP" slices.

Figures (3) and (4) show the behavior of the control columns. Figure (3) represents the axial load versus average concrete axial strain, while Figure (4) shows the axial load versus the concrete lateral strains. In addition, Table (3) shows the ultimate load and ultimate strain of this group accompanied with the observed failure strain. It can be seen that all the tested columns showed overall similar axial response up to their ultimate load. The ultimate load and corresponding axial strain varied depending on the configuration of the lateral steel reinforcement. Beyond the ultimate load, the descending branch of the load-strain curves had a real relation with the shape and spacing of lateral stirrups. In addition to the previous remarks, the following findings can be noticed from the figures:

- 1- Column C1-HS20, which was poorly confined, failed by the spalling of its concrete cover followed by buckling of longitudinal reinforcement bars and sudden drop in its axial load carrying capacity. Due to the poor confinement configuration of this column, its ultimate strain was 71% lower than axial concrete compressive strain (0.002). Column C1-HS20 has rapid stiffness degradation beyond its ultimate load. This was mainly attributed to the large stirrups spacing. On the other side, decreasing the stirrups spacing to 10 cm for column C2-HS10 slightly improved the ultimate load by 4.4%.
- 2- Column C3-CS10, which was laterally reinforced by interlocking circular stirrups significantly shows improved ultimate load and post peak behavior. The ultimate load of this column is higher than those for columns C1-HS20 and C2-HS10 by 25.60% and 20% respectively. The descending branch of this column was significantly improved in comparison with those of the current group (GROUP A).
- 3- From figure (4), it can be observed that column C3-CS10 can withstand higher horizontal concrete strain in comparison with columns C1-HS20 and C2-HS10, which indicates the superior ductility of the interlocking circular stirrups in comparison with separate hoops.

Table (3) Results of columns confined by steel reinforcement

Column Identification	Ultimate Load (Ton)	Strain at Ultimate Load ϵ_{ult}	Strain at Failure Load ϵ_f	$\frac{\epsilon_f \times 100}{\epsilon_{ult}}$	Notes
C1-HS20	183.0	0.00142	0.001905	134%	Control column
C2-HS10	191.0	0.00220	0.00262	120%	Control column
C3-CS10	230.0	0.00240	0.00319	133%	Control column

Columns Laterally Reinforced by "GFRP" Interlocking Slices (GROUP (B))

Figures (4) through (9) show the influence of various parameters which may affect the behavior of columns laterally reinforced by the interlocking "GFRP" slices. The studied parameters were the effect of spacing, slice width, and the horizontal alignment of the interlocking "GFRP" slices. Table (4) represents the experimental results. By studying the aforementioned figures, the following remarks can be drawn:

- 1- From figure (5), it is obvious that decreasing the slice spacing of the "GFRP" slices from 20 cm for column C4-GF20 to 10 cm for column C7-GF10 significantly increased ductility. Beyond the ultimate load, the stiffness degradation of column C4-GF20 was much higher than that of column C7-GF10. Regarding the axial load carrying capacity, the difference between the ultimate loads of the above-mentioned columns did not exceed 4%.
- 2- From figure (6), it can be noticed that increasing the slice width from 3 cm for column C4-GF20 to 6 cm for column C5-GF20 slightly increased the ultimate load and ductility. The difference between the axial load strain curves of the two columns did not exceed 5%.
- 3- The effect of increasing the slice width is more obvious for columns of slice spacing 10 cm. Increasing the slice width from 1.50 cm for column C8-GF10 to 3 cm for Column C7-GF10 resulted in increasing their axial load carrying capacity and ductility as well. The difference between their ultimate loads was 14%.
- 4- For all columns laterally reinforced by 1.50 cm width "GFRP" interlocking slices, the failure was recognized by rupture of the outer slice accompanied by strong snapping sound. The rupture of the "GFRP" slice was followed by buckling of the longitudinal reinforcement and sudden drop in the applied load.
- 5- As seen from Figure (8) and Figure (9), there is no clear trend can distinguish one of the proposed horizontal alignments over the other. On the other hand, it was found that staggered horizontal alignment is much more accepted from construction point of view.

Potentiality of Using "GFRP" Waste Pipes as Lateral Reinforcement

- 1- Figure (10) shows that the ultimate load of column C4-GF20 was higher than that of the control columns C1-HS20 by 15%, also the behavior of the former column showed significant improved ductility.
- 2- Figure (11) represents a direct comparison between the behavior of column C7-GF10 and that of control columns having the same pitch distance. Column C7-GF10 has superior behavior regarding ultimate load and ductility if compared to columns C2-HS10 and slightly worst overall structural performance in comparison with C3-CS10. The ultimate load of C7-GF10 is higher than that of C2-HS10 by 12.40% and lower than C3-CS10 by 5.5%.
- 3- From figure (12), it could be derived that column C8-GF10 with interlocked "GFRP" slices of 1.50 cm width had almost the same ultimate load of that of column C2-HS10; however its behavior was better from ductility point of view.
- 4- Although lateral steel reinforcement and GFRP slices have different stress-strain curves, columns laterally reinforced by GFRP slices have showed good comparable behavior to that of conventionally reinforced concrete columns from ductility point of view. Considering columns have same spacing between the lateral reinforcement, the last finding can be attributed to larger volume of confined concrete in columns reinforced by the GFRP slices in comparison with that columns laterally reinforced by steel stirrups (the width of the GFRP slice are much more bigger than the diameter of the steel stirrup rebar).
- 5- Photos (5,6,7,8) show the mode of failure of columns C1-HS20, C4-GF20, C7-GF10, and C8-GF10 from the left to the right. As seen from the photos, the failure of column C4-GF20 was as similar as that of column C1-HS20. In addition to that, a real rupture of the "GFRP" slices can be seen in Photo (7) for column C7-GF10.

Table (4) Results of columns confined by GFRP slices

Column identification	Ultimate Load (Ton)	Strain at Ultimate Load ϵ_{ult}	Strain at Failure Load ϵ_f	$\frac{\epsilon_f \times 100}{\epsilon_{ult}}$	Notes
C4-GF20	210.0	0.0015	0.00669	446.0%	
C5-GF20	217.0	0.0022	0.0068	310.0%	
C6-GF20	194.0	0.00159	0.00605	380.0%	
C7-GF10	218.0	0.00200	0.00652	326.0%	
C8-GF10	191.0	0.00248	0.005425	218.0%	
C9-CS10	202.0	0.00250	0.0052	208.0%	

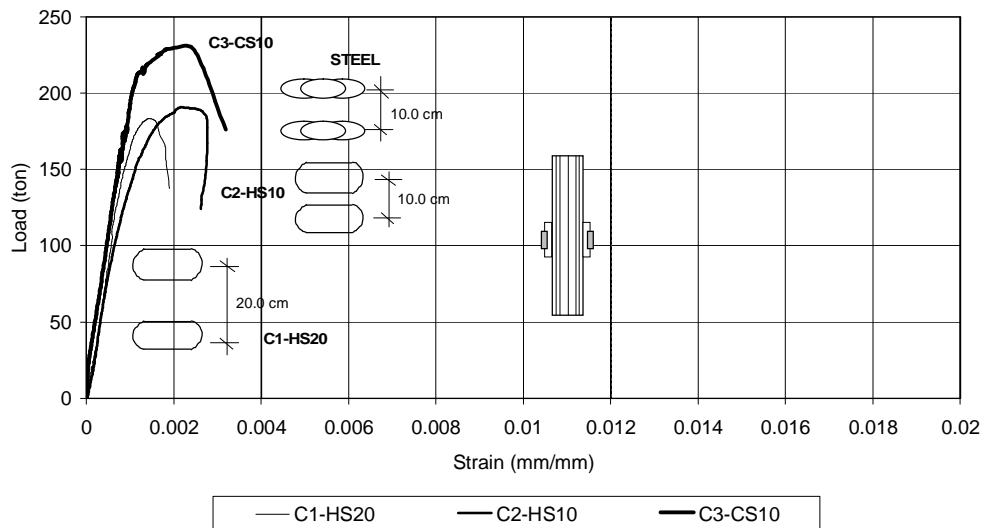


Fig. 3: Column Axial Load versus Average Concrete Vertical Strain for Columns Laterally Reinforced by Steel Stirrups

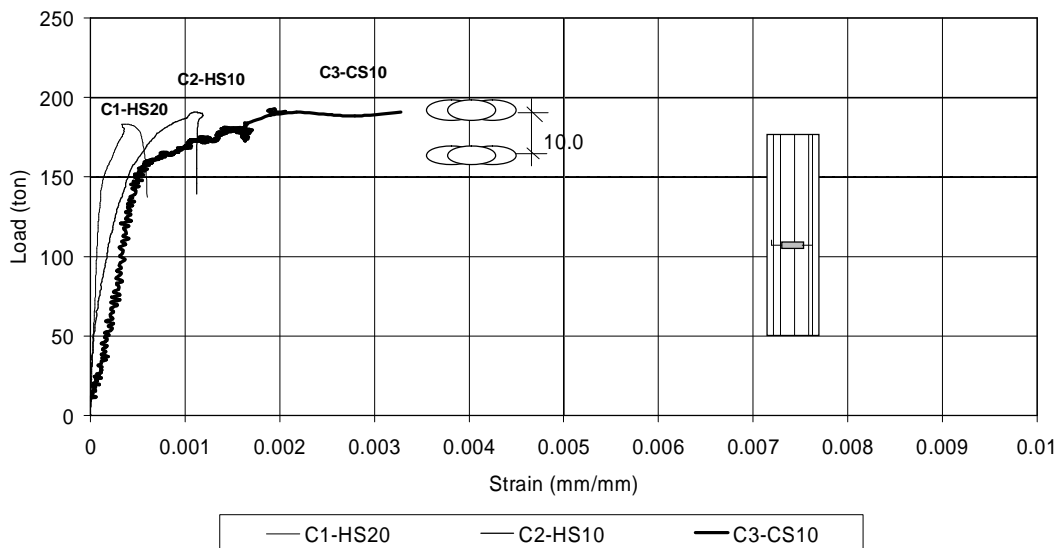


Fig. 4: Column Axial Load versus Average Concrete Horizontal Strain for Columns Laterally Reinforced by Steel Stirrups

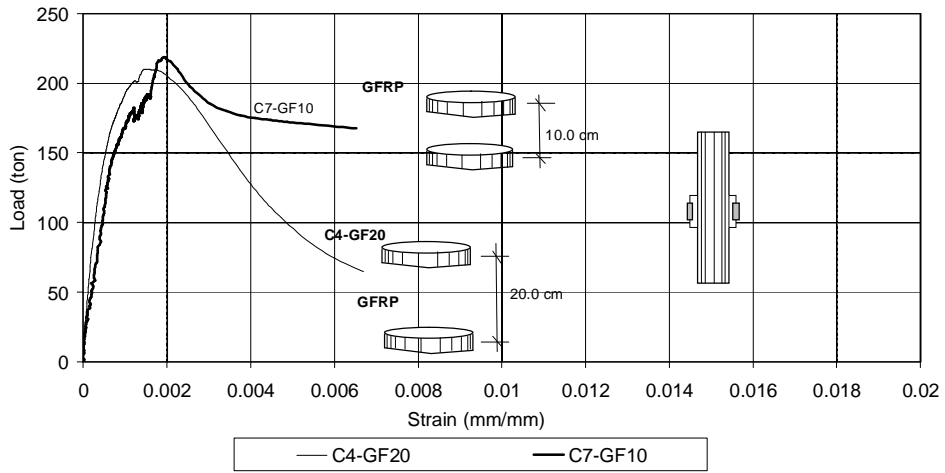


Fig. 5: Column Axial Load versus Average Concrete Vertical Strain for Columns Laterally Reinforced by GFRB Slices (Effect of Spacing between Slices)

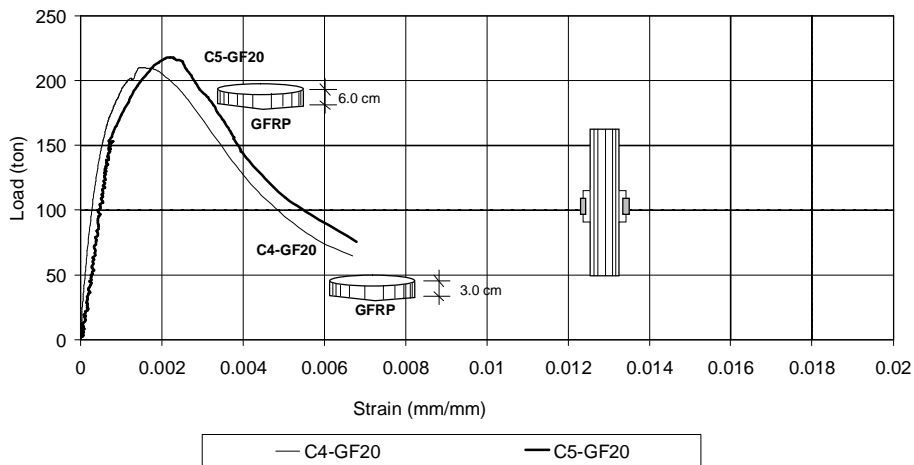


Fig. 6: Column Axial Load versus Average Concrete Vertical Strain for Columns Laterally Reinforced by GFRB Slices (Effect of Slice Width – Slice Spacing 20 cm)

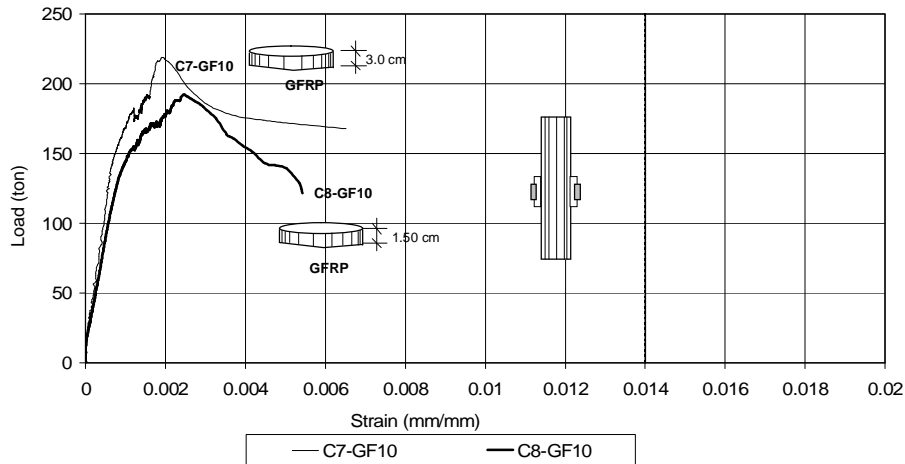


Fig. 7: Column Axial Load versus Average Concrete Vertical Strain for Columns Laterally Reinforced by GFRB Slices (Effect of Slice Width – Slice Spacing 10 cm)

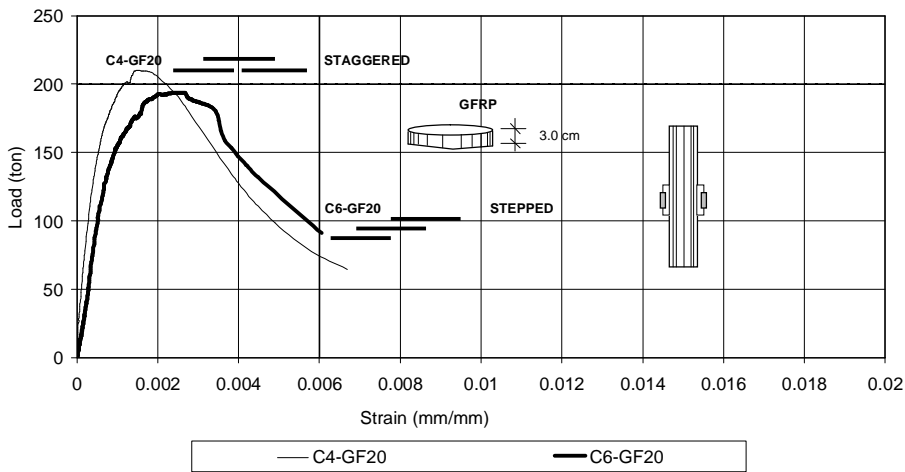


Fig. 8: Column Axial Load versus Average Concrete Vertical Strain for Columns Laterally Reinforced by GFRB Slices (Effect of Horizontal Alignment - Slice Width 20 cm – Slice Spacing 3.0 cm)

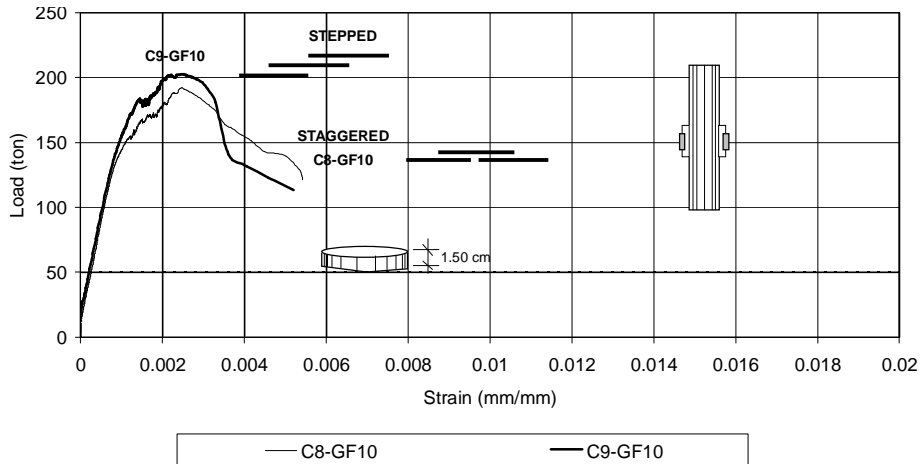


Fig. 9: Column Axial Load versus Average Concrete Vertical Strain for Columns Laterally Reinforced by GFRB Slices (Effect of Horizontal Alignment - Slice Width 10 cm – Slice Spacing 1.5 cm)

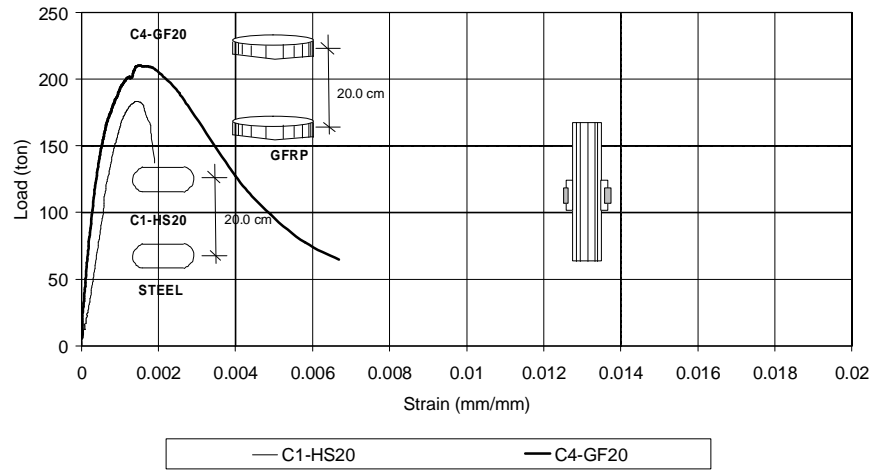


Fig. 10: Column Axial Load versus Average Concrete Vertical Strain (Comparison between GFRB and Steel Stirrups Spaced at 20 cm)

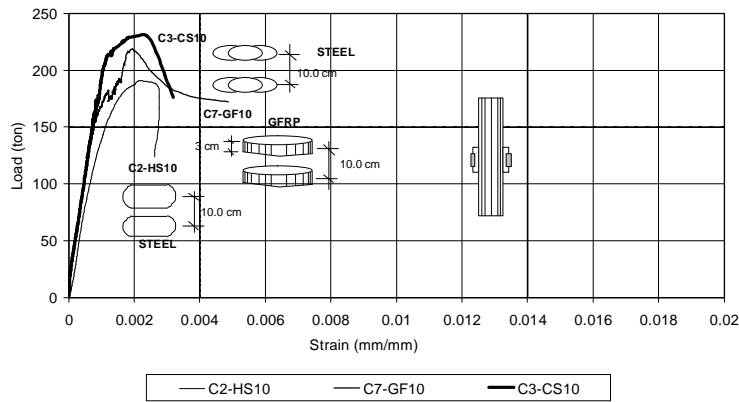


Fig. 11: Column Axial Load versus Average Concrete Vertical Strain (Comparison between GFRB Slice of Width 3.0 cm and Steel Stirrups Spaced at 10 cm)

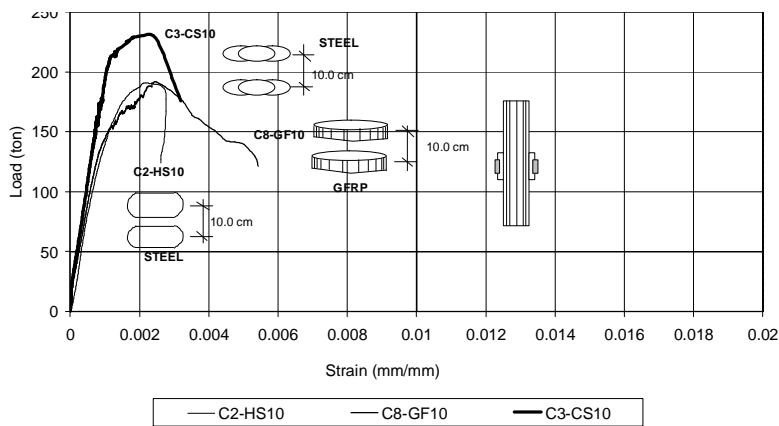


Fig. 12: Column Axial Load versus Average Concrete Vertical Strain (Comparison between GFRB Slice of Width 1.5 cm and Steel Stirrups Spaced at 10 cm)



Photo (5) Mode of failure of column
C1-HS20

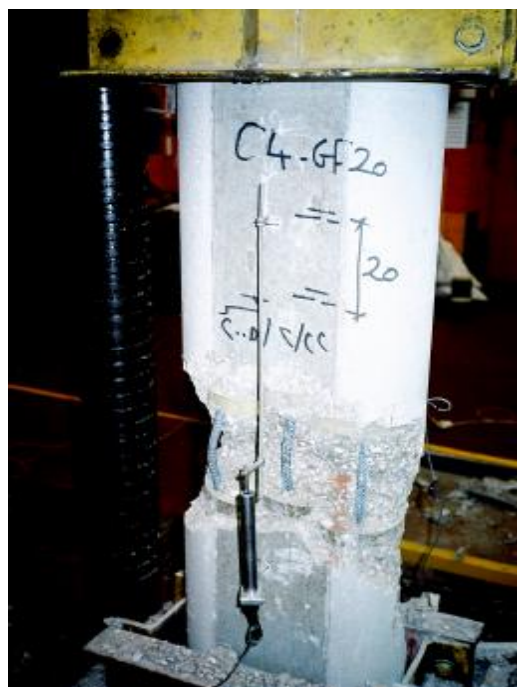


Photo (6) Mode of failure of column
C4-GF20



Photo (7) Mode of failure of column
C7-GF10



Photo (8) Mode of failure of column
C8-GF10

THEORETICAL EVALUATION OF EXPERIMENTAL RESULTS

The purpose of this part of the study is to compare the experimental ultimate loads of the tested columns with that predicated based on the Egyptian code for the design and construction of concrete structures (ECCS 203-2001).

The Egyptian Code gives the following equation to calculate the axial load carrying capacity of compression members:

$$P_{u1} = 0.35 f_{cu} \cdot A_c + 0.67 f_y \cdot A_s \quad \text{Eq.3}$$

Where:

f_{cu} = Compression strength of plain concrete as measured from standard cubes

A_c = Gross area of column section

A_s = Area of longitudinal steel.

f_y = Yield strength of longitudinal steel

The above equation was driven from the formula:

$$P_{u1} = \left(\frac{0.85 \cdot (0.8 \cdot f_{cu}) \cdot A_c}{\gamma_c} + \frac{f_y \cdot A_s}{\gamma_s} \right) / 1.1 \quad \text{Eq.4}$$

Where:

γ_c = The concrete strength reduction factor, which is equal to 1.75 according to Eq. 3-16-a of the code.

γ_s = Steel strength reduction factor, which is equal to 1.34 according to Eq. 3-16-b of the code.

1.1 = Constant value accounts for minimum eccentricity equal to 5%.

0.8 = Correction factor correlates cylinder and cube strengths.

0.85 = A factor take into consideration effect of element shape and rate on loading.

Ignoring both steel and concrete strength reduction factors, and ignoring the factors which account for the effect of eccentricity and rate of loading, the Egyptian formula can be written as:

$$P_{u2} = 0.8 f_{cu} \cdot A_c + f_y \cdot A_s \quad \text{Eq.5}$$

Table (5) contains the values of axial load capacities using the ECCS formula (Eq.4,5) with and without strength reduction factors, the eccentricity constant factor, and element shape factor. It can be seen that, the theoretical ultimate load taking the factor of safety into consideration is 81.50 ton (P_{u1}) while this value is 171.0 ton (P_{u2}) without the strength reduction factors. The value of (P_{u1}) will be used as a reference of the theoretical ultimate load in the following discussions.

- 1- If the single hoops were used as lateral reinforcement, the experimental ultimate loads of columns C1-HS20 and C2-HS10 were higher than the theoretical ultimate load according the Egyptian formula ($P_{u1}=81.50$ ton) by 224.5% and 234% respectively while, this percentage was significantly increased to 282% if the interlocking circular steel stirrups were used.
- 2- All columns laterally reinforced by the waste "GFRP" slices gave experimental ultimate loads higher than the theoretical value. The minimum experimental ultimate load among the tested columns was higher than the theoretical value by 234% for column C8-GF10 while the maximum percentage was 267 for column C7-GF10.
- 3- It can be noticed that, the Egyptian code formula can be safely used to predicate the working load of the columns laterally reinforced by the "GFRP" slices taking into consideration that

the "GFRP" slices of 3.0 cm width is the minimum practical width can be used and within the cross section studied through this research.

Table (5) Comparison between Experimental and theoretical ultimate loads

Column Id.	$P_{exp.}$ (ton)	P_{u1} (ton) ECCS-2001	P_{u2} (ton) ECCS-2001	$P_{exp.} / P_{u1}$	$P_{exp.} / P_{u2}$	Notes
C1 – HS20	183.0	81.5	171.0	224.5%	107%	Control column
C2 – HS10	191.0			234%	112%	
C3 – CS10	230.0			282%	134%	
C4 – GF20	210.0			258%	123%	Columns laterally reinforced by GFRP slices
C5 – GF20	210.0			258%	123%	
C6 – GF20	194.0			238%	113.5%	
C7 – GF10	218.0			267%	127%	
C8 – GF10	191.0			234%	112%	
C9 – GF10	202.0			248%	118%	

Where P_{u1} is the theoretical ultimate load taking the factor of safety into consideration
 And P_{u2} is the theoretical ultimate load without factor safety

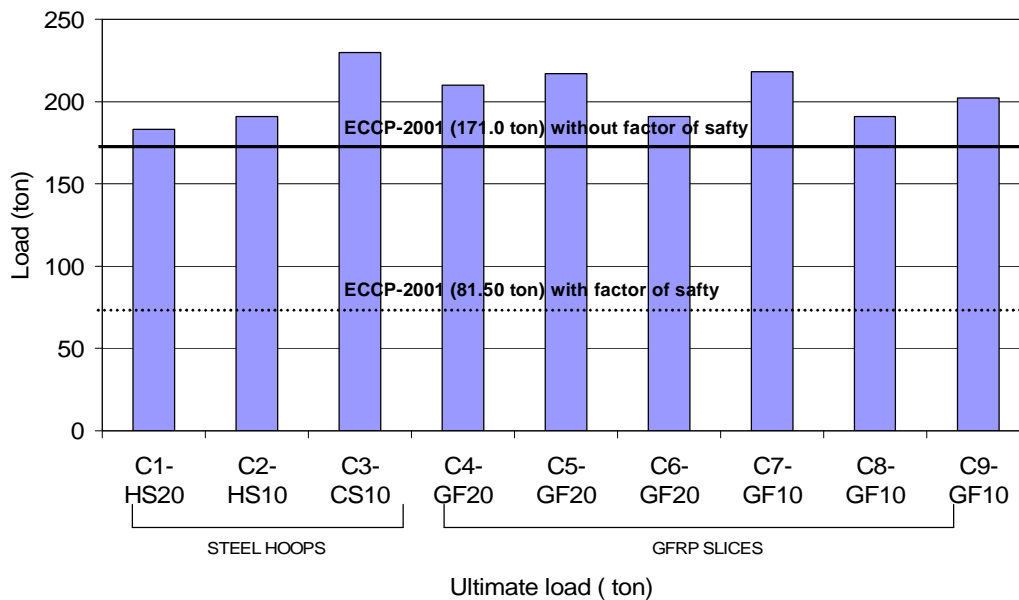


Fig. 13: Comparison between Theoretical and Experimental Capacities of the Tested Columns

CONCLUSIONS

The following conclusions can be drawn:-

- 1- Based on the experimental results, the axial behavior of columns laterally reinforced by GFRP slices are comparable to that of conventionally reinforced concrete columns, however the validity of the proposed reinforcement technique needs additional research work.
- 2- From ductility point of view, columns reinforced by the interlocking "GFRP" slices showed pronounced better behavior if compared with columns conventionally reinforced by either single hoops or interlocking circular steel stirrups.

- 3- The horizontal alignment of the interlocking "GFRP" slices did not significantly affect the behavior. Although staggered alignment is much more convenient from the fabrication point of view.
- 4- Decreasing the spacing between the interlocking "GFRP" slices improve the overall axial behavior of the "GFRP" laterally reinforced columns. This finding is in line with the known literature of conventionally reinforced concrete columns.
- 5- The formula of Egyptian code of concrete structure for calculating the ultimate loads of axially loaded reinforced concrete columns can be used with accepted factor of safety to predict the ultimate load of columns laterally reinforced by the "GFRP" interlocking slices. Additional future investigations are needed to verify this conclusion for columns having higher cross sectional aspect ratio.
- 6- Future research efforts are required to study the durability of the proposed reinforcement technique in all severe environments.

ACKNOWLEDGEMENT

I am highly appreciating the direct support from Future Pipe Industries Company (FPI). Grateful thanks to the staff of material laboratory, Housing and Building National Research Center (HBRC) in Egypt, for their hard effort through the experimental work of the National study. Great appreciations to *Eng. Wael Hassan* from (HBRC) for the effort he has done through the final stage of the study.

REFERENCES

1. ASTM D 2290 – 92: "Standard Test Method for Apparent Tensile Strength of Ring or Tubular Plastics and Reinforced Plastics by Split Disk Method"
2. ECCS 203 – 2001: "Egyptian Code for the Design and Construction of Concrete Structures," Housing and Building Research Center, Egypt.
3. Khaloo, A. R., El-Dash, K. M., Ahmed, S. H., 1999: "Model for Lightweight Concrete Columns Confined by Either Single Hoops or Interlocking Double Spirals," ACI Structural Journal, V. 96, No. 6, pp. 883-890.
4. MOSSALLAM, A. I., 1999: "Confinement Effectiveness of Axially Loaded Concrete Members Confined by Lateral Reinforcement," M.SC Thesis, Faculty of Engineering, Cairo University, Egypt.
5. SAYED, M. S., 2005: "Recycling of Factory Rejected GFRP Pipes as Transverse Reinforcement For Reinforced Concrete Short Circular Columns," Proceeding of The Forth Middle East Symposium For Composite Materials in Infrastructure Applications, Alexandria, Egypt.
6. SCOTT, B. D., PARK, R., PRIESTLEY, M. J. N., 1982: "Stress-Strain Behavior of Concrete confined by Overlapping Hoops at Low and High Strain Rates," ACI Structural Journal, V. 79, No. 1, pp. 13-27
7. Sheikh, S., Toklucu, 1993: "Reinforced Concrete Columns Confined by Circular Spirals and Hoops," ACI Structural Journal, V. 90, No. 5, pp 542-553.
8. TOUTNJI, H., SAAFI, M., 2002: "Stress-Strain Behavior of Concrete Columns Confined with Hybrid Composite Materials," Materials and Structures, V. 35, pp. 338-347.
9. Wang et al., 1978: "Stress-Strain Curves of Normal and Lightweight Concrete in Compression," ACI Structural Journal, V. 75, No. 11, pp. 603-611.

STATISTICAL ASSESSMENT OF STRENGTH ACCEPTANCE CRITERIA IN THE EGYPTIAN CODE OF PRACTICE

M. M. El Attar, H. H. Abo Ghanima, and O. A. Hodhod
Structural Engineering Department, Cairo University, Giza, EGYPT

ABSTRACT

In this paper, a review of the statistical basis for analyzing the results of strength tests and their relation to the strength of the whole production is given. The paper also, presented and discussed the strength acceptance criteria in the ECP, BS, and ACI codes. The statistical interpretations of these criteria and the observed deficiencies in them have been highlighted. A parametric study on the effects of sample standard deviation, sample size, probability of type (I) error and acceptable percentage of low test results on the required concrete sample average compressive test result have been conducted. Based on the performed parametric study and the highlighted deficiencies in the current ECP strength acceptance criteria, the authors have proposed new criteria for accepting reinforced and plain concrete strength test results.

Keywords: statistics, strength test, acceptance criteria, Egyptian code

INTRODUCTION

Concrete quality is generally assessed by measuring its cube (or cylinder) compressive strength. Variability of cube (or cylinder) strength is a stochastic process that urges the use of statistical methods to arrive at a reasonable estimation of the mean strength of the whole production based on the strength test results of limited, and most frequently, isolated samples. The concrete strength acceptance criteria in the Egyptian Code of Concrete Design and Construction Practice (ECP) have evolved from the 1970 version to the 1990 version trying to provide more stringent acceptance criteria, nevertheless, the statistical basis behind them are not clear (El-Desoky, 2000 and Abo Ghanima, 2005).

In the ECP (1990) and ECCS-203 (2001) it was stated that concrete is deemed conforming if:

- 1- For strength test results less than 20; no test result is allowed to be less than the characteristic strength AND the difference between maximum and minimum test results is not allowed to exceed 25% of the average crushing test result.
- 2- For test results greater than 20; for every 20 test results one test result is allowed to be less than the characteristic strength by 15% AND the difference between the maximum and minimum test results is not allowed to exceed 25% of the average crushing test result.

Taerwe (1991) indicated that many international codes and standards such as ISO, Czech and Yugoslav codes adopt strength acceptance criterion in the form of:

$$f_{cu} + \delta f_{cu} \quad (1)$$

In this paper, the authors give a general background of the statistical basis behind acceptance rules of concrete strength; apply general statistics rules to the problem of estimating the mean value of concrete strength from the measured values of samples of different sizes. The authors, also, study the effects of "within sample variability" on the acceptance rules. Finally, and based on the performed investigation, the authors propose not only, statistically-conforming strength acceptance criteria but Egyptian practice and legislative conforming as well.

METHODOLOGY

In order to achieve the objectives of the study, the statistical basis of the conditions of strength acceptance in the British, ACI and Egyptian codes is investigated by studying each variable in their specified concrete strength acceptance criteria. The statistical parameters of compressive strength of a concrete sample with specified number of specimens are statistically related to the corresponding compressive strength parameters of the whole production. The statistical procedure of hypothesis testing is one suitable approach for establishing the relation between the statistical parameters of the sample and those of the population. In this investigation, the left tail hypothesis test is the most appropriate method to be used in the statistical analysis since the null hypothesis is $\mu \geq \mu_0$ (i.e. average strength test results \geq target strength). (Abo Ghanima, 2005)

Left-Tailed Hypothesis Test of Population Mean

The systematic steps to perform a left-tailed hypothesis test are as follows: (Bowers, 1990)

- i) Set the value (μ_0) in the null hypothesis which indicates the hypothesized population mean;
- ii) Choose a value for the probability of Type (I) error (α), which is the probability of wrongly rejecting a good lot by the sampling plan. This probability indicates the producer's risk (usually taken one of these values 0.01, 0.05, or 0.10);
- iii) Determine the corresponding value of ($t_{n-1, \alpha}$) from the "student's t" table, (n is the sample size);
- iv) Use the sample mean \bar{X} , sample variance s^2 and hypothesized μ_0 values to calculate the value of the standardized test statistic $(\bar{X} - \mu_0) / \sqrt{(s^2 / n)}$
- v) The decision rule is then:

Decision rule for left-tailed hypothesis test of $H_0: \mu \geq \mu_0$ against $H_1: \mu < \mu_0$ accept H_0 if $(\bar{X} - \mu_0) / \sqrt{(s^2 / n)} \geq t_{n-1, \alpha}$ reject H_0 otherwise

ANALYSIS

In this study, the statistical problem is formulated as follows: there exist a number of randomly selected concrete test specimens. The individual compressive strength values have been obtained from a proper compressive strength test. The average strength (\bar{X}) and standard deviation (s) of this sample have been calculated. It is required to check whether this sample represents a population that has a mean strength of ($\mu_0 = f_{target}$) or not. It should be noted that

$$f_{target} = f_{cu} + k \sigma \tag{2}$$

Where,

f_{cu} = characteristic strength

k = constant depending on the acceptable percentage of low tests

σ = population standard deviation

To check this hypothesis in a left-tailed test, the problem takes the form:

$$H_0 : \mu \geq \mu_0 \tag{3} \text{ null hypothesis}$$

$$H_1 : \mu < \mu_0 \tag{4} \text{ alternate hypothesis}$$

The test statistic is calculated as follows:

$$(\bar{X} - \mu_0) / \sqrt{(s^2 / n)} = (\bar{X} - f_{target}) / \sqrt{(s^2 / n)} \tag{5}$$

Then the student's t value is obtained for the different probabilities of type (I) error, (α) and the sample size ($t_{n-1, \alpha}$). Performing the required mathematical manipulation, the hypothesis acceptance condition is now put in the form:

$$X \geq f_{cu} + s [k + (t_{n-1, \alpha}) / \sqrt{n}] \tag{6}$$

i.e. $X \geq f_{cu} + \delta f_{cu} \tag{7}$

It is evident that δf_{cu} is a function of the sample size, error (I) probability, acceptable percentage of low test results, and the dispersion of the test results. The values of δf_{cu} have been calculated for $(\alpha) = (0.01, 0.05, 0.10)$ because these are the most commonly used values. Sample sizes have been varied between 2 and 8 to cover the recommended sample sizes in the studied codes. The standard deviation values have been varied between 10 and 80 kg/cm² to cover a wide range of quality control levels (excellent to poor) as this range of standard deviation is quite wide to cover practical values. Tables 1 to 3 give the numerical results of the study while Figures 1 to 3 are graphical depictions of the results.

As shown in Equation (6), there is a linear relation between the standard deviation of the sample and δf_{cu} (for specified n , α) which is illustrated in Figs 4 to 6.

It is also evident that increasing the sample size (in case the same standard deviation is maintained) will lead to higher δf_{cu} . This is logical conclusion since it means that the data dispersion of the large sample is closer to the actual value of the population and the test tends to reject a larger number of tests although they are conforming to the hypothesis. In this case, it is of utmost importance to properly specify the sample size (Bowers, 1990). In this adopted statistical hypothesis testing approach, a sample of 2 cubes only is not suitable since the value of δf_{cu} is negative. Consequently, the minimum sample size that can be taken is (3). It is also, intuitive, that increasing the sample size should decrease its standard deviation and hence it should lead to smaller value of δf_{cu} . In addition, it can be noticed that as the probability of committing error type (I) increases, δf_{cu} decreases. This logical conclusion is understood because if the percentage of low tests is minimized, the average strength of the cubes of the project must be increased (δf_{cu} for $\alpha = 0.01 > \delta f_{cu}$ for $\alpha = 0.05 > \delta f_{cu}$ for $\alpha = 0.10$).

DISCUSSION

Egyptian Code of Practice Compliance Requirements

The Egyptian code indicates that concrete strength is deemed conforming if:

- 1- For strength test results less than 20; no test result is allowed to be less than the characteristic strength AND the difference between maximum and minimum test results is not allowed to exceed 25% of the average crushing test result.
- 2- For test results greater than 20; for every 20 test results one test result is allowed to be less than the characteristic strength by 15% AND the difference between the maximum and minimum test results is not allowed to exceed 25% of the average crushing test result.

British Standard Compliance Requirements

British standard (BS 5328) indicates concrete mix is safe if:

- 1) average crushing strength for the first two tests or first three tests or any four consecutive tests must satisfy the limits in Table 4
- 2) no crushing strength test is less than the characteristic strength by certain limits indicated in Table 4

American Concrete Institute's Strength Requirements

The concrete producer must provide a strength that is higher than the specified strength, called the required average strength f_{cr} . The required average strength can be determined from the following formula:

$$f_{cr} = f_c + p_s$$

Where:

f_{cr} = required average strength, psi

f_c = specified strength, psi

p = probability factor based on the percentage of tests the designer will allow to fall below f_c

s = expected standard deviation for the project, ψ

Table 5 lists criteria for selecting different probability factors based upon the risk if the concrete strength falls below the specified strength [ACI 214, 1997].

Deficiencies of the Egyptian Acceptance Criteria

The Egyptian code of practice has created a very difficult to achieve acceptance criteria as pointed out by (El-Desoky, 2000) and (Ali, 2004). The statistical analysis of the set conditions for accepting the strength test results shows that:

- 1- The definition of test result is not clearly given
- 2- For the first 20 tests, no test result should go below f_{cu} and the difference between the highest and the lowest results should not exceed 25% of the average. This means that the standard deviation of the results is assumed around 10% of the characteristic strength. This is a low value given the concrete production conditions in most projects which are still semi manual operation with little control on mix constituents. The collected test results show great variations of test results for the same project and the same concrete manufacturer. An acceptance criterion that takes into account this reality is much more appropriate.
- 3- The producer's and consumer's risks associated with the current criteria are not defined.

As demonstrated in section 4.3, the ACI code has related the accepted concrete strength to the specified concrete characteristic strength and the standard deviation of the test results. Although, this is a very sound approach from statistics point of view, it is more demanding computationally.

In section 4-6, a proposal for suitable strength acceptance criteria will be given.

Interpretation of the British Acceptance Criteria

The basic deficiency of the British acceptance criteria is the lack of controlling the sample standard deviation and/or strength dispersion. This deficiency creates some statistically unacceptable situations such as shown in the following example:

Four test specimens which represent an extreme case of very poor quality control (where a strength test in BS is the average of two compressive test results) have the following strength values: 190 kg/cm², 250 kg/cm², 200 kg/cm², 400 kg/cm². The test results are; 220 kg/cm², 300 kg/cm². The average of the two tests is which exceeds $f_{cu} = 250$ kg/cm² by 10 kg/cm² as required and the minimum test result is less than f_{cu} by only 30 kg/cm² also as required. In this case it is acceptable by the British code. However, statistical analysis shows for sample size of 4 and the standard deviation of these results which is 96 kg/cm² the average sample strength should exceed the characteristic strength by 40 kg. It should be noted that such problem would have not risen if it is expected that the concrete production is under the proper quality control. It is also evident that, the British acceptance criteria have not been related to the value of the characteristic concrete strength, i.e. characteristic strengths between 200 kg/cm² and 400 kg/cm² are alike.

Recommendations for Strength Acceptance in the Egyptian Code of Practice

Conditions of the British code can be used to conclude suitable conditions for the Egyptian code since the probability of low tests in both of them is 0.05. Since a test result in the British Standard is the average of two cubes, hence we can conclude from Table 2 that the condition of exceeding the first two test results f_{cu} by 10 kg/cm² is taken with $n = 4$ and $s = 22$ kg/cm². The condition of exceeding the first three test results f_{cu} by 20 kg/cm² is taken with $n = 6$ and $s = 25$ kg/cm². The condition of exceeding any four test results f_{cu} by 30 kg/cm² is taken with $n = 8$ and $s = 30$ kg/cm². i.e. increases standard deviation as the sample size increases. But these conditions cannot be taken for the Egyptian Code of Practice because the standard deviation in Egypt is expected to be much greater than England since there is no good control in concrete production in Egypt as England.

New conditions based on statistical basis as other codes are recommended. Also, conditions for reinforced concrete and plain concrete will be recommended since strength in plain concrete is of minor consequence in design. In Egypt the unit of counting cubes is 3, so the value of δf_{cu} for $\alpha = 0.05$, $n = 6$ and $s = 60 \text{ kg/cm}^2$ which is double the standard deviation for the British Standard is taken in reinforced concrete conditions. The value of δf_{cu} for $n = 3$, $\alpha = 0.10$ and $s = 60 \text{ kg/cm}^2$ will be taken in plain concrete conditions.

CONCLUSIONS

In this paper, a review of the statistical basis for analyzing the results of strength tests and their relation to the strength of the whole production is given. The paper also, presented and discussed the strength acceptance criteria in the ECCS-203, BS, and ACI codes. The statistical interpretations of these criteria and the observed deficiencies in them have been highlighted. A parametric study on the effects of sample standard deviation, sample size, probability of type (I) error and acceptable percentage of low test results on the required concrete sample average compressive test result have been conducted. Based on the performed parametric study and the highlighted deficiencies in the current ECCS-203 strength acceptance criteria, the authors have proposed new criteria for accepting concrete strength test results as follows:

Recommended Strength Acceptance Criterion for Reinforced Concrete Strength Test Results:

- a) No less than 3 test cubes should be used in estimating concrete strength,
- b) The average strength of the tested cubes taken from concrete elements in the project should exceed the characteristic strength by 50 kg/cm^2 .

Recommended Strength Acceptance Criterion for Plain Concrete Strength Test Results:

- a) No less than 3 test cubes should be used in estimating concrete strength,
- b) The average strength of the tested cubes taken from concrete elements in the project should exceed the characteristic strength by 15 kg/cm^2 .

These recommendations are valid for small number of test results. However, they are conservative for larger number of test results.

REFERENCES

1. Abo Ghanima, H. H., "A Comprehensive Knowledge-Based System for Quality Control of Concrete Manufacturing", MSc thesis, Structural Eng. Dept., Cairo University, 2005.
2. ACI 214, "Simplified Version of the Recommended Practice for Evaluation of Strength Test Results of Concrete", 1997.
3. Ali, M. S., "Quality Control of Concrete in Small Projects and Effect of Variability of its Constituents", MSc thesis, Structural Eng. Dept., Cairo University, 2004.
4. Bowers, D., "Statistics for Economics and Business", pp. 107 – 160, 1990.
5. BS 5328, "Specification for the Procedures to be used in Sampling, Testing and Assessing Compliance of Concrete", 1990.
6. ECCS-203, "Egyptian Code of Practice for Design and Construction of Concrete Structures", 2001.
7. ECP, "Egyptian Code of Practice for Design and Construction of Concrete Structures", 1990.
8. El-Desoky, S. A., "Criteria for Specifying Quality Requirements for Concrete to Comply with the Characteristic Strength", Engineering & Practical Sciences Magazine, August 2000.
9. Holicky, M.; and Vorlicek, M.; "Draft of an ISO-Standard on Statistical Quality Control", in "Quality Control of Concrete Structures", Taerwe and Lambotte eds., June 12-14, Ghent, Belgium, 1991.

10. Mikulic, D., Pause, Z., and Skenderovic, A.; "Quality Control and Acceptance Criteria for Concrete and Its Ingredients (Yugoslav Experience)", in "Quality Control of Concrete Structures", Taerwe and Lambotte eds., June 12-14, Ghent, Belgium, 1991.
11. Taerwe, L.; "Basic Concepts for Conformity Control of Concrete", in "Quality Control of Concrete Structures", Taerwe and Lambotte eds., June 12-14, Ghent, Belgium, 1991.

Table 1: Values of $d f_{cu}$ for Different Sample Sizes “n” and Strength Standard Deviations “s” (a = 0.01 and k = 2.32)

n	2	3	4	5	6	7	8
s (kg/cm²)	$d f_{cu}$ (kg/cm²)						
10	-201.8	-17.01	0.5	6.44	9.46	11.32	12.6
20	-403.6	-34.02	0.99	12.89	18.93	22.64	25.2
30	-605.42	-51.03	1.49	19.33	28.39	33.97	37.8
40	-807.2	-68.04	1.99	25.77	37.85	45.28	50.4
60	-1210.95	-102.06	2.98	38.67	56.76	67.92	75.6
80	-1614.5	-136.09	3.97	51.54	75.7	90.56	100.8

Table 2: Values of $d f_{cu}$ for Different Sample Sizes “n” and Strength Standard Deviations “s” (a = 0.05 and k = 1.64)

n	2	3	4	5	6	7	8
s (kg/cm²)	$d f_{cu}$ (kg/cm²)						
10	-28.24	-0.46	4.63	6.87	8.17	9.06	9.7
20	-56.49	-0.92	9.27	13.73	16.35	18.11	19.4
30	-84.74	-1.38	13.9	20.6	24.52	27.17	29.1
40	-113	-1.83	18.53	27.47	32.7	36.24	38.8
60	-169.47	-2.75	27.8	41.2	49	54.36	58.2
80	-225.96	-3.67	37.06	54.93	65.39	72.48	77.6

Table 3: Values of $d f_{cu}$ for Different Sample Sizes “n” and Strength Standard Deviations “s” ($\alpha = 0.10$ and $k = 1.28$)

n	2	3	4	5	6	7	8
s (kg/cm²)	$d f_{cu}$ (kg/cm²)						
10	-8.96	1.91	4.61	5.49	6.77	7.36	7.8
20	-17.93	3.83	9.22	11.89	13.55	14.72	15.6
30	-26.89	5.74	13.83	17.83	20.32	22.08	23.4
40	-35.85	7.65	18.45	23.77	27.1	29.44	31.2
60	-53.79	11.48	27.67	35.66	40.64	44.16	46.8
80	-71.71	15.3	36.89	47.54	54.2	58.88	62.4

Table 4: Requirements of Satisfaction of the Characteristic Strength According To British Standard BS 5328

Characteristic Strength(Kg/cm ²)	Test Results	Minimum Limit For Average Crushing Test To Exceed The Characteristic Strength (Kg/cm ²)	Maximum Allowable Limit For Any Test Result To Be Less Than The Characteristic Strength (Kg/cm ²)
200 OR MORE	FIRST TWO RESULTS	10	30
	FIRST THREE RESULTS	20	30
	ANY FOUR CONSECUTIVE TESTS	30	30

Table 5: Recommendations for ρ_s to Be Used In Computing the Required Average Strength Based On Critical Nature of Strength of Concrete

Type Of Structural Member	Probability Of Low Tests	Recommended Values For ρ_s For Computing Required Average Strength ($f_{cr} = f_c + \rho_s$)
Strength is critical (main element; column or main girder or prestressed concrete)	1 in 100	2.32s
Strength below f_c is not critical but a test below $f_c - 25$ is critical (secondary element)	Variable	2.32s - 25 kg/cm ²
Strength of concrete is of minor consequence in design (plain concrete)	1 in 5	0.8s

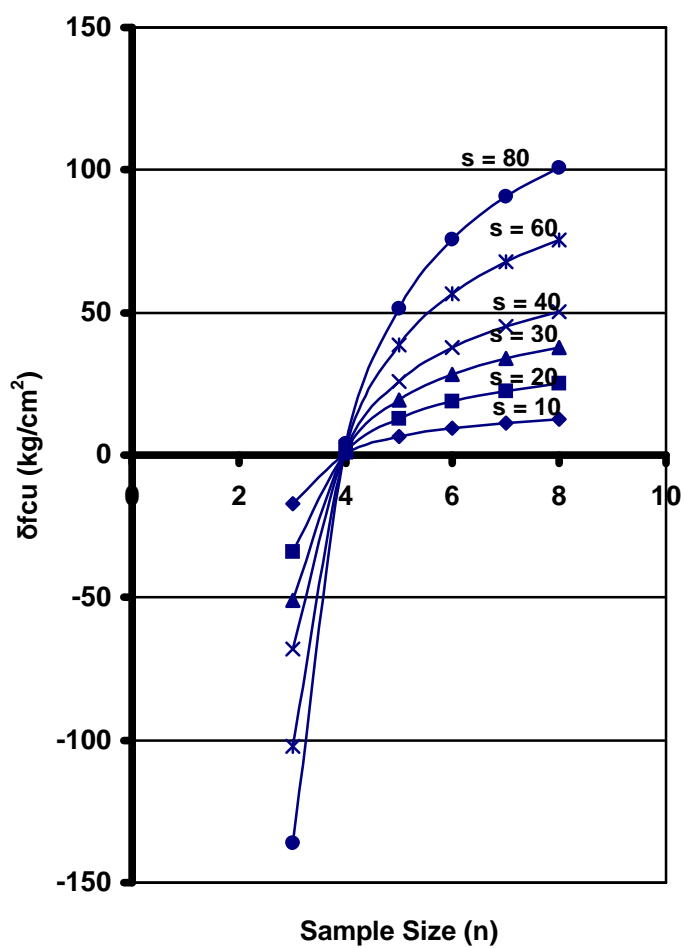


Fig. 1: Effect of sample Size (n) on δf_{cu} ,
 ($\alpha = 0.01$ and $k = 2.32$)

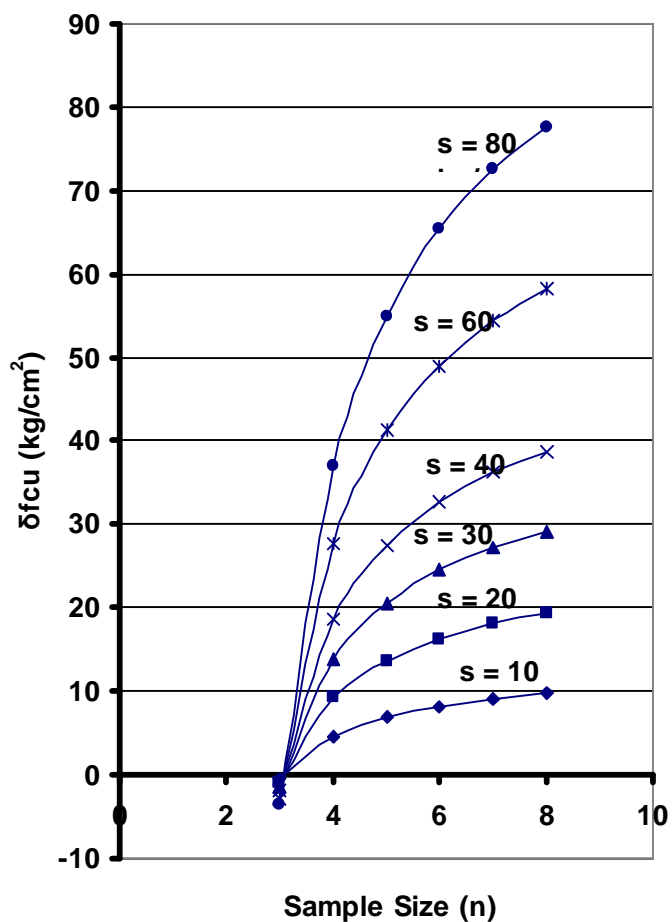


Fig. 2: Effect of sample Size (n) on $d f_{cu}$,
 ($\alpha = 0.05$ and $k = 1.64$)

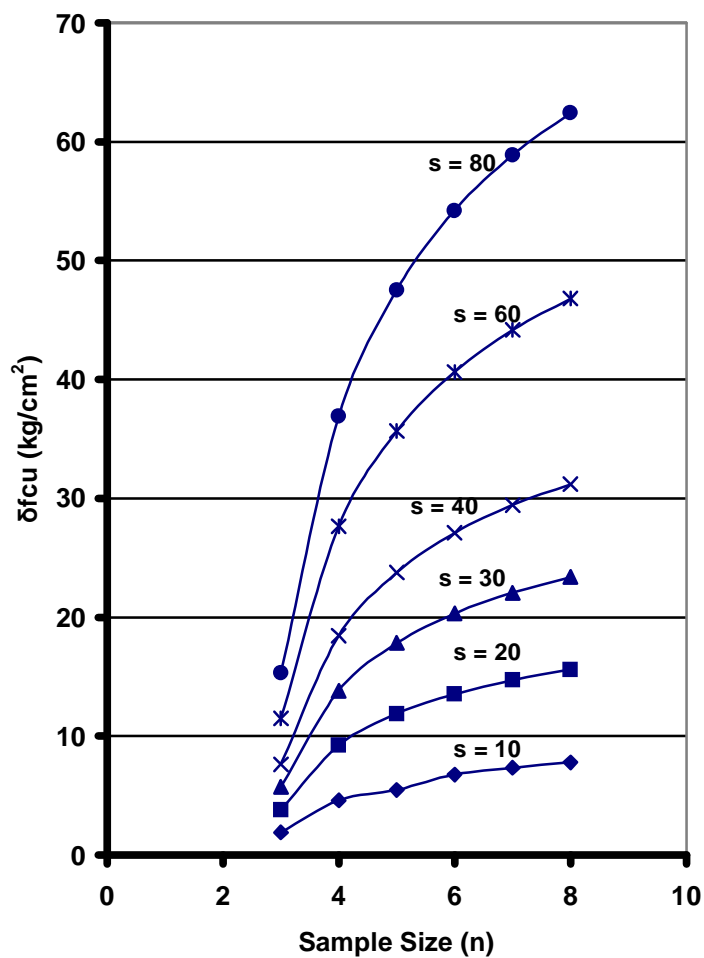


Fig. 3: Effect of sample Size (n) on δf_{cu} ,
 ($\alpha = 0.10$ and $k = 1.28$)

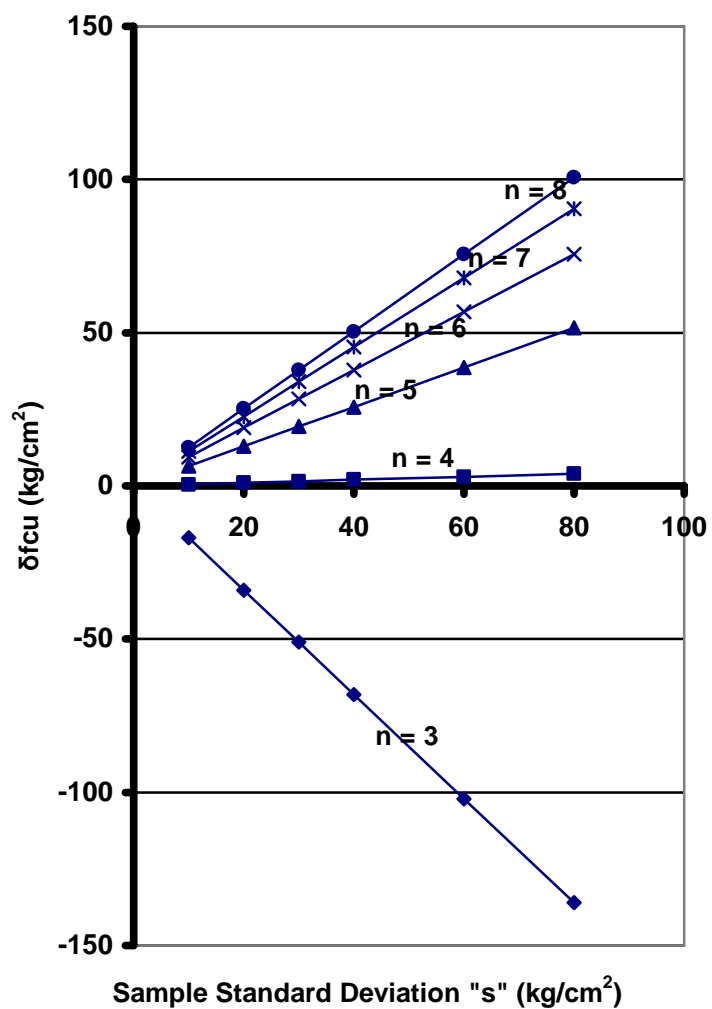


Fig. 4: Effect of Sample Standard Deviation "s" on δf_{cu}
($\alpha = 0.01$ and $k = 2.32$)

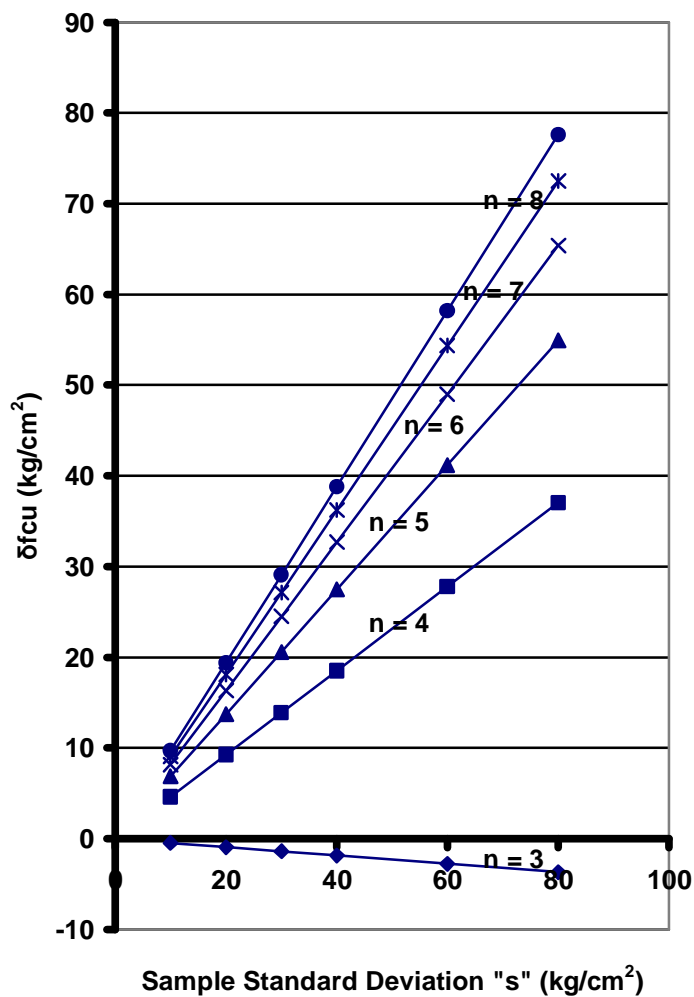


Fig. 5: Effect of Sample Standard Deviation "s" on $d f_{cu}$ ($\alpha = 0.05$ and $k = 1.64$)

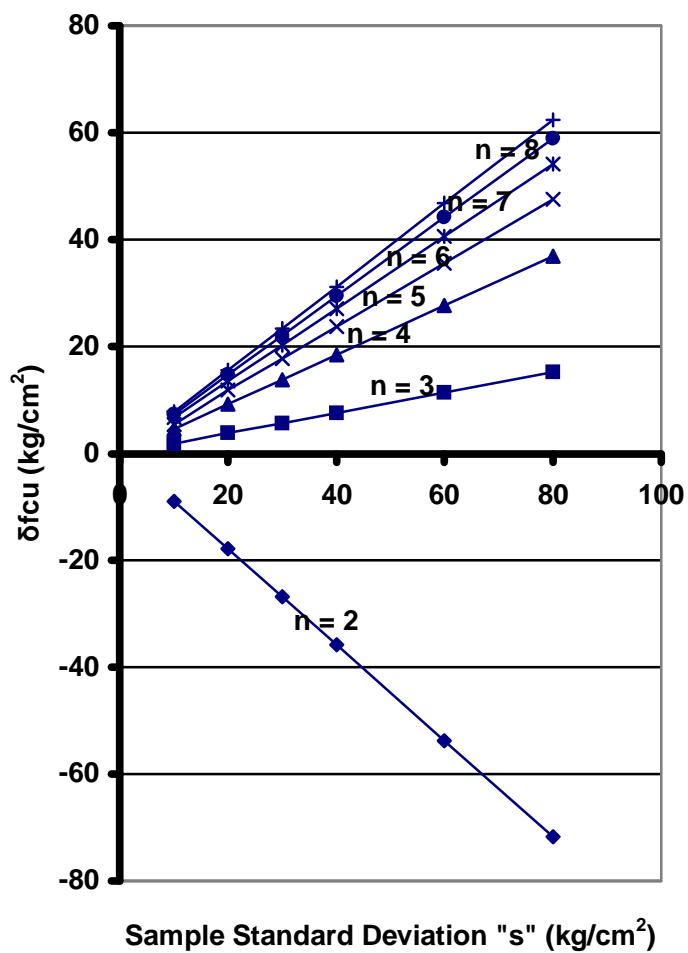


Fig. 6: Effect of Sample Standard Deviation “s” on Δf_{cu} ($\alpha = 0.10$ and $k = 1.28$)

TORSIONAL CAPACITY OF REINFORCED CONCRETE COLUMNS

Y. M. Hussein

Researcher, Reinforced Concrete Dept., Housing and Building National Research Center

ABSTRACT

Concrete columns in buildings may be subjected to torsional moments under the effect of lateral loads, especially when both the building and the columns shapes are irregular. In bridges, due to the bridge alignment or unsymmetrical breaking forces the columns are subjected to torsional moments. An experimental and theoretical study was conducted to evaluate the torsional capacity of concrete columns. The test program included eight normal strength concrete columns applied to torsion. The experimental tests were executed at Reinforced Concrete Laboratory in Housing and Building Research Center. Two columns had square cross sections and the other six columns had L-shape cross sections. The studied parameters were the shape of column section, the amount of lateral reinforcement, and the level of axial load. The tested specimens were aligned horizontally and subjected to the required level of axial load, then, pure torsional moment was subjected through two concrete arms. The test results are discussed and analyzed to evaluate the torsional capacity of both the square and L-shape concrete columns. In the theoretical study, a space truss model which considers concrete softening was modified to include the effect of the axial load. A computer program based on the modified model was adapted to predict the columns torsional capacity.

KEYWORDS: reinforced concrete columns, torsional capacity, space truss model

INTRODUCTION

Torsional moments can be separated into two basic categories, compatibility torsion and equilibrium torsion. Equilibrium torsion occurs when the external load has no alternate path except to be resisted by torsional resistance. However, compatibility torsion arises when torsional moment is induced from the compatibility of deformations between members meeting at a joint¹. Equilibrium torsion should be resisted by special torsional reinforcement. In bridges and irregular buildings columns may be subjected to equilibrium torsion. In the Egyptian code ECCS 203-2004² there are no special design provisions for columns subjected to torsional loading (i.e. sections subjected to combined torsion and axial force). In ACI code 318-2002³ the column torsional capacity at any axial load level is calculated based on a constant value of cracking angle. Moreover, in literature a few previous works can be found concerning the torsional capacity of reinforced concrete columns.

The objectives of this research are:

- § Study experimentally the torsional capacity of regular and irregular columns at different levels of axial load and volumetric stirrups ratios.
- § Propose a theoretical model to predict the torsional capacity of reinforced concrete columns.

EXPERIMENTAL WORK

The test program; the dimensions of tested columns; the test setup; and the test procedure are presented.

Test Program

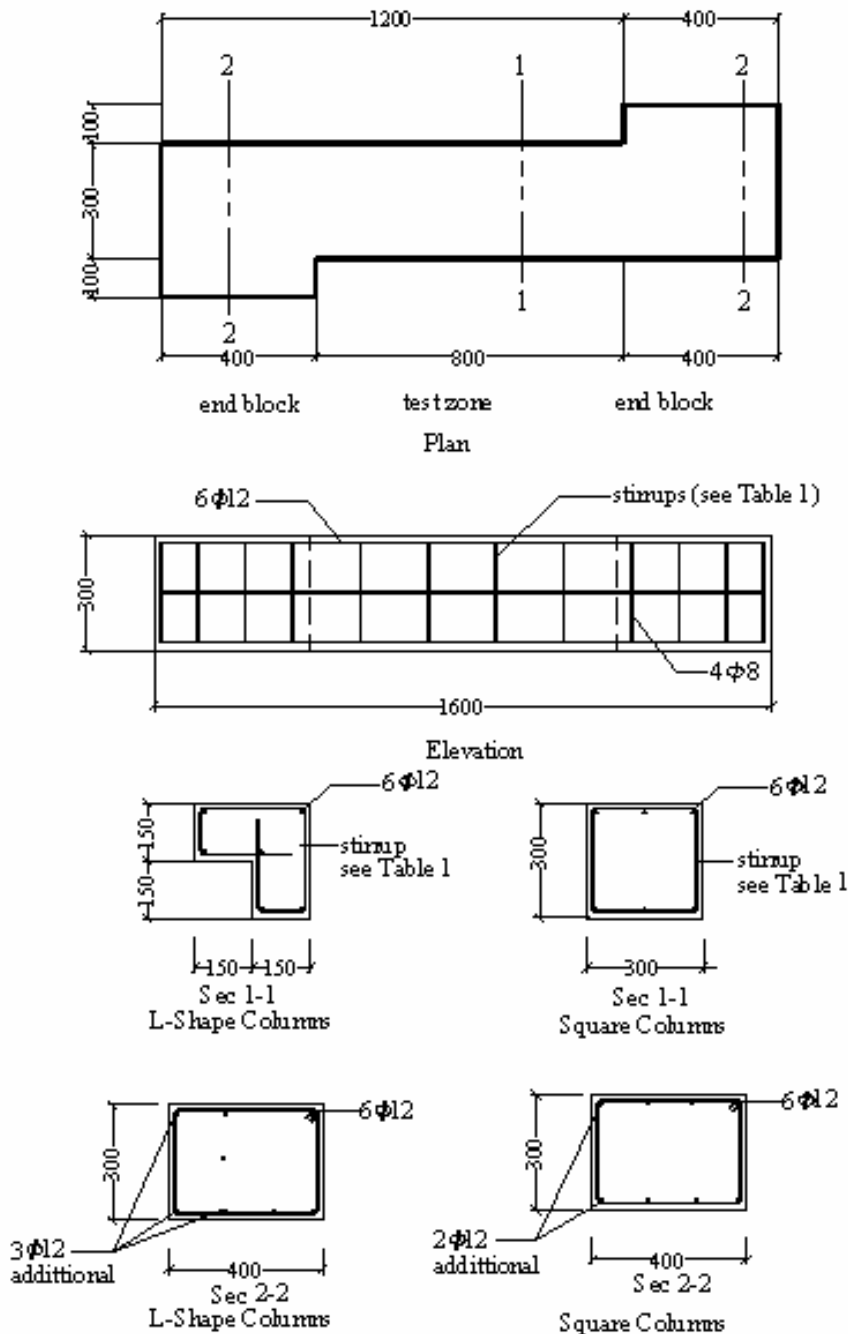
The test program included eight normal strength concrete columns. The studied parameters are: column shape, amount of lateral reinforcement, and level of axial load. The columns were divided into three groups: A, B, and C. Group A included two columns with square cross section at different values of volumetric stirrups ratios (VSR = 0.288% and 0.577%; respectively), and subjected to a constant axial load ($0.23 A_g \cdot f_{cu}$). Group B included three columns with L-cross section at different values of volumetric stirrups ratios (VSR = 0.385%, 0.770%, and 1.54%; respectively) and subjected to constant axial load ($0.28 A_g \cdot f_{cu}$). Group C included three columns with L-cross section with the same volumetric stirrups ratios as group B and subjected to different levels of axial loads (0, 0.14 $A_g \cdot f_{cu}$, and 0.42 $A_g \cdot f_{cu}$). Table 1 shows the details of the tested specimens.

Table 1: Details of Test Program

Group	Type	Cross section shape	Axial load/ $A_g \cdot f_{cu}$	Stirrups	Volumetric stirrups ratio VSR %	Concrete compressive strength f_{cu} MPa
A	C1R	Square section	0.23	Ø8/200	0.288	24.4
	C2R	Square section	0.23	Ø8/100	0.577	24.4
B	C1L	L-section	0.28	Ø8/200	0.385	26.5
	C2L	L-section	0.28	Ø8/100	0.770	26.5
	C5L	L-section	0.28	Ø8/50	1.54	26.5
C	C3L	L-section	0.0	Ø8/200	0.385	26.5
	C4L	L-section	0.14	Ø8/100	0.770	26.5
	C6L	L-section	0.42	Ø8/50	1.54	26.5

Dimensions and Details of Tested Columns

The tested columns had a length of 1600 mm divided into three zones. The middle zone was the test zone and representing the column with square or L-shape cross section. The dimensions of the column cross section in this zone are shown in Figure 1. The other two zones were the two end blocks which had skew alignment at both sides of the test zone. The longitudinal reinforcement of all the columns was 6 high grade steel bars (grade 400/600) while the lateral reinforcement in the test zone was mild steel stirrups of 8 mm diameter (grade 280/450). The spacing of stirrups was varied according to the required volumetric stirrups ratios shown in Table 1. The end blocks were reinforced with additional lateral reinforcement and external lateral strengthening in some columns to prevent premature failure of the end block.



Note: all dimensions in mm

Fig. 1: Details of Tested Columns

Test Setup

The columns were tested under a certain level of axial load while the torsional load was applied gradually up to the specimen failure. The column was aligned horizontally inside a 3000 kN closed horizontal frame and supported vertically on two concrete blocks. The axial load was applied using 1000 kN hydraulic jack equipped with 1360 kN compression load cell. Two ball hinges were mounted at the column ends to permit rotation and prevent any torsional fixation at the ends. The torsional moment was obtained by applying the reactions of a rigid steel girder at two skew positions on the middle of the column end blocks which were shifted with eccentricity 175 mm from column centerline. The steel girder was loaded at its mid span with a 1000 kN

hydraulic vertical actuator. The vertical actuator was mounted to a 4000 kN laboratory test rig to resist the upward vertical reaction. Two rotational bearings were used as vertical support at the middle of the column end blocks to permit twisting of specimen at both ends. One of these bearings was equipped with rollers to permit specimen elongation in the longitudinal direction of the column. Figure 2 shows the details of the test setup.



Fig. 2: Test setup

Testing System and Measurements

The columns were tested using a data acquisition measurement and control online computer feedback system programmed with LabView language. This system was prepared to perform displacement control tests. The following measurements sensors were used to record loads, displacements and deformations:

- § 1360 kN load cell attached to horizontal jack to measure variation of axial load
- § 680 kN load cell attached to the vertical actuator to measure vertical load
- § Four linear variable displacement transducers (LVDT) +/- 50 mm stroke mounted vertically at two opposite positions at both ends of the test zone to measure the twisting angle.
- § Two strain gages mounted on the stirrups (S1 and S2) at the middle of the test zone and two other strain gages mounted on the longitudinal reinforcement (S3 and S4).

Test Procedure

The columns were subjected to displacement control test as follows:

- § Initial readings for all the sensors were recorded.
- § The axial load was applied up to the required level and kept constant during the test.
- § The torsional moment was applied gradually at displacement steps controlled by the feed back signal of the LVDT used as displacement controller.
- § The column was loaded by torsional moment up to failure.

TEST RESULTS

The modes of failure and the crack patterns of the tested columns are discussed. The relationships between the torsional moment and the twisting angle are presented. Degradation of axial load during column failure is discussed. The strains in both the lateral and longitudinal reinforcement are analyzed.

Crack Pattern and Failure Mode

All tested columns failed in torsion. Diagonal cracks appeared all around the surfaces of the column. In group A (columns with square section at different values of VSR and constant axial load), column C1R exhibited failure due to yielding of stirrups followed simultaneously by crushing of concrete accompanied with spalling of concrete cover. The existence of axial load increased the compression in the concrete strut. Column C2R showed a ductile behavior and failure occurred due to yielding of stirrups. In group B (columns with L-section at different values of VSR and constant axial load), column C1L exhibited brittle failure due to yielding of stirrups followed simultaneously by crushing of concrete strut. However, columns C2L and C5L had sufficient lateral reinforcement to prevent splitting and limit the lateral tensile strain in the concrete strut. These columns showed ductile behavior and failures were governed by stirrups yielding. In group C (columns with L-section at different axial load levels $0.0 A_g f_{cu}$ to $0.42 A_g f_{cu}$) a similar ductile behavior was observed and yielding of stirrups governed the failure. The modes of failure of the tested columns are presented in Table 2. In all columns except column C3L the longitudinal reinforcement did not reach yielding.

The modes of failure mentioned in Table 2 indicate that a partial space truss model has been developed in all columns except the one in which no axial load was applied. The term partial space truss model means that both types of torsional steel did not reach yielding at failure. The existence of axial load reduces the tensile strains in the longitudinal steel and prevents it from yielding at failure. The failure patterns are shown in Figure 3. The angle of crack of the tested columns varied according to the level of axial load as shown in Table 2. It is obvious that the angle of crack decreased with increasing the level of axial load.

Table 2: The Modes of Failure and Cracking Angles

Group	Type	Angle of crack α°	Axial load/ $A_g f_{cu}$	Mode of failure
A	C1R	28.6	0.23	Stirrups yielding followed simultaneously by concrete crushing
	C2R	34.2	0.23	Yielding of stirrups
B	C1L	28.6	0.28	Stirrups yielding followed simultaneously by concrete crushing
	C2L	33.1	0.28	Yielding of stirrups
	C5L	-	0.28	Yielding of stirrups
C	C3L	49.6	0.0	Yielding of stirrups and longitudinal reinforcement
	C4L	38.2	0.14	Yielding of stirrups
	C6L	27.75	0.42	Yielding of stirrups



(a) column C1R



(b) column C2R



(c) column C1L



(d) column C2L



(e) column C3L



(f) column C4L



(g) column C5L



(h) column C6L

Fig. 3: Failure patterns of tested columns

Torsional Moment and Twisting Angle

The relationships between the torsional moment and the twisting angle for the tested columns are shown in Figure 4. In addition the ultimate torsional moment (torsional capacity) and the corresponding twisting angles are shown in Table 3. The torsional capacity of columns in groups A and B showed that increasing the VSR improved the column torsional capacity up to a certain level of VSR (M_u of C2R > M_u of C1R and M_u of C2L > M_u of C1L), after which the increase of VSR enhanced the column torsional ductility. The biggest ultimate torsional moments in group B was obtained for column C2L with VSR 0.77% and axial load of $0.28 A_g f_{cu}$, when the VSR was doubled in column C5L the torsional capacity did not improve. The increase of torsional capacity of column C2L compared with column C5L was unexpected and may be referred to variation of concrete strength or nature of test setup. However, the ductility of column C5L increased considerably compared with ductility of column C2L.

Similarly, comparing the torsional capacity of columns in groups C and B showed that increasing the axial load level improved the column torsional capacity up to a certain level of axial load (M_u of C2L > M_u of C4L and M_u of C1L > M_u of C3L), however when the axial load exceeded that level the torsional capacity remained constant and the ductility decreased (compare columns C5L and C6L). The ultimate load of columns with low VSR (C1R and C1L) was reached at a low value of twisting angle and then the load decreased progressively. In the other tested columns the ultimate load was reached at a high value of twisting angle and then decreased gradually showing improved ductility.

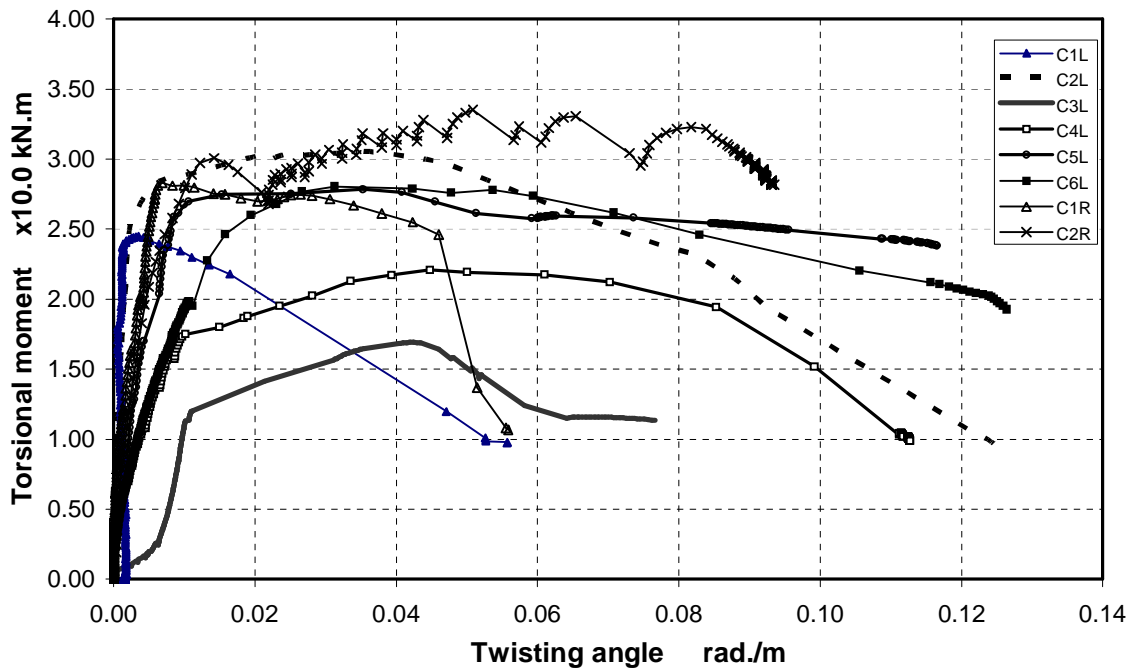


Fig. 4: Torsional Moment-Twisting Angle Relationship

Table 3: The ultimate torsional moment and corresponding twisting angle

Group	Type	Ultimate Torsional moment x10 kN.m	Corresponding twisting angle rad./m	Axial load/ $A_g \cdot f_{cu}$	Torsional Ductility (Refer to section 4.5.2)
A	C1R	2.82	0.0068	0.23	9
	C2R	3.35	0.0508	0.23	14
B	C1L	2.45	0.0035	0.28	10
	C2L	3.08	0.0379	0.28	15
	C5L	2.76	0.0400	0.28	>20
C	C3L	1.69	0.0429	0.0	13
	C4L	2.20	0.0440	0.14	15
	C6L	2.78	0.0400	0.42	19

Degradation of Axial Load

In all tested columns the axial load was almost unchanged until the columns reached their ultimate torsional moments, except in column C4L subjected to $0.14 A_g \cdot f_{cu}$ the axial load increased with the applied torque and reached 1.12 times its original value at the ultimate torsional moment. Degradation of axial load after reaching the ultimate torque is shown in Figure 5. The axial load of column C1R remained constant up to a twisting angle of 0.046 rad./m, then the load dropped suddenly. However, in column C2R the axial load was almost constant up to the test end. In column C1L the axial load dropped suddenly at twisting angle of 0.017 rad./m where the applied torsional moment decreased to 80 % of its ultimate value. In column C2L the axial load decreased to 80% of its original value at a twisting angle of 0.06 rad./m where the applied torsional moment decreased to 90% of its ultimate value, then the axial load decreased by a faster rate. In column C4L the axial load reduced to 80% of its original value where the applied torsional moment was reduced to 70% of its ultimate value. In columns C5L and C6L degradation of the axial load at the columns failure did not exceed 15 % of its original value. These columns could sustain the applied axial load in spite of the occurrence of severe torsion cracks, cover spalling, and degradation of torsional capacity, however the concrete core was undamaged due to the high VSR.

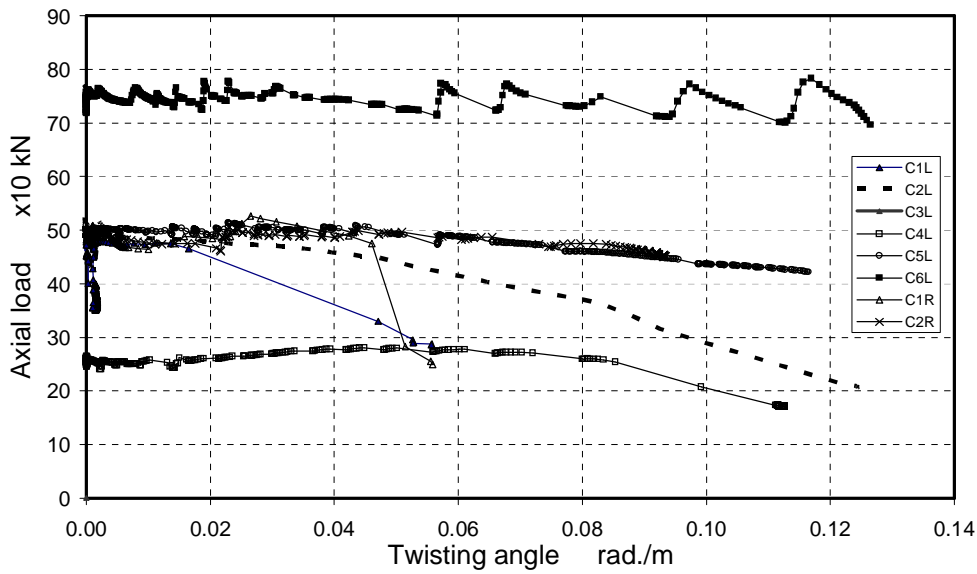


Fig. 5: Axial Load-Twisting Angle Relationship

Strains in Lateral and Longitudinal Reinforcement

The strain measurements could not be obtained in columns of group A and columns C1L and C2L in group B. In column C3L subjected to no axial load the strains reached steel yielding in both the stirrups and longitudinal reinforcement. In columns C4L, C5L, and C6L tested under axial load ranging between $0.14 A_g f_{cu}$ to $0.42 A_g f_{cu}$, the strains in the stirrups reached yielding. The strains in the longitudinal reinforcement changed from compression strain to tensile strain after applying the torsional moment, however, at failure these strains did not reach yielding. Figure 6 shows the relationship between the torsional moment and the strain in stirrups (S1 and S2) and longitudinal reinforcement (I3 and I4) for column C5L.

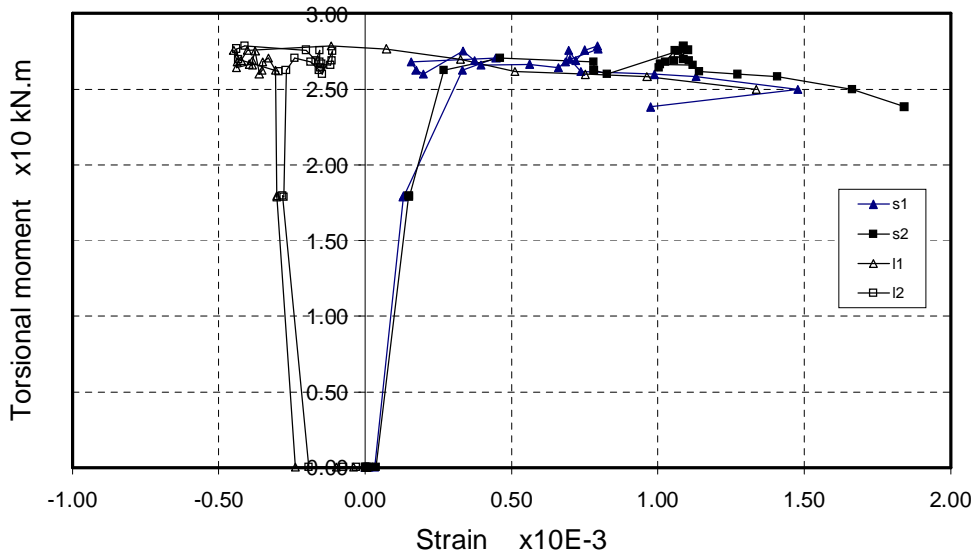


Fig. 6: Torsional Moment-Stirrups Strain Relationship for Column C5L

Evaluation of Test Results

Torsional Capacity

The torsional capacity increased due to the presence of axial load. At low stirrups ratio (SVR = 0.385%) brittle failure occurred due to crushing of concrete strut and the increase in torsional capacity did not exceed 45% compared to columns tested under no axial load. When the stirrups ratio was sufficient to prevent splitting of concrete strut (SVR = 0.77%), the torsional capacity increased more than 60%. Increasing the stirrups ratio above that level enhanced the column torsional ductility but did not improve the gain in the strength. Increasing the axial load level more than $0.28 A_g f_{cu}$ did not improve the torsional capacity, however the column torsional ductility decreased.

Torsional Ductility

The torsional ductility (D) of the columns is defined here as follows:

$$D = \theta_f / \theta_y$$

Where:

θ_f is the angle of twist corresponding to 20% reduction of ultimate torsional moment or applied axial load

θ_y is the angle of twist at yield

Table 3 shows the torsional ductility of the tested columns. The column torsional ductility depends on the level of axial load and the volumetric stirrups ratio VSR. Increasing the level of the axial load led to the reduction in the column torsional ductility. However, the increase of the VSR enhanced the column torsional ductility considerably.

Angle of Crack

The angle of crack decreased due to the presence of axial load. Table 2 represents the angle of crack measured on the surface of columns after failure. The cracking angle increased with the increase of the stirrups ratio for the same amount of longitudinal reinforcement.

THEORETICAL ANALYSIS

A theoretical analysis based on a modified space truss was conducted. The model proposed by Fouad⁴ to compute the torsional capacity of normal and high strength concrete beams considering concrete softening was modified to account for the axial load. In addition the computer program prepared by Fouad⁴ was modified to predict the theoretical torsional capacity of columns with rectangular sections. Experimental tests on columns with square sections were used to verify the theoretical results. The basic principles of the model were found to be valid to the pre-stressed concrete beams subjected to torsional moment. The proposed model was used to predict the torsional capacity of 21 pre-stressed concrete beams found in literature^{1,5,6,7}.

Modified Space Truss Model

Equilibrium equations

The axial load was considered in the equilibrium equations of the space truss model. The first equilibrium equation is obtained by taking moment about the column longitudinal axis

$$q = M / 2A_o \quad (1)$$

The other equilibrium equations are derived by taking equilibrium of the force triangle shown in Figure 7. The contribution of axial load was presented in the second equilibrium equation.

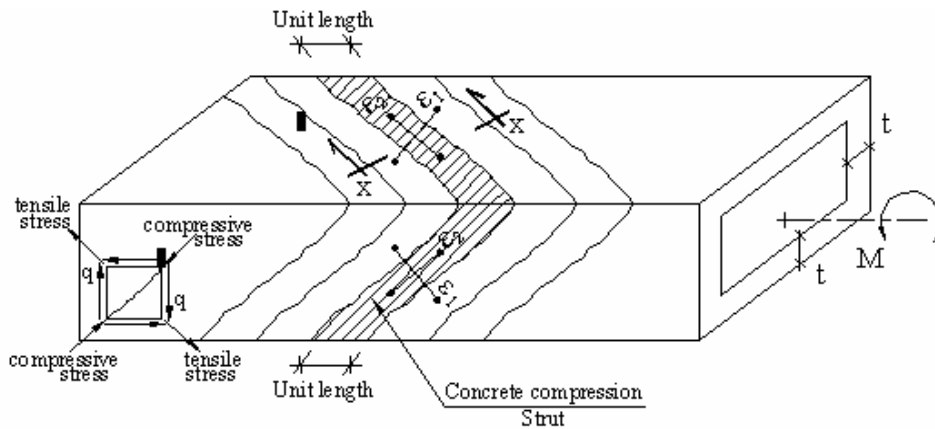
$$A_L f_L = p_o q \cot \alpha - P \tag{2}$$

$$A_t f_t = q s \tan \alpha \tag{3}$$

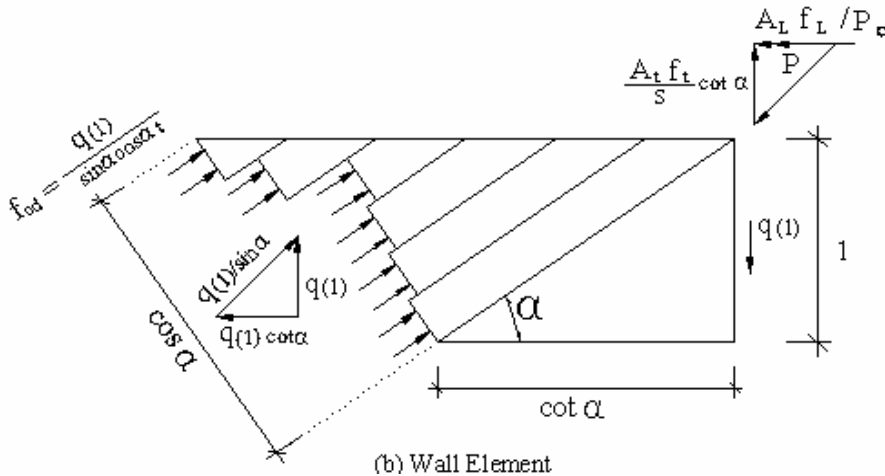
$$q = f_{cd} t \sin \alpha \cos \alpha \tag{4}$$

Where:

- q shear flow
- M Torsional moment
- A_o area enclosed by centerline of shear flow zone
- A_L, A_t area of longitudinal and transversal reinforcement, respectively
- s spacing of stirrups
- t thickness of shear flow zone
- α crack angle
- f_{cd} average compressive strength in concrete strut
- f_L, f_t stress in longitudinal and transversal reinforcement, respectively
- P axial load
- p_o perimeter of area enclosed by centerline of shear flow zone



(a) Stresses at Concrete Struts



(b) Wall Element

Fig. 7: Equilibrium of Column Subjected to Torsion

Equations (1) through (4) represent the four basic equilibrium equations of the space truss model including the effect of axial load.

Compatibility Equations

The same compatibility equations derived for the space truss model without axial load are considered. There are six basic equations relating the angle of twist, the angle of crack, the shear distortion of the wall, the strain in the longitudinal reinforcement, the strains in the stirrups, the concrete strains parallel and perpendicular to the concrete struts (ϵ_1 and ϵ_2), the curvature of the concrete struts, and the compressive surface strains. For the details of these equations refer to Fouad⁴.

Concrete Softening Model for Compression in Concrete Strut

The model represents the softening occurring in concrete strut due to lateral tensile strain by reducing the values of both ultimate stress and ultimate strain by strength a reduction factor β as follows:

$$f_p = \beta f_c \quad , \quad \epsilon_p = \beta \epsilon_c \quad (5)$$

Where:

- f_p ultimate compressive strength of softened concrete
- f_c ultimate compressive strength of concrete
- ϵ_p strain at ultimate compressive strength of softened concrete
- ϵ_c strain at ultimate compressive strength of concrete

The strength reduction factor β depends on the values of concrete compressive and tensile strains.

The average compressive stress in concrete strut is computed as follows:

$$f_{cd} = k_1 f_p \quad (6)$$

Where k_1 is an averaging factor obtained by the integration of the softened stress strain curve.

Computer Program

The computer program prepared by Fouad⁴ was modified to include the effect of axial load. The program is an iterative procedure to solve the equilibrium and compatibility equations to obtain the torsional capacity, the corresponding twisting angle and the strains in concrete and reinforcement.

Experimental Verification

The results of the square columns in group A were used to verify the theoretical analysis. The torque-twisting angle relationships for both experimental and proposed theoretical model are shown in Figure 8. Table 4 shows the ultimate torsional capacity of these columns obtained experimentally and theoretically.

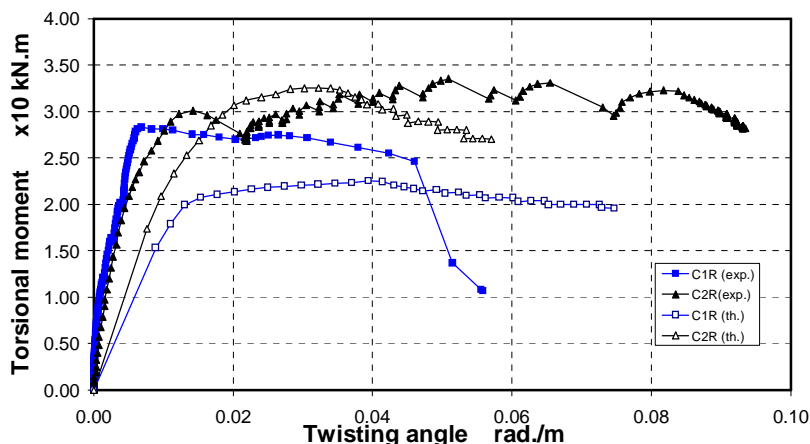


Fig. 8: Torsional Moment-Twisting Angle Relationship for Columns in Group A

Comparison with Test Results of Pre-stressed Members Found in Literature

The torsional capacities of 21 pre-stressed members found in literature ^{5, 6, 7} were predicted using the proposed model. Detailed description of the properties of these members is given in references (1), (5), (6), and (7). Table 4 represents the ratio of theoretical and experimental torsional capacity. It is found that, the ratio of the experimental ultimate torque M_{exp} to theoretical ultimate torque M_{th} ranges from 1.00 to 1.26 in all specimens except PC3 and PC4.

Table 4: Comparison between Experimental Results and Results Obtained by Proposed Program

Reference	Notation	Ultimate Torque M_{exp} x10 kN.m (experimental)	Ultimate Torque M_{th} x10 kN.m (theoretical)	M_{exp}/M_{th}
Columns in group A	C1R	2.83	2.25	1.25
	C2R	3.35	3.25	1.03
Mitchell and Collins, 1978 (5)	P1	8.35	7.64	1.092
	P2	8.23	7.68	1.071
	P3	5.41	5.38	1.005
	P4	9.16	7.66	1.195
Eldegwy and McMullen, 1985 (6)	PA1	2.31	1.98	1.166
	PA2	2.21	1.98	1.116
	PA3	2.99	2.86	1.045
	PA4	3.46	3.06	1.130
	PA5	3.81	3.26	1.168
	PB1	2.26	1.88	1.202
	PB2	2.80	2.68	1.044
	PB3	3.32	2.86	1.095
	PB4	3.83	3.03	1.260
	PC1	2.01	1.65	1.218
	PC2	2.60	2.40	1.083
	PC4	3.92	2.67	1.468
Chander, Kempt, and Wilhelm, 1970 (7)	C/5	0.87	0.79	1.101
	C/9	0.98	0.85	1.152
	E/6	0.80	0.79	1.012
	E/10	0.92	0.85	1.082

CONCLUSIONS

From the experimental and theoretical studies the following conclusions are derived:

- 1- For columns with volumetric stirrups ratio more than or equal to 0.57% increasing the axial load level up to $0.28 A_g.f_{cu}$ enhanced the torsional capacity of the column to more than 60% compared to the column with zero axial load and ductile torsional failure occurred.
- 2- The columns with volumetric stirrups ratio less than or equal to 0.385% and subjected to axial load level more than $0.23 A_g.f_{cu}$ failed in brittle torsional failure mode.
- 3- Increasing the volumetric stirrups ratio more than 0.77% improved the column torsional ductility but did not enhance the column torsional capacity for the same axial load level $0.28 A_g.f_{cu}$.
- 4- Increasing the axial load level to $0.42 A_g.f_{cu}$ did not improve the column torsional capacity compared with columns tested under axial load level of $0.28 A_g.f_{cu}$ and had the same VSR of 1.54%, however the column ductility decreased.
- 5- The angle of torsional crack of the tested columns ranged between 28° to 38° according to the level of axial load and volumetric stirrups ratio.
- 6- The modes of failure of the tested columns indicate that a partial space truss model has been developed in all columns subjected to axial load level equal to or more than $0.14 A_g.f_{cu}$, and yielding occurred in stirrups only.
- 7- The longitudinal reinforcement did not reach yielding in all tested columns except the one in which no axial load was applied. This indicates that the requirements of additional longitudinal reinforcement for torsional resistance in columns is much less than these requirements in beams.
- 8- The proposed modified space truss model seems to could predict the torsional capacity of square columns with reasonable agreement especially when failure occurred due to yielding of stirrups.
- 9- The proposed model seems to be able to predict the torsional capacity of pre-stressed beams.

REFERENCES

1. Ghoneim, M.G., and MacGregor, J. G., "Evaluation of Design Procedures for Torsion in Reinforced and Pre-stressed Concrete," Structural Engineering Report No. 184, Department of Civil Engineering, University of Alberta, Edmonton, February 1993.
2. "Egyptian Code for Design and Construction of Concrete Structures", ECCS-203, 2004.
3. ACI Committee 318, "Building Code Requirements for Reinforced Concrete (ACI 318-02)," American Concrete Institute.
4. Fouad, E., "Behavior of Reinforced Normal and High Strength Concrete Beams Subjected to Combined Shear and Torsion," Ph.D. thesis, Faculty of Engineering, Cairo University, 2000
5. Mitchell, D. and Collins, M.P., "Influence of Prestressing on Torsional Response of Concrete Beams," PCI Journal, Vol. 23, No. 3, May-June 1978, pp. 54-73.
6. Eldegwy, W. and McMullen, A., "Prestressed Concrete Tests Compared with Torsion Theories," PCI Journal, Vol. 30, No. 5, Sept.-Oct. 1985, pp. 96-127.
7. Chander, H., Kemp, E.L., and Wilhelm, W.J., "Behavior of Prestressed Concrete Rectangular Members Subjected to Pure Torsion," Civil Engineering Studies, Report No. 2007, Department of Civil Engineering, West Virginia University, Morgantown, 1967, 100pp. (cited in reference 4)

EFFECT OF WEB INCLINATION ON THE BEHAVIOR OF COLD FORMED STEEL C-PURLINS

A. M. Fadel

Associate Professor, Housing and Building National Research Center, Cairo, Egypt

Email: a.fadel@hbrc.edu.eg

ABSTRACT

C and Z sections are two of the most common cold-formed steel shapes in use today. In case of portal frames those sections are used as purlins that carry loads not parallel to their webs, which lead to stresses in both major and minor directions of the sections. To effectively use those sections the webs are made to have the same inclination angle as for the portal frame rafter. A comparison between the behavior of C-purlins having vertical and inclined webs has been made to show the effect of web inclination on the capacity of the C-purlins. The members selected are widely used in practice and have (h/t) that varies from 60 to 123. The thicknesses of the used C -purlins are 1.5, 2.0, 2.5 and 3.0 mm. The height of the used sections are 200 and 250 mm. 30 sections have been studied to show the effect of the web inclination angle on the behavior of the C-purlins. The web slope varies from 0 to 20%. The direct strength method has been used to compare the local, distortional and overall buckling stresses for C-purlins having vertical and inclined webs. Results are discussed and recommendations are given for the use of the C-purlins having inclined webs.

Keywords: Cold formed, C-purlins, Inclined web, Local Buckling, Distortional Buckling, Overall Buckling.

INTRODUCTION

Cold-formed steel members provide substantial savings due to their high strength-to-weight ratio. As a result, they have become very popular in the construction of industrial, commercial, and factory buildings. An important advantage of cold-formed steel is the greater flexibility of cross-sectional shapes and sizes available to the structural steel designer.

Through cold-forming operations, steel sheets, strips or plates can be shaped easily and sized to meet a large variety of design options. Such a large number of design possibilities create a very important challenge of choosing the most economical cold-formed shape in design of steel purlins. Many researches had been carried out to obtain the optimum dimension of sections used as purlins [1]. Through analytical and experimental works had been carried out recently to enhance the design expressions stated by international codes for both C and Z sections and to distinguish between local, distortional and lateral-torsional buckling [2].

Described in this paper is an approach for the effective use of the C-purlins to carry the load directly in their major directions and minimizing the effect of the lateral component of the applied load, which acts upon the minor direction of the purlins. Comparison between the behaviors of the C-purlins having webs inclined by 5, 10, 15 and 20 % with the vertical axes had been made and discussed. The direct strength method [3] had been used to compare the behavior of the C-purlins having inclined webs with those having vertical webs.

FINITE STRIP ANALYSIS

Finite strip analysis is a specialized variant of the finite element method. For elastic stability of cold-formed steel structures, it is one of the most efficient and popular methods. Cheung and Tham (1998) [4], explain the basic theory while Hancock and Schafer (1997) provide specific details for the stability analysis done using this method. Hancock and his researchers pioneered the use of the finite strip analysis for the stability of cold-formed steel members and convincingly demonstrated the important potential of the finite strip analysis for both cold-formed steel design and behavior. Schafer's research group has used finite strip analysis extensively and has made available the academic program, CUFSM [5], for the finite strip analysis which has been used in this research.

The direct strength method, which has been used in this research emphasizes the use of finite strip method for elastic buckling determination. Finite strip analysis is a general tool that provides an accurate elastic buckling solution with a minimum amount of effort and time. Finite strip analysis, as implemented in conventional programs, does have limitations, the most important ones are:

- the mode assumes the ends of the member are simply supported, and
- the cross-section may not vary along its length (uniform properties longitudinally).

These limitations preclude some analyses from readily being done with the finite strip method, but despite these limitations the tool is useful and a major advance over plate buckling solutions and plate buckling coefficients "K's" that only partially account for the important stability behavior of cold-formed steel members. The freely available computer program, CUFSM that is used in this research, employs the finite strip method for elastic buckling determination of any cold-formed steel cross-sections.

BUCKLING CURVE AND HALF-WAVE LENGTH

The buckling curve is the relation between the load factor and the half-wave length. The finite strip method assumes that the longitudinal deformation occurs at half a sine wave, which is called a half-wave length. The analysis is performed for systematically increasing half-wave lengths to determine the buckling behavior (mode shape and load factor) of the member. It has to be noted that the half-wave length is not strictly equal to the un-braced length, as any identified mode may repeat itself multiple times within a given un-braced length.

A bifurcation buckling analysis is conducted in this research using finite strip method. The member is loaded with a reference stress distribution; the buckling stress is equal to the load factor times the reference stress distribution. More precisely, the load factor is the eigenvalue of the relevant buckling problem and the eigenvector is the buckling mode.

LOCAL, DISTORTIONAL AND GLOBAL BUCKLING MODE SHAPES

Fig. 1 shows the various buckling modes. Local buckling involves significant distortion of the cross-section, but this distortion involves only rotation, with no translation at the fold lines of elements with edge-stiffened flanges.

For distortional buckling, both rotation and translation at the fold lines of the elements shall take place. In some members like in simple angles, it is very difficult to differentiate between local and distortional buckling and in such cases no local buckling shall take place.

The global or "Euler" buckling mode, flexural, torsional, or flexural-torsional for columns, and lateral torsional for beams, occur as the minimum mode at long half-wave lengths. Global buckling modes involve translation (flexure) and/or rotation (torsion) of the entire cross-section. No distortion exists in any of the elements in the long half-wave length buckling modes.

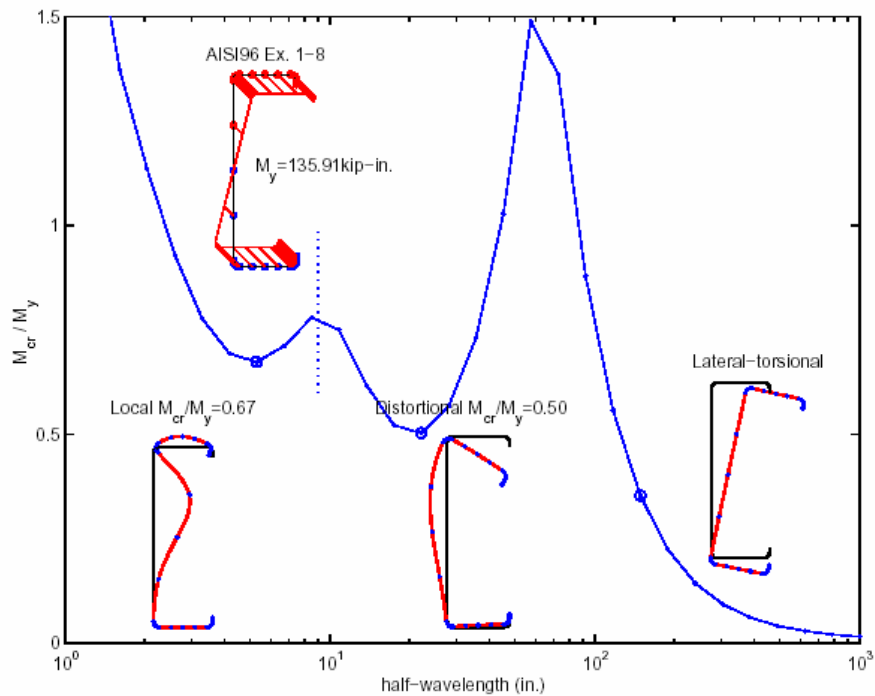


Fig. 1: Local, Distortional and Global (Flexural) Buckling Modes in Bending [3]

ANALYSIS OF COLD FORMED C-PURLINS HAVING VERTICAL OR INCLINED WEBS

Fig. 2 shows the layout of purlins located above rafter of portal frame for both cases of purlins having perpendicular web and purlins having inclined webs. For simplicity, the case of purlins having perpendicular webs will be referenced in this paper as purlins having vertical webs. Fig.2 (a) shows the load acting on the purlins having perpendicular (or vertical) web; the resultant R in this case shall be resolved to two components as shown in the figure. Fig.2 (b) shows the load acting on the purlins having inclined webs; the resultant R in this case shall be carried directly in the major direction of the purlin. Note that the web inclination angle of the purlin is the same as the angle of inclination of the rafter.

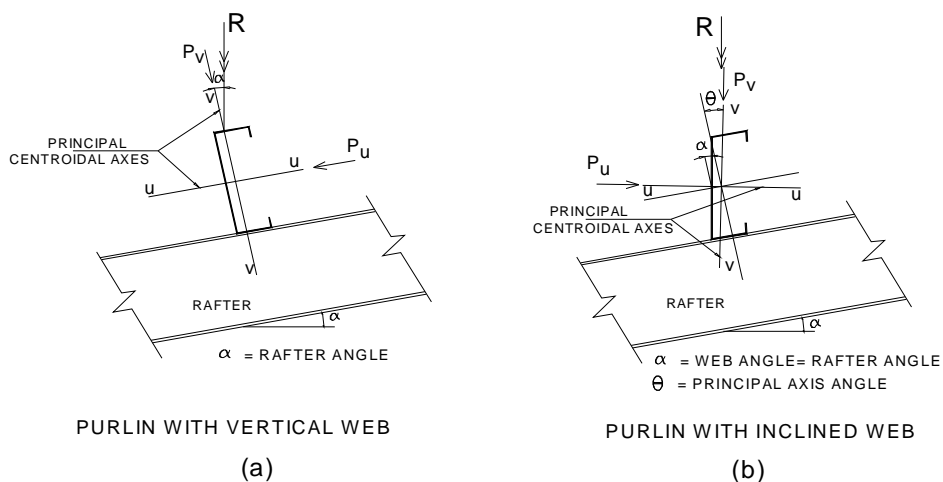


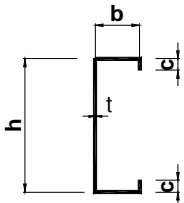
Fig. 2: Layout of Purlins Having Perpendicular Web and Inclined Web

Six different cold formed C-purlins have been used in the analysis, each of them have web slope of 0, 5, 10, 15 and 20%, which makes the total number of sections analyzed is 30 sections. Table 1 shows the dimensions of the selected C-purlins used. The notation 200C20-05 (e.g.) means that the height of the C-section is 200 mm, the thickness is 2 mm; the web slope is 5%.

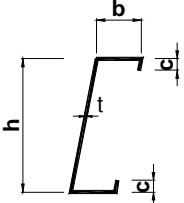
All the 30 sections (6 sections times 5 inclination angles) have been studied under the effect of pure bending assuming that the maximum stress at the top and bottom of the section is 2400 kg/cm². The purlins studied have simple span of 6 meters carries a load of sandwich panels of 15 kg per square meter plus the own weight of the purlin and a live load of 50 kg per square meter, the spacing between purlins is taken 1.20 m. Comparison between the actual stresses resulting from the applied loads for different slopes of webs and the corresponding cases of C-purlins having vertical webs have been made for the 30 sections studied.

Table 1: Dimensions of the Selected Cold Formed C-purlins

NOTATION	h (mm)	b (mm)	c (mm)	t (mm)
200C15-00	200	60	20	1.5
200C20-00	200	60	20	2
200C25-00	200	60	20	2.5
200C30-00	200	60	20	3
250C20-00	250	60	20	2
250C25-00	250	60	20	2.5



C-PURLIN WITH VERTICAL WEB



C-PURLIN WITH INCLINED WEB

Determination of the Principal Axes

Table 2 shows the moments of inertia of the sections analyzed about the principal centroidal axes at different web slopes and the angle of rotation (θ) with vertical line.

Slope	0 %		5 %		10 %		15 %		20 %	
q	0°		- 3.13°		- 6.24°		- 9.30°		-12.50°	
	I _u	I _v								
200C15	350.4	30.1	351.5	30	355	29.8	360.8	29.6	358.5	29.1
200C20	467.2	40.1	468.7	40	473.3	39.8	481.1	39.4	478	38.8
200C25	583.9	50.1	585.9	50	591.7	49.7	601.3	49.3	597.5	48.5
200C30	700.7	60.2	703.1	60	710	59.7	721.6	59.2	717	58.2
q	0°		- 3.03°		- 6.03°		- 9.01°		-11.78°	
	I _u	I _v								
250C20	792.4	43.1	792.7	42.6	800.4	42.4	813.4	41.9	794.9	41.9
250C25	990.5	53.9	990.9	53.3	1000.5	53	1016.7	52.4	993.7	52.3

* All values of I_u and I_v are in cm⁴

The results obtained, Fig. 3 shows that the maximum normal stress calculated about the principal centroidal axes of the C-purlin 200C30-00 (vertical web) is 1.08 t/cm² while the corresponding values for C-purlin 200C30-20 (web slope = 20%) is 0.42 t/cm². The ratio between the stresses for the C-purlin having inclined web to that for the C-purlin having vertical web is equal to 39.3% in this case, which means that a reduction in the stress of 60.7%, has been obtained in this case.

Fig. 4 shows that maximum normal stress calculated about the principal centroidal axes of the C-purlin 250C25-00 (vertical web) is 1.10 t/cm² while the corresponding values for the C-purlin 250C25-20 (web slope = 20%) is 0.42 t/cm². The ratio between the stresses for the C-purlin having inclined web to that for the C-purlin having vertical web is equal to 37.9 %, which means that a reduction in the stress of 62.1%, has been obtained in this case.

Fig. 5 and Fig. 6 show comparisons between the buckling curves for C-purlins having vertical webs and C-purlins having inclined webs. From these figures we can notice that the local buckling load factor for the C-purlins having inclined webs is lower than that for C-purlins having vertical webs by not more than 0.90 % (for 250C20-20). In other words, the elastic critical local buckling moment for the C-purlins having inclined webs is lower than that for the C-purlin having vertical webs by not more than 0.90 %. The distortional buckling load factor for the C-purlins having inclined webs is higher than that for C-purlins having vertical webs by 6.5 % (for 200C30-20). In other words, the elastic critical distortional buckling moment for the C-purlins having inclined webs is lower than that for the C-purlins having vertical webs by 6.5 %. The overall elastic buckling curves for C-purlins having inclined webs and C-purlins having vertical webs are almost identical which means that the lateral torsional buckling of the purlins are not affected by the inclination of the web.

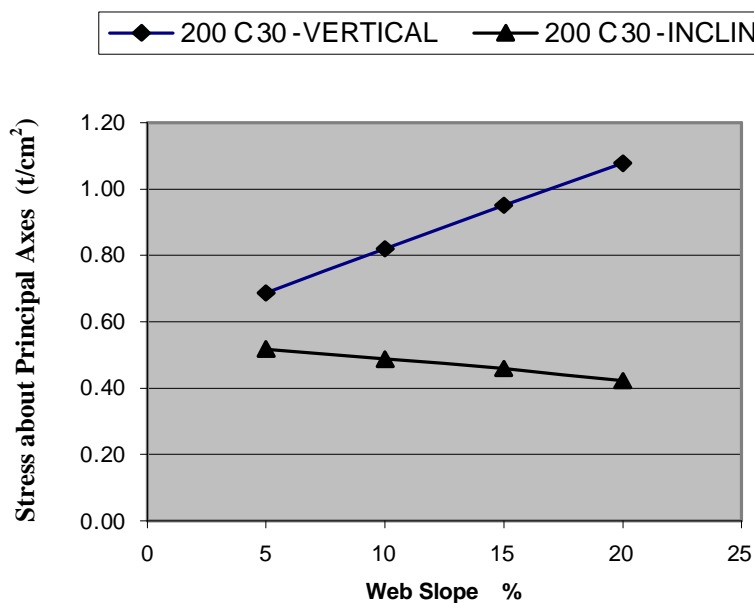


Fig. 3: Comparison between C-purlins Having Vertical and Inclined Webs for 200C30

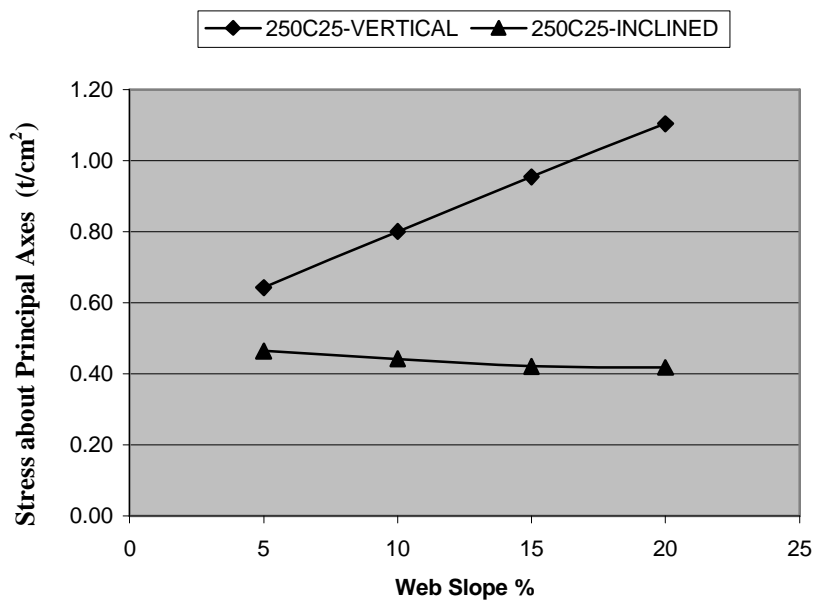


Fig. 4: Comparison between C-purlins Having Vertical and Inclined Webs for 250C25

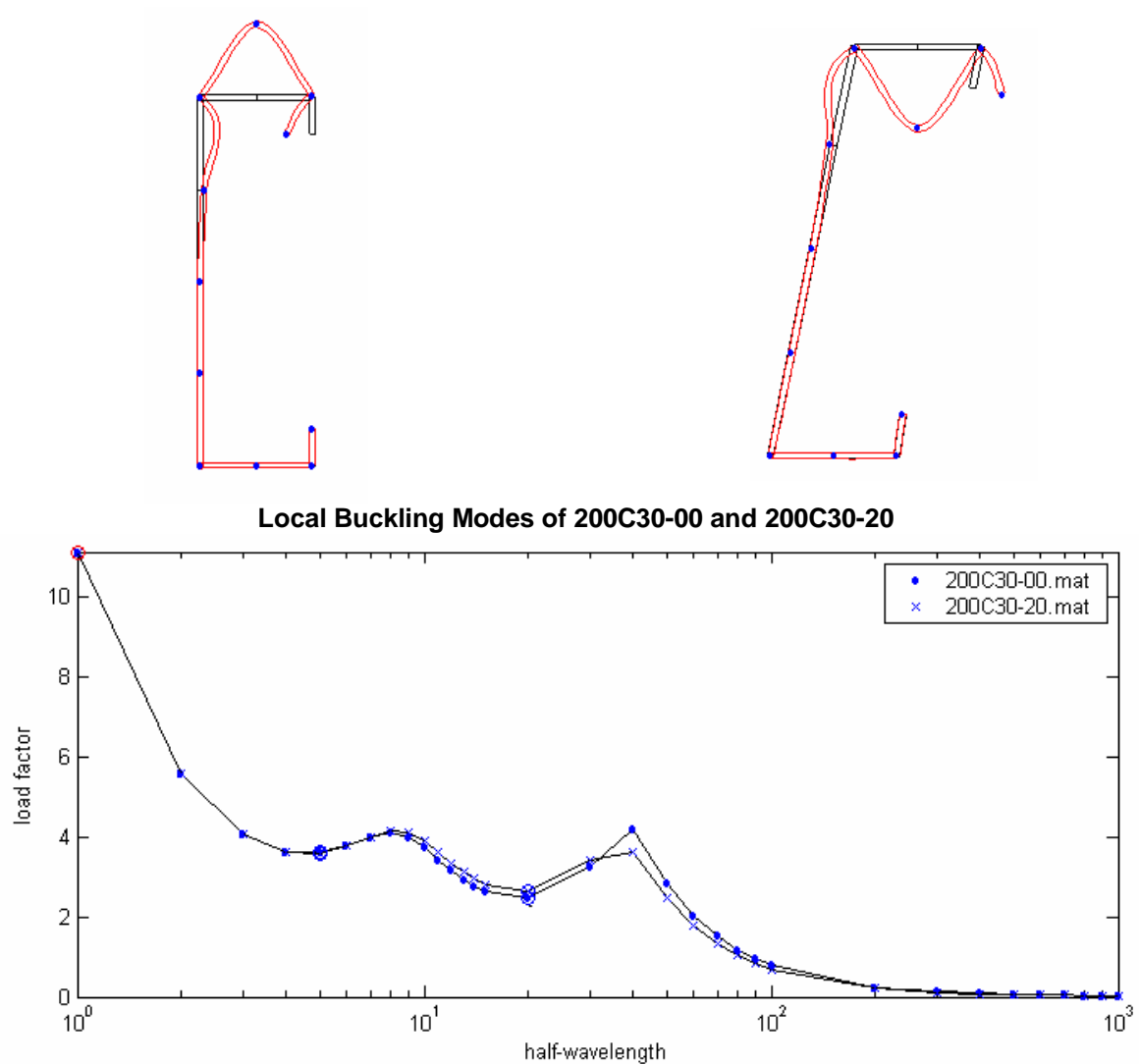


Fig. 5: Comparison between Buckling Curves of 200C30-00 and 200C30-20 [5]

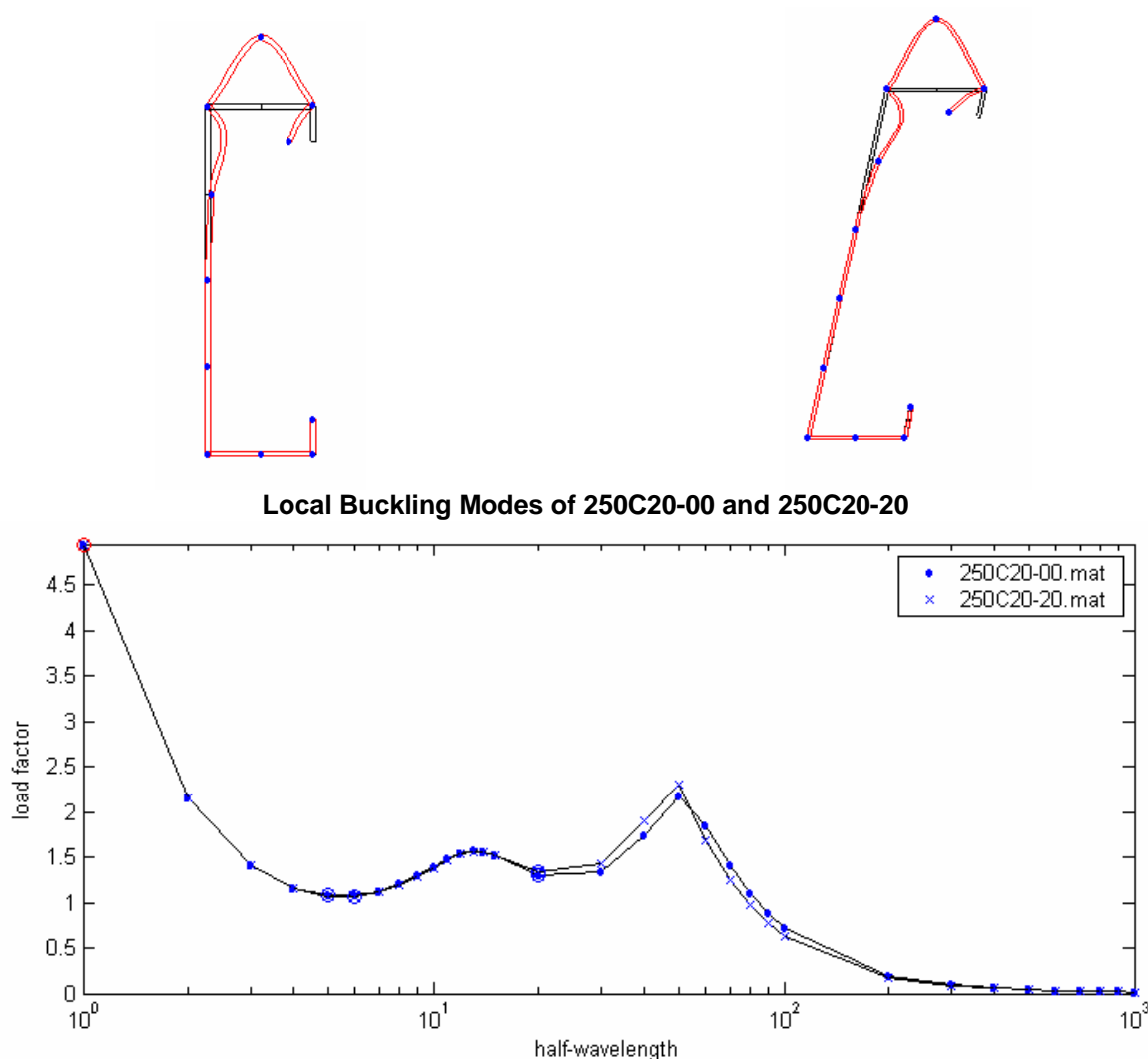


Fig. 6: Comparison between Buckling Curves of 250C20-00 and 250C20-20 [5]

RESULTS AND DISCUSSIONS

From Figures 3 and 4 we can notice that by rotating the web of the C-purlins by the same slope of the portal frame rafter; the maximum normal stress calculated about the principal centroidal axes of the purlins is greatly reduced due to the reduction of the load component acting upon the weak axis of the C-purlin.

Fig. 7 shows the comparison between the web slope and the reduction in the stress calculated about the principal centroidal axes for C-purlins 200C15 to 200C30 and 250C20 to 250C25 for the case of no tie rods used. From this figure we can see that the stress calculated about the principal centroidal axes for the C-purlins having inclined webs is 60.7 % less than that for the C-purlins having vertical webs for 200C15, 200C20, 200C25 and 200C30 purlins at slope of 20 %. Also the stress calculated about the principal centroidal axes for the C-purlins having inclined webs is 62.1 % less than that for the C-purlins having vertical webs for 250C20 and 250C25 purlins at slope of 20 %.

Fig. 8 shows the comparison between the web slope and the reduction in the stress calculated about the principal centroidal axes for C-purlins 200C15 to 200C30 and 250C20 to 250C25 for the case of using one tie rod at mid span of the purlins. From this figure we can see that the

stress calculated about the principal centroidal axes for the C-purlins having inclined webs is 30.1 % less than that for the C-purlins having vertical webs for 200C15, 200C20, 200C25 and 200C30 purlins at slope of 20 %. Also the stress calculated about the principal centroidal axes for the C-purlins having inclined webs is 30.4 % less than that for the C-purlins having vertical webs for 250C20 and 250C25 purlins at slope of 20 %.

Fig. 9 shows the comparison between the web slope and the reduction in the stress calculated about the principal centroidal axes for C-purlins 200C15 to 200C30 and 250C20 to 250C25 for the case of using two tie rods at third points of the span of the purlins. From this figure we can see that the stress calculated about the principal centroidal axes for the C-purlins having inclined webs is 19.9 % less than that for the C-purlins having vertical webs for 200C15, 200C20, 200C25 and 200C30 purlins at slope of 20 %. Also the stress calculated about the principal centroidal axes for the C-purlins having inclined webs is 18.5 % less than that for the C-purlins having vertical webs for 250C20 and 250C25 purlins at slope of 20 %.

Fig. 10 shows the relation between the web slope and the percentage of reduction in lateral moment of inertia capacity (about axis v-v) of C-purlins having inclined webs relative to those having vertical webs. From this figure we can see that the maximum reduction in the moment of inertia of C-purlins having inclined web is 3.2% than the corresponding C-purlins having vertical webs.

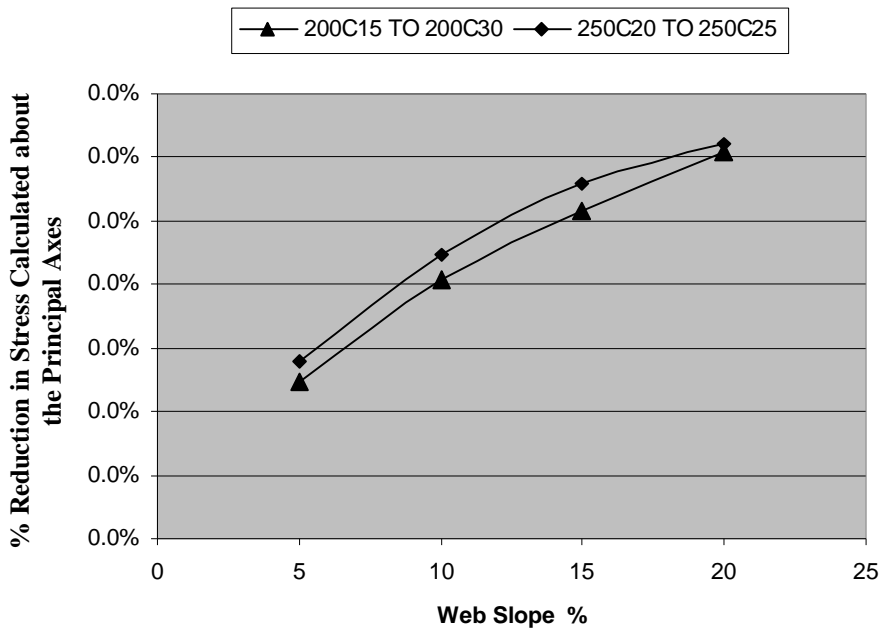


Fig. 7: Relation between Web Slope and Reduction in Stress Calculated About the Principal Axes of C-purlins (Case of No Tie Rods)

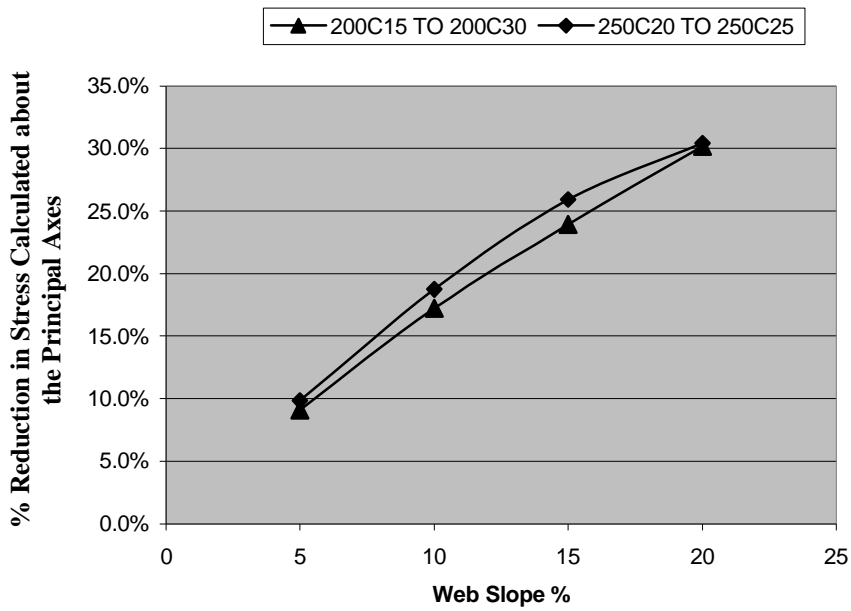


Fig. 8: Relation between Web Slope and Reduction in Stress Calculated About the Principal Axes of C-purlins (Case of One Tie Rod)

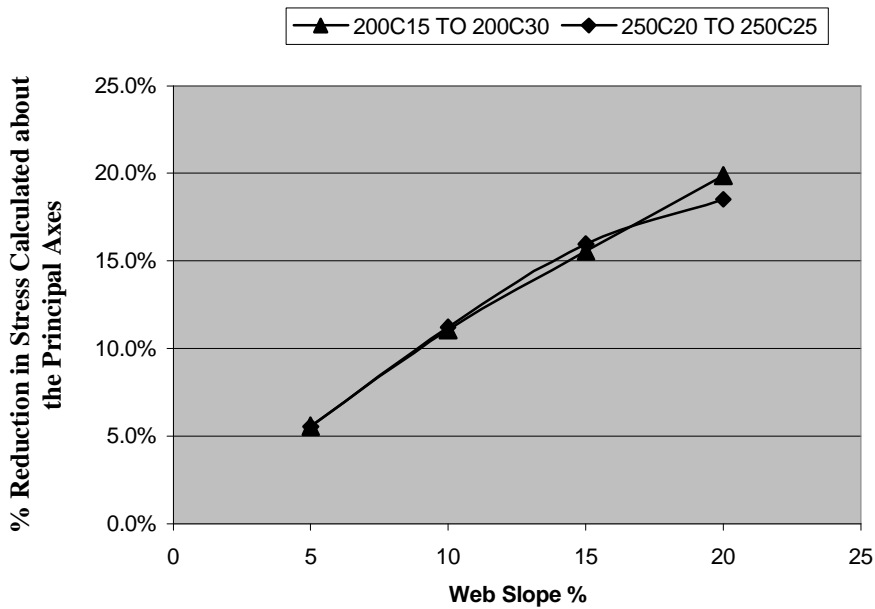


Fig. 9: Relation between Web Slope and Reduction in Stress Calculated about the Principal Axes of C-purlins (Case of Two Tie Rods)

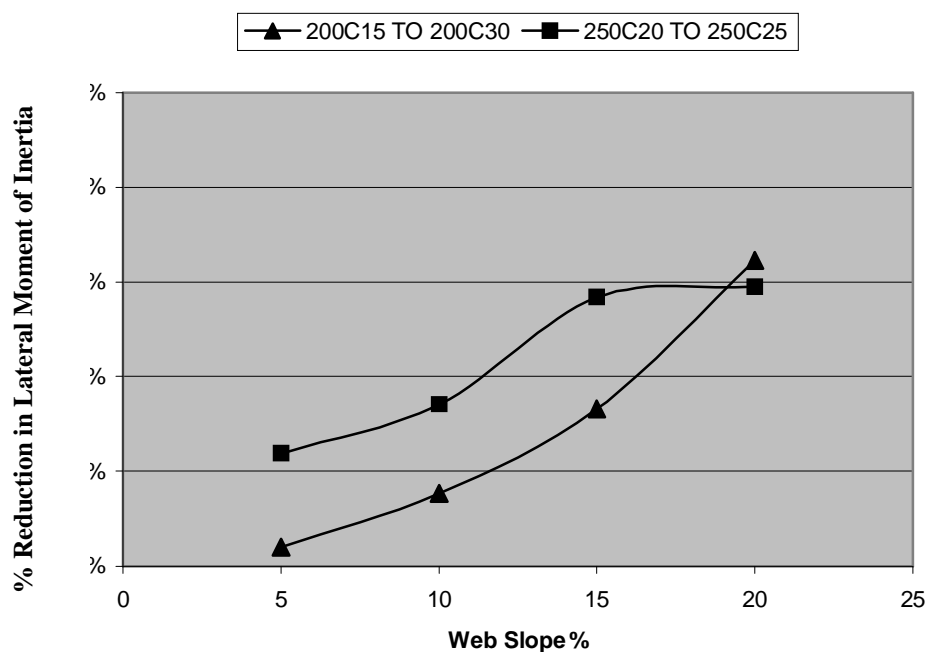


Fig. 10: Relation between Web Slope and Reduction in Lateral Moment of Inertia of C-Purlins

CONCLUSIONS

The analysis to study the behavior of C-purlins having inclined webs under loads parallel to their webs is made and compared with that for C-purlins having vertical webs subjected to loads not parallel to the web. The lateral moment of inertia capacities of the C-purlins having inclined webs are lower than the corresponding values for the C-purlins having vertical webs by not more than 3.2%. The torsional capacities of the C-purlins having inclined webs are almost the same as those for C-purlins having vertical webs.

The use of C-purlins having inclined web greatly affects the design of purlins. A reduction in the stress calculated about the principal axes reaches up to 62.1% compared with the C-purlins having vertical webs.

The author recommends the use of C-purlins having inclined webs provided that the web inclination angle shall be the same as the rafter inclination angle; this will lead to considerable loss in weight of purlins.

A more accurate nonlinear analysis is currently in progress to study the effect of the point of application of load on the C-purlin top flange and its effect on the behavior of both types of C-purlins having vertical or inclined webs. The comparison between Z purlins having vertical and inclined webs is also made.

REFERENCES

1. Wei Lu, "Optimum Design of Cold-Formed Steel Purlins Using Genetic Algorithms", Ph.D., 2003, Helsinki University of Technology, Department of Civil and Environmental Engineering, Laboratory of Steel Structures.
2. Cheng Yu and Benjamin W. Schafer, "Local Buckling Tests on Cold-Formed Steel Beams", Journal of Structural Engineering, ASCE, December 2003.
3. Benjamin W. Schafer, "Manual for Direct Strength Method of Cold-Formed Steel Design", draft- January 7, 2002, for American Iron and Steel Institute – Committee on Specifications.
4. Cheung, Y.K., and Tham, L.G. "Finite Strip Method", CRC press. 1998.
5. CUFSM, free software, www.ce.jhu.edu/bschafer/cufsm, version 2.6.

AN INTEGRATED SOFTWARE FOR THE DESIGN OF BEAM-TO-COLUMN RIGID CONNECTIONS

H. I. Hassanain

*Assistant Lecturer, Housing & Building National Research Center, Dokki, Giza,
E-mail: h.hassanain@hbrc.edu.eg*

ABSTRACT

An integrated software for the design of beam-to-column rigid connections (STCON v1.0) was developed under the Visual Basic environment. The software (STCON v1.0) is a part of a comprehensive plan to develop an integrated software for the design of many steelwork connections, base connections and splices. The software covers most of the parameters associated with the end plated rigid beam-to-column connections; end plate extension, haunch girders, different material properties and bolt types. The software package comprises a concept of driven-user data checking, also it integrates the advantages of spreadsheets and programming languages together in a non-automated "what-if" optimization process. The STCON v1.0 was verified using PROKON v1.7.1 software through several case studies it can handle.

Keywords: beam-to-column connections, driven-user data checking, input validation, non-automated optimization, what-if analysis.

1 INTRODUCTION

Different available commercial software packages such as SAP2000[®][7], STAAD PRO[®][8], COSMOS/M[®][2], PROKON[®][6] and ETABS[®][3] are currently used in consultant works as well as research institutes not only for the purpose of structural analysis but for the purpose of designing main structural elements as well. Generally, they are capable of designing columns, beams, beam columns in a rather well-suited general formulation to accommodate for space actions, end conditions and most of them can even account for the global behaviour of the structure as well.

Most of the above mentioned software packages do not have modules for steel connections design unless it is in a primitive development status. To solve the problem of the lack of steel connections design software, structural consultants and design engineers tend to construct spreadsheets to accomplish the tedious and repetitive calculations inherent with these types of connections. Spreadsheets have the mere disadvantage of inflexibility for general solutions that programming languages do not have. So, a software package was developed using Visual Basic[®] to gather all available advantages in an All-In-One program.

In addition, one of the prime issues regarding the industry of software is the application of the law of intellectual rights, which may restrict the illegal use of several structural analysis and design software packages. This would result in either abandoning the use of such sophisticated analysis techniques or purchasing legal packages with foreign currency.

The prime objective of the present work is to promote the national programming industry and to highlight some frequently poorly implemented engineering aspects.

In the present paper, the preliminary version of steel connections software package (STCONv1.0) is presented. This version included one module for the design of beam-to-column rigid connections and another one for the design of portal frame apex connection. Newer

versions include modules for the design of base connections; either hinged or fixed; and beam-column splice as well as beam-to-column junction as shown in figure (1). The package is intended to be developed to account for some extra modules in the future. Visual Basic 6.0[®] was utilized in constructing the software along with Crystal Report 10[®] reporting software.

2 BEAM-TO-COLUMN RIGID CONNECTION

2.1 Overview

Beam-to-column rigid connection is a group of elements connecting beams to columns in a framed structure and thus it is capable and responsible for transmitting straining actions (axial, shear forces and bending moments) from one element to the other. Different configurations are usually implemented for this type of connection as shown in figure (2), among them the end plated moment connection, (Fig. 2c), is the most widely used. The endplate may be either welded to the beam giving a nearly vertical interface plane at the endplate (Fig. 3a) or welded to the column giving a nearly horizontal one (Fig.3b).

The attachment of endplate to the column is easier in handling during construction, gives more economic design and higher factor of safety due to the higher compressive axial force in the column than that in the beam. However, the attachment of endplate to the beam end is preferable by most of the designers.

The attachment of endplate to the beam end has the advantage of applicability in multi-storey buildings where the columns are made continuous across the floor level and spliced within the floor height, preferably at floor mid height or within the middle third of floor height. Thus, this software package considers only the configuration of extended column-trimmed beam which is applicable to both multi-storey structures and single story pitched roof.

2.2 Code Requirements

The Egyptian code of practice of steel construction and bridges ECP-ASD2001 [9] requires several checks on this type of connection. These checks include checks on welds, bolts, end plate bending, column web crippling at the vicinity of the beam compression flange, column flange thickness at the vicinity of the beam tension flange and column web shear at the corner panel. These are the checks implemented in the package so far.

Additional checks such as column web tensile stresses (yielding if ultimate conditions are considered) at the beam tension flange, column web compressive buckling, column flange bearing and endplate bearing will be implemented in the future.

2.3 Methods of Analysis

Approved approximate methods of analysis for the bearing type and friction type bolted end plated connection listed in [5] are adapted in this software. This method assumes that the endplate remains straight within the tension zone after deformation due to bending resulting in a linear distribution in bolts elongation; with a rectangular contact area in compression zone in the bearing type and no separation of plates in friction type.

Bernoulli's assumption of linear stress distribution is applied for the check of stresses on weld lines considering both resultant shear stresses and equivalent stresses as stated by the ECP-ASD 2001.

Column web crippling at the vicinity of the beam compression flange is checked considering the maximum strength of the beam compression flange, not the actual forces, as specified by the ECP-ASD 2001.

3 STCON V1.0'S FEATURES

The STCON v1.0 interface was designed to serve many features and has many advantages that can be summarized as follows:

3.1 Input flexibility

The STCON V1.0 input interface has the latest input flexibility facilities. All input fields can be handled with either keyboard or the pointing device. All connection types and configurations are interpreted by images that help to identify the components of the connection as shown in figure (4).

3.2 Connection configuration

The STCON V1.0 can handle four different configurations for the extended column– trimmed beam rigid connection according to the end plate extension as shown in figure (5):

- Extended endplate top and bottom; beyond the top and bottom flanges of the beam or haunch, this configuration is recommended for reversal of loading and seismic-resistant frames.
- Extended endplate top only; the endplate is extended beyond the top flange of the beam and flushed to the bottom flange of the beam or haunch, this configuration is used when no reversal of loading is anticipated.
- Extended endplate bottom only; the endplate is extended beyond the bottom flange of the beam or haunch and flushed to the top flange of the beam, this configuration is used when metal decks are used interfering with any components above beam top flange.
- The flushed end plate which is used when the two conditions specified in (2) and (3) are combined together.

3.3 Haunch girders

For all the above four configurations, the beam can be optionally strengthened with a haunch making a total of eight configurations, which the software can handle.

3.4 Material properties for beam, column, welds and bolts

The ECP assumes no differentiation in material properties between columns and beams in its checks, e.g., check for crippling of column web and column flange thickness at beam tension flange vicinity. STCON v1.0 includes this differentiation in material properties between columns and beams which is a common practice in multi-story structures with heavy loading where columns are made of higher grade of steel while beams are made of mild steel to control the deflection in them. Thus, the above mentioned checks are made according to [4] taking steel grade into account.

3.5 Bolt types

Three types of bolts can be utilized in STCONv1.0; ordinary bolts in bearing type connections even though they are almost obsolete, high tension bolts of both bearing type and friction type. Limitation of bolt grade to be used as friction bolt is built in the software.

3.6 Load cases

No practical limit for the load cases the STCON v1.0 can handle. Also, reversal of straining actions is accounted for and complete control of adding, modifying and deleting of any load case is in hand.

3.7 Input validation:

3.7.1 Restrictions for input data completeness

All the above mentioned features are gathered in the first form of the module which identifies the input from the main element design stage. Other design input for the connection components and connecting parts are gathered in the second form. Moving from the first form to the second one, STCON v1.0 insures that the data entered are complete, the software prohibits the user from advancing unless all mandatory data are entered as shown in fig. (6).

3.7.2 Restrictions for interface-wise input data validation

Input validation is a well-known concept for all interactive-interface software programmers. It is a concept that insures that the types of data entered by the user are limited to the data types they refer to, e.g., a field representing a distance or a dimension is restricted to positive numeric values only and no alphabetical characters can be entered in that field. This concept of interface-wise input validation can be regarded as driven-user data checking.

3.7.3 Restrictions for engineering-wise input data validation

The concept of interface-wise input validation was extended to engineering-wise input validation. This may be considered as the most important feature implemented in STCON v1.0 software. Input data are checked automatically as they are entered. For example, while defining a section for a beam or a column, STCON v1.0 validates that the web height cannot be of zero or negative value and prohibits the user from advancing (Fig. 7) unless he/she corrects the mistyped input error (Fig. 8). A series of 25 checks validates each input data entry for both logic and code requirements (Fig. 9). Most of these checks cover the aspects of minimum pitches between bolt rows, edge distances, maximum weld size to specific plates, minimum plate thickness and local buckling requirements. Like the check of data completeness, STCON v1.0 also prohibits the user from running the problem unless all input data are validated as shown in figure (10). This feature is important to get an error-free runs especially when doing the so-called what-if analysis as explained in the next section.

3.8 What-if analysis

The main advantage of spreadsheets over software programs is their input simplicity especially during the so-called "what-if analysis". The "what-if analysis" is usually done after a successful run of a problem looking for a more suitable solution, i.e., it can be viewed as a non-automated optimization process. So, STCON v1.0 is designed to have the spreadsheet advantages in a software package.

By smooth navigation through the data, the user can adjust any parameter and look "**WHAT**" will happen "**IF**" he/she alters a certain parameter, keeping in mind that engineering-wise input validation insures that every "**IF**" is logically valid and applicable according to the ECP ASD2001 requirements and no "**IF**" is non-applicable.

3.9 On-screen output summary

An on-screen output summary is provided to simulate the spreadsheet, (Fig. 11), to get the results at-a-glance especially during the what-if analysis

3.10 Extended calculation notes output:

An extended calculation note output is provided both in softcopy as a text file to give the user complete control on the output format and in report format using Crystal reports 10[®] for professional reporting.

3.11 Drawing module

A drawing module is provided for further visual check of the input data (Fig. 13), with complete zooming and panning options (Fig. 14). Newer version is intended to be provided with DXF exporting options.

4 VERIFICATION PROBLEMS

Several problems were analyzed by STCONv1.0 for the variety of configurations it covers. Sixteen examples are solved using STCONv1.0, PROKONv1.7.1 and manual calculations representing four different endplate extension configurations, with and without haunches and using both bearing type high strength bolts and high strength friction grip bolts.

Comparison of results to manual calculations is perfectly verified for all configurations. PROKONv1.7.1 being based on LRFD codes while STCONv1.0 being based on ASD codes prohibits the full comparison but a good relevance of utilization factors between STCONv1.0 and PROKONv1.7.1 is observed.

5 CONCLUSIONS

A software package for beam-to-column rigid connection analysis and design is developed using Visual Basic 6.0 to help analyzing and checking all components of this type of connection.

The software considers four different configurations for the endplate extension, with or without haunches, different material properties for columns, beams, welds and bolts, different bolt types, and unlimited load cases with reversal loading.

The software package comprises a concept of driven-user data checking through restrictions for both interface-wise and engineering-wise input data validation. Advantages of spreadsheets and programming are integrated together in a non-automated "what-if" optimization process. The software package is equipped with navigation tools, input and output file handling, reporting tools and drafting tools to be suitable for practical usage.

An integrated version of the software package that imports input data from SAP2000® with complete control is currently under development and will be released soon. This version imports the geometry of beam and column sections and slope along with the loading combinations for all the joints specified by the user and creates the input files for them.

ACKNOWLEDGEMENT

The author would like to acknowledge the efforts of **Eng. Wael Abdel-Mageed Hasan**, Institute of Statistical Studies & Research (ISSR), who broke through considerable milestones in the present software package especially in file handling and software inter-relations through valuable discussions and suggestions due to his premium proficiency in Visual Basic.

Also many thanks are due to **Prof. Dr. Metwally Abo Hamd**, Head of Civil Engineering Centre for Research & Studies (C.E.C.) – Faculty of Engineering, Cairo University and **Prof. Dr. Sherif A. Murad**, Faculty of Engineering, Cairo University for their valuable suggestions about the software development.

The author also would like to acknowledge **PROKON software Consultants Ltd.** for providing him with the demo version of their software package.

REFERENCES

1. Ballio G. & Mazzolani F.M., "Theory and Design of Steel Structures", 1st ed., Chapman and Hall, New York, 1983.
2. COSMOS/M User Manual, Version 1.7, Structural Research and Analysis Corporation, Santa Monica, California, 1994.
3. ETABS User Manual, Computer and Structures Inc. CSI, Berkley, USA, 2002.
4. Kulak G.L., Fisher J.W. & Struik J.H., "Guide to Design Criteria for Bolted and riveted Joints", 2nd ed., John Wiley & Sons, New York, 1987.
5. Machaly S.B. "Behaviour, Analysis and Design of Steelwork Connections", 4th ed., 2002.
6. PROKON User Manual, Ver. 1.7.01, Prokon Software Consultants Ltd., Dec. 2000.
7. SAP2000 User Manual, Computer and Structures Inc. CSI, Berkley, USA, 2002.
8. STAAD PRO User Manual, Release 2004, Research Engineers Intl., 2003.
9. The Egyptian Code of Practice for Steel Construction and Bridges (Allowable Stress Design), Code No. (205), 1st ed., ECP-ASD2001, 2004.

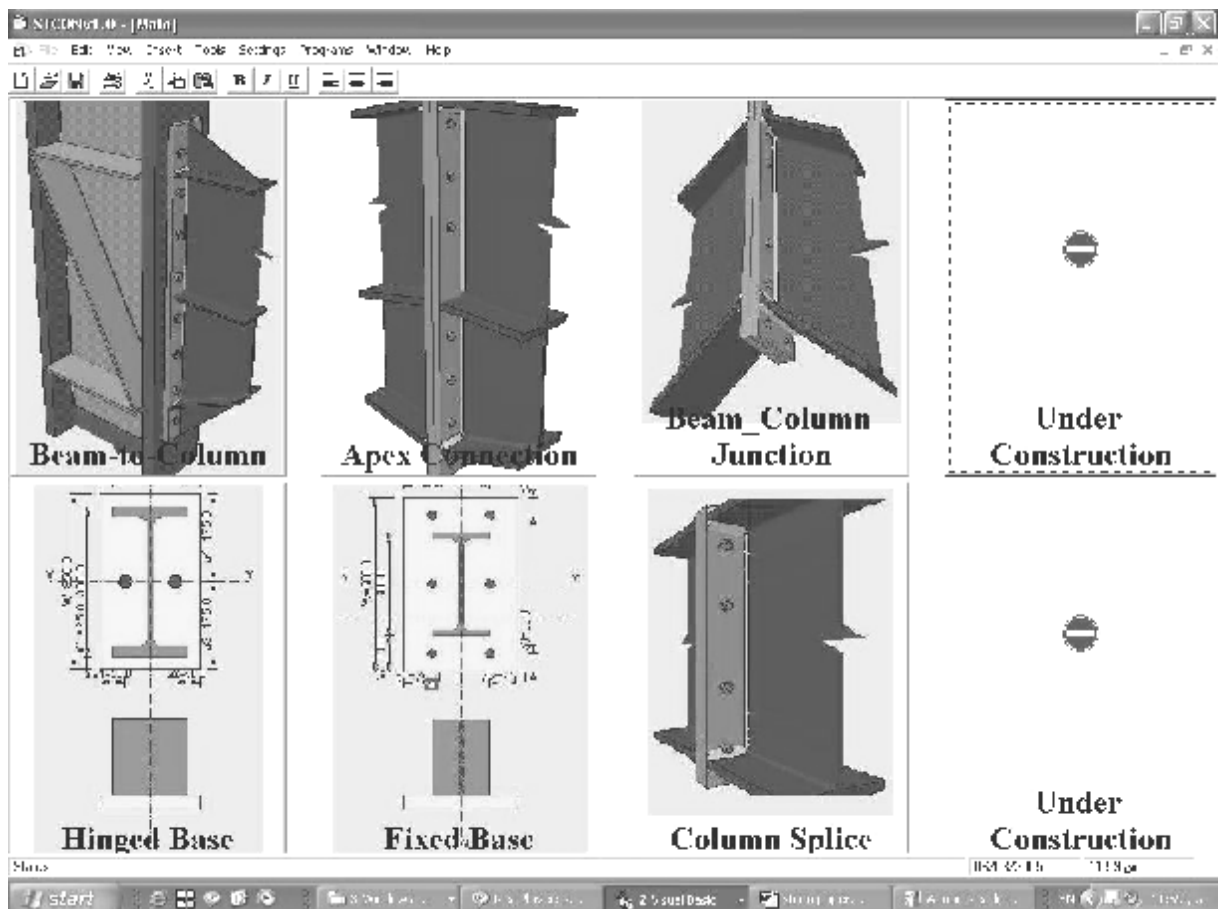


Fig. 1: STCON v1.0 main modules

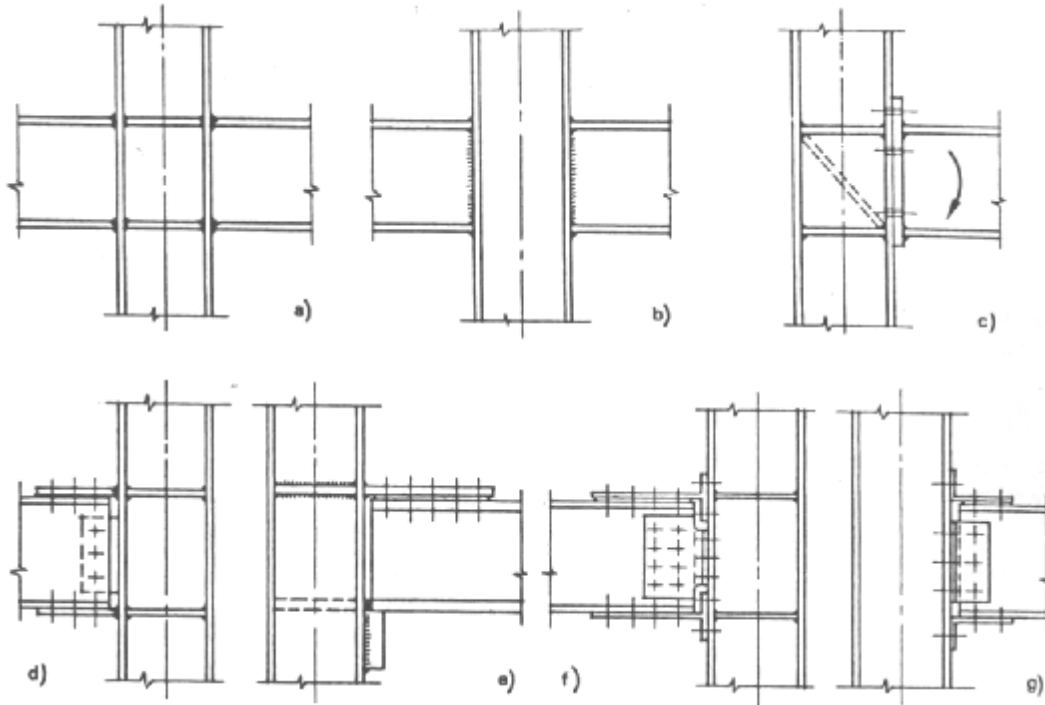


Fig. 2: Different configurations for beam-to-column rigid connection (Courtesy Ballio & Mazzolani, 1983 [1])

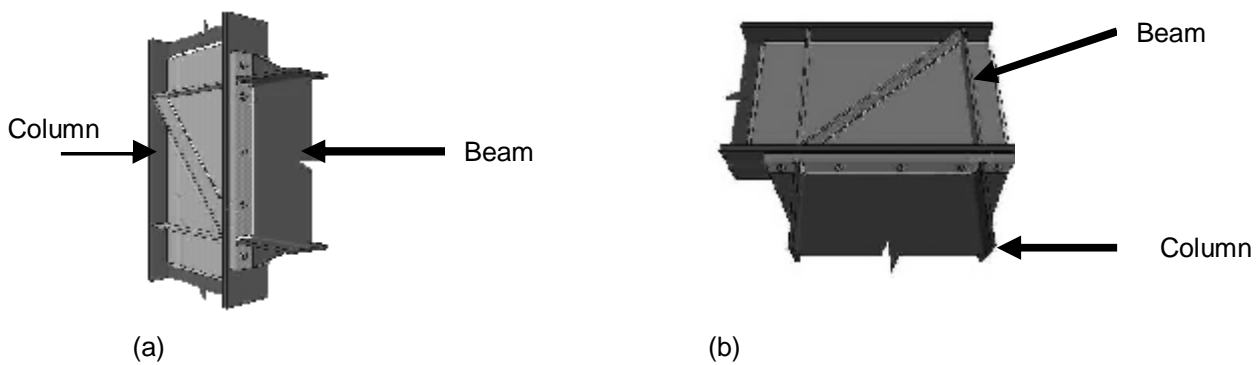


Fig. 3: End-plated beam-to-column rigid connection: (a) Extended column-trimmed beam, (b) Trimmed column-extended beam.

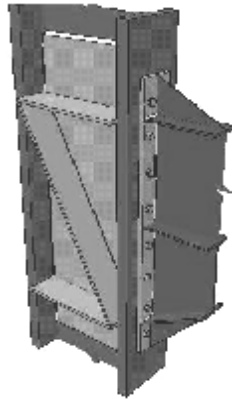


Fig. 4: Components of beam-to-column rigid connection

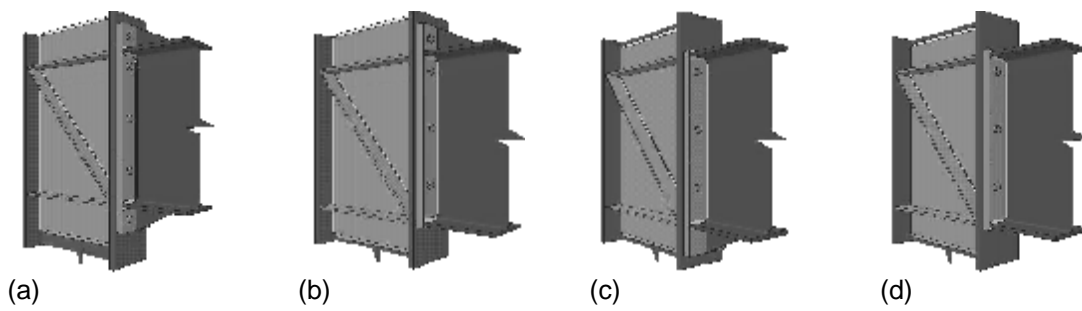


Fig. 5: Different configurations according to end plate extension

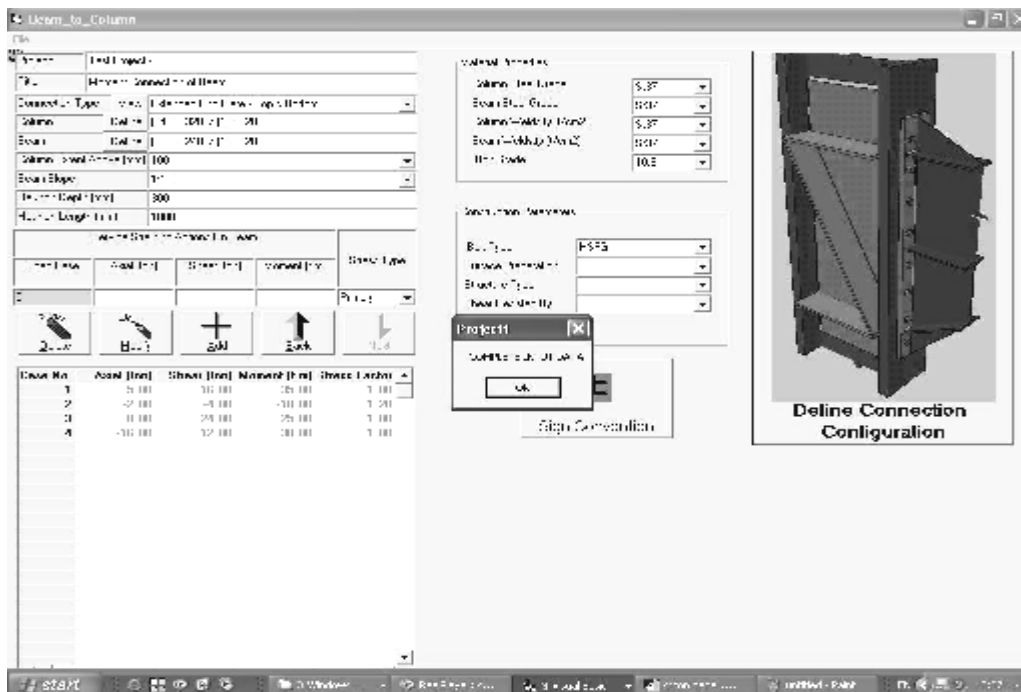


Fig. 6: STCON v1.0 prohibits the user from advancing unless all mandatory data are entered.

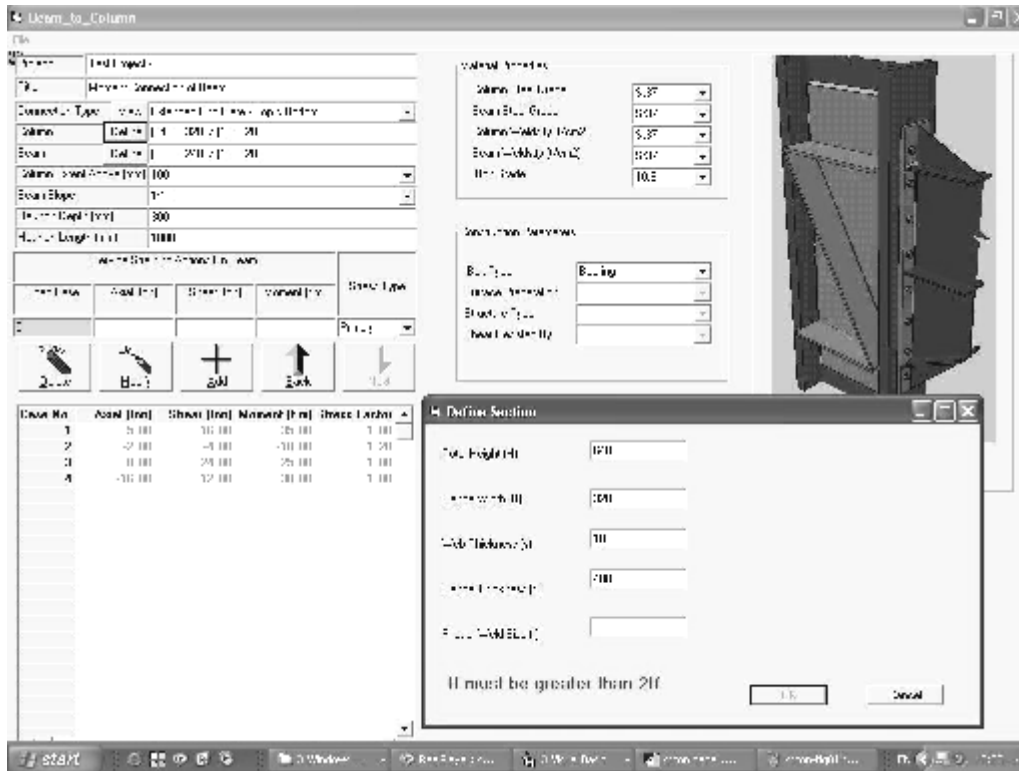


Fig. 7: Input data are logically checked

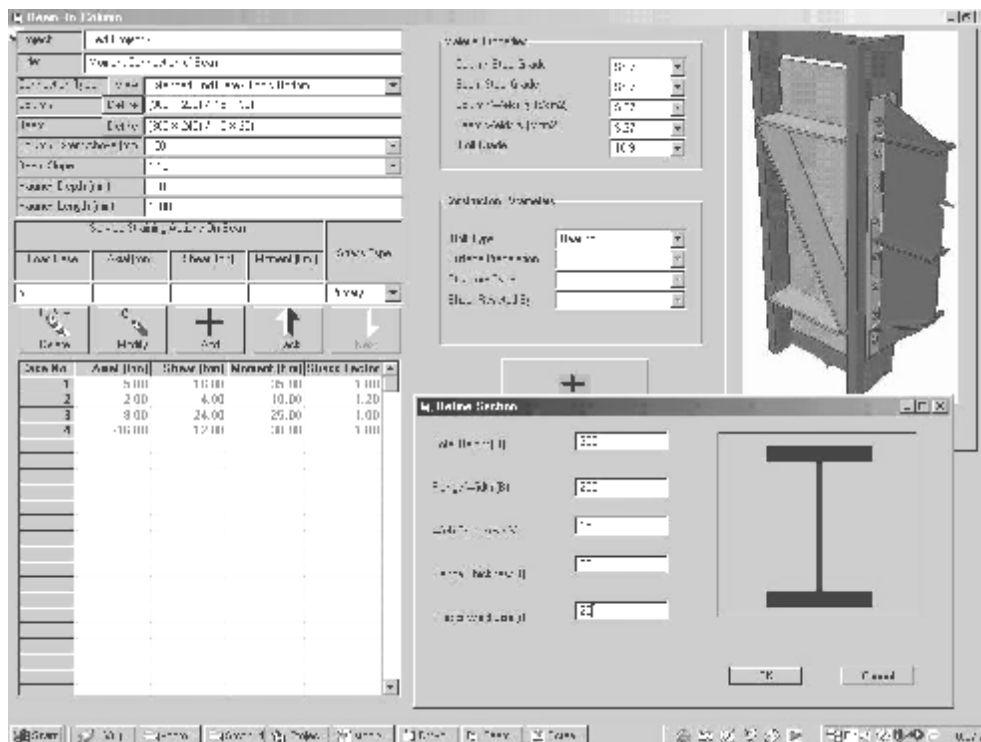


Fig. 8: Correcting errors returns the control to the user

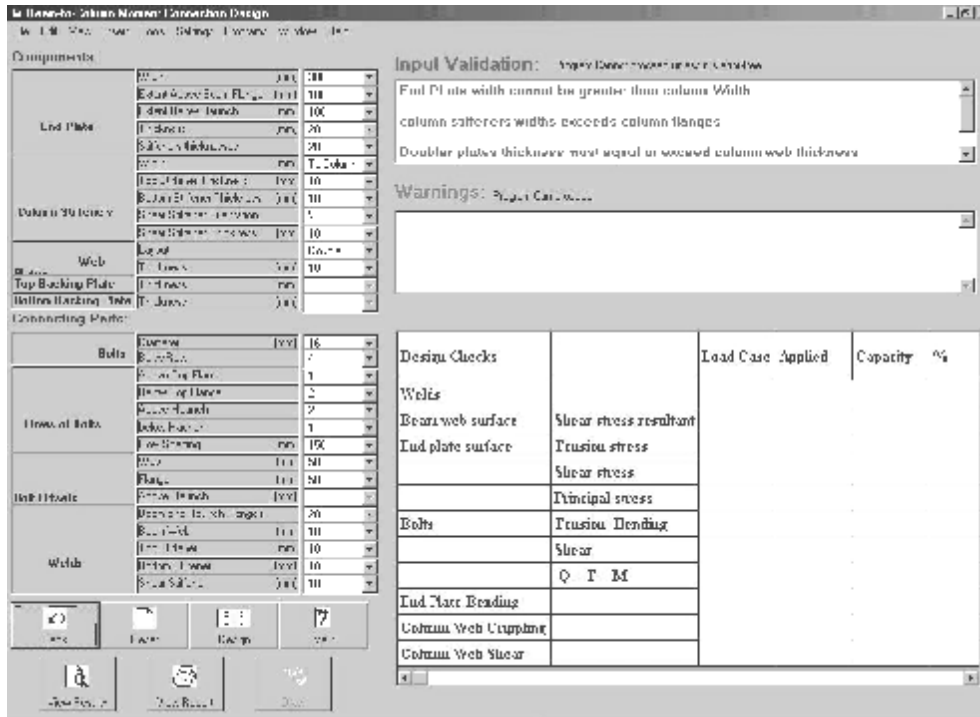


Fig. 9: Engineering-wise input validation

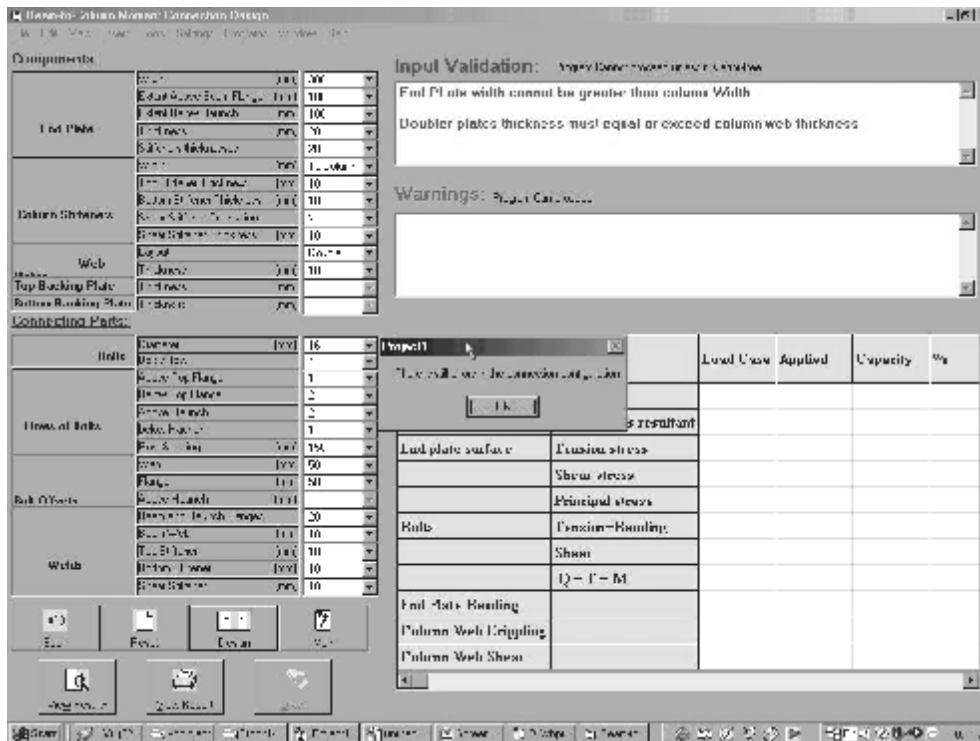


Fig. 10: STCON v1.0 prohibits the user from advancing unless all input are valid.

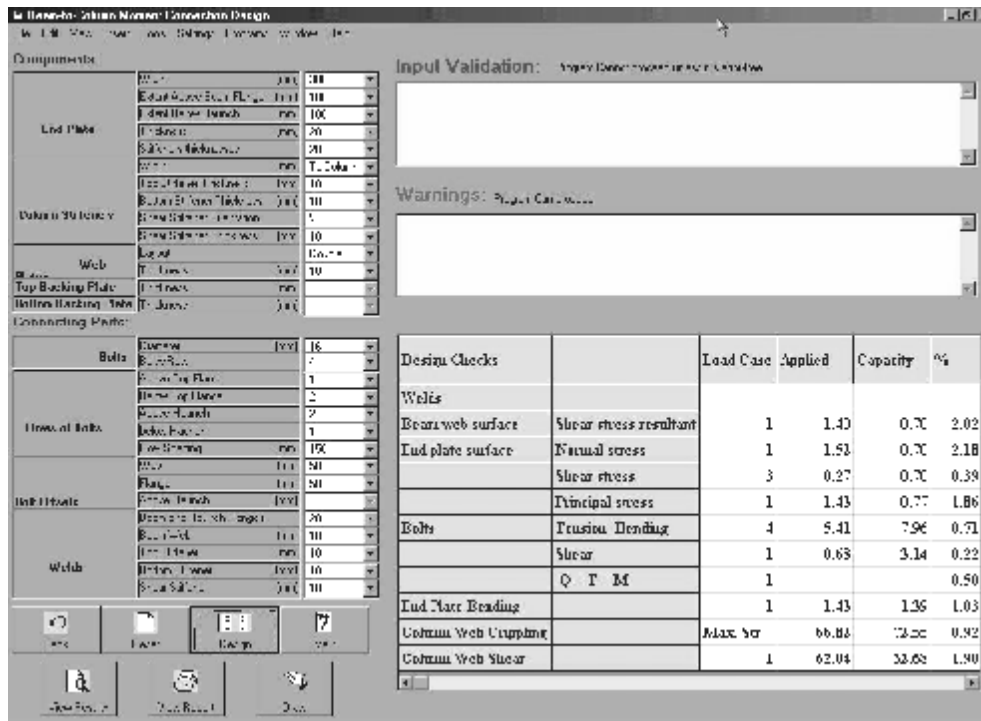


Fig. 11: On-screen output summary

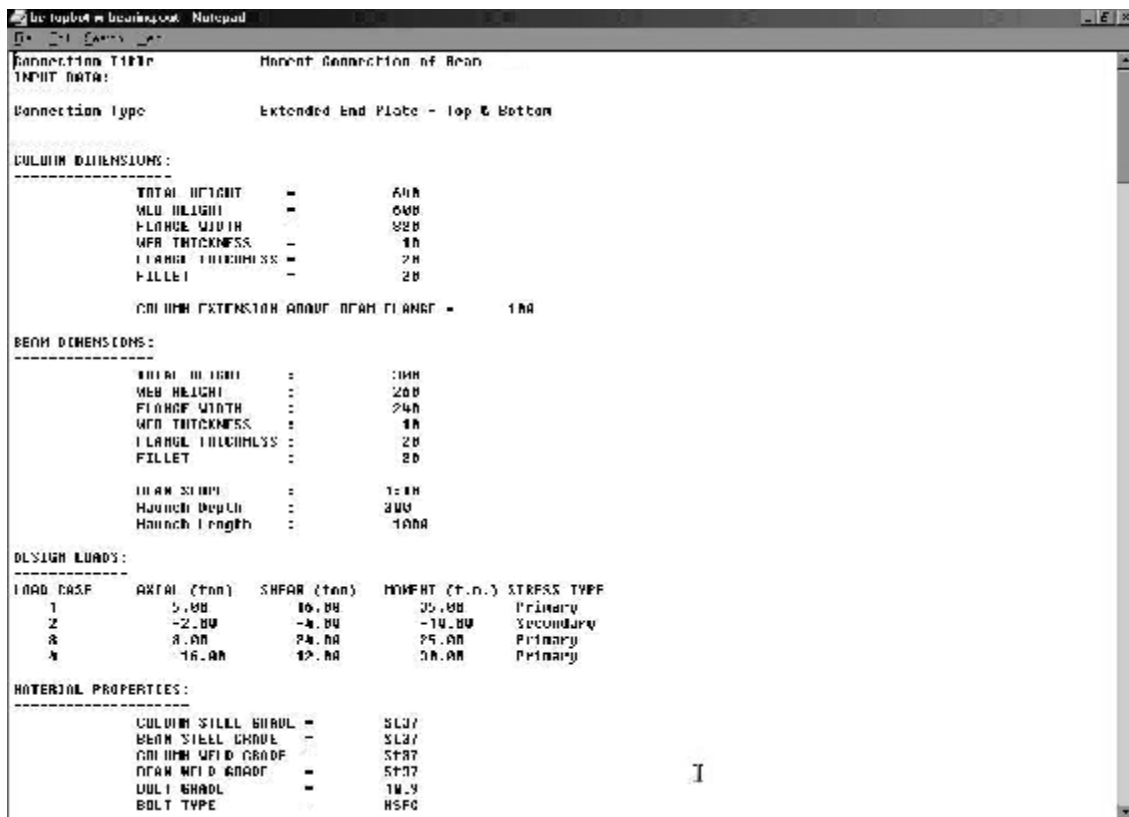


Fig. 12: Extended calculation notes output

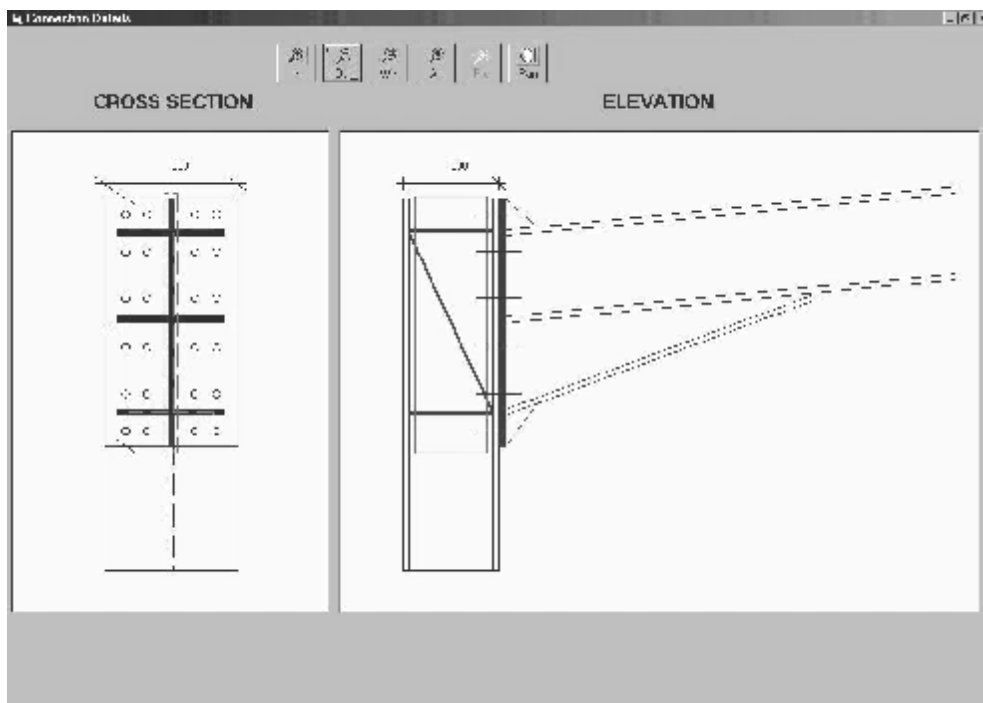


Fig. 13: Drawing module

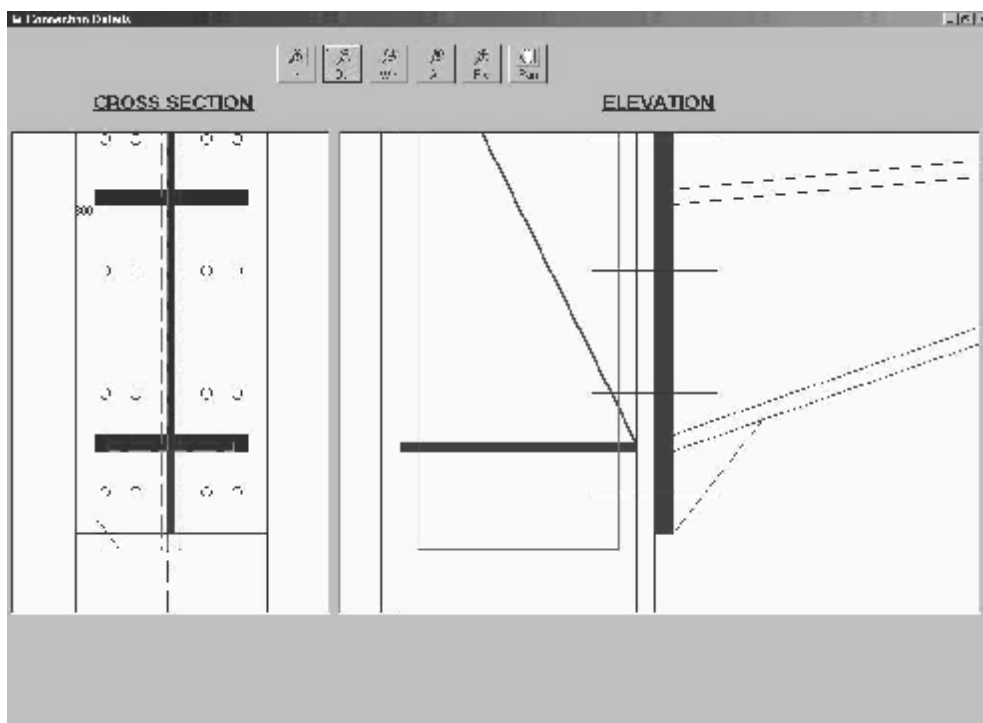


Fig. 14: Complete zooming and panning options

POST-SUBURBIA ARABIA

W. EIRIK HEINTZ

American University of Sharjah

ABSTRACT

This paper explores the growing influence of Western design in the Persian Gulf country of the United Arab Emirates. It focuses on how American design and ideology have transformed the landscape of the desert kingdom of the UAE and how these “American” ideals have been transformed through a unique Arab interpretation. From the macro-scale of the city to the micro-scale of the single-family home, the built environment of the UAE is probably the closest example of an American design ideology outside North America. While many in the Arab community are opposed to American foreign policy, they often embrace many aspects of American culture and lifestyle. The discovery of oil in the mid-twentieth century created the region’s wealth and brought an influx of capital and foreign workers who, together with the nationals, have created a diverse and dynamic society with global aspirations.

INTRODUCTION

Located on the northeastern edge of the Arabian Peninsula on the shores of both the Arabian Gulf and the Gulf of Oman, the United Arab Emirates has seen astonishing growth over the past 40 years. Trade has long been the mainstay of the city’s economy but the discovery of oil in 1966 led to the development of more modern social and economic infrastructure. (Dubai Explorer 2002). This rapid development leads to the need for imported labor. Today, about 80 percent of the population of 3.5 million is expatriates. Many of these expatriates are laborers who hail from the Indian Subcontinent. However a number are well educated Westerners who work alongside the Emirates nationals to bring about the nation’s rapid development. The UAE has enjoyed a 10 percent GDP annual growth for the past decade, and the population has increased 25 percent in the past five years. (ameinfo) Both the Emirates and the growing expatriate population have embraced a consumerist lifestyle and its design implications, which are perhaps typified by the American popular culture. Design is imported for an eager population that knows America through its movies, television, clothes, music, chain restaurants and other consumer products.

The UAE is building its communities and cities much closer to the American model rather than a European or indigenous model. The notable architecture and urban developments of the last decade and those planned for the future are much more similar to North American suburban development. These new, high profile developments are designed to attract business, capital and tourism. Often, their scale and novelty are designed to elicit media attention. One reason for the adaptation of the American model is that many of the architects and designers responsible for the cities new development are from North America. Another reason is that these new developments rely on an infrastructure of automobile access. It seems that the automobile-dependent, multi-centered city layout is the urban form that best supports the rapid development and the scale of global business. Like major American cities, those of the UAE are designed around a pluralistic and diverse population.

European influence is evident in many of the UAE cities. A British protectorate until 1971, the UAE was definitely influenced by this relationship. The road system features roundabouts at many intersections—a definite British influence. Many of the older parts of Dubai, built in the early 1980s, show a European influence. For example, the city blocks in the neighborhood of

Kerama incorporate mixed-use development, with commercial space on the ground floor and apartments above. These modernist blocks define the street edge and open-up on the interior of the city blocks to shared areas. Most of these urban developments are generic in design however, and better suited to a European climate and density.

The traditional Arabian city, although viewed nostalgically by Western tourists, does not have the infrastructure to support businesses seeking to participate in the global economy. It is dense, labyrinthine and pedestrian-based. Its small space and lack of the latest technologies are not supportive of the modern business model. The old town is better suited to small-scale commerce.

The fragmentation of the city to a multi-centered amorphic layout is not necessarily at odds with the tradition of Arabian cities. Historically, areas of Arab cities were divided up into particular neighborhoods and dotted with various *souks* (markets) that specialized in particular goods. While residential and business areas were combined, each type of business had its own zone or *souk*. For example, one would find a plant *souk*, a spice *souk*, the gold *souk*, the carpet *souk* and so on. This traditional zoning has been expanded to create new urban developments that represent the “goods” of present and future Dubai. Enclaves such as Media City (advertising, public relations, media *souk*) Internet City (information technology *souk*), Knowledge Village and University City (university *souk*) and Festival City have become islands scattered throughout the urban and suburban landscape of Dubai and the neighboring emirate of Sharjah. The difference with these new urban developments is that they are much larger and many have become detached from the fabric of the city. They are self-contained units located beyond the city core.



Front Gate at Dubai Internet City



Typical building at Dubai Knowledge Village

As mentioned above, the new development that describes the cities of the UAE is designed around the automobile. With a large population of citizens and expatriates who can afford their own vehicle and with an excellent system of roads and highways, the freedom and convenience that is afforded by the automobile is understandable. This coupled with the lack of any other real public transportation system as an alternative, means that as the population explodes, traffic increases exponentially. The Dubai and the neighboring Emirate of Sharjah municipalities are continually building, widening and creating new road systems to keep up with growth. American suburbanization led to the abandonment of the city core. In Dubai, this has not happened. The pedestrian city of the old town continues to be a thriving, congested space of buying, selling and trading. They have just been transformed and populated by merchants with less global and more regional aspirations. The city center has lost some of its primacy to new large-scale shopping malls. One reason for this is due largely in part to the climate. For at least six months of the year, it is too hot and humid to be outside. Locals and expatriates of financial means opt for leaving their air-conditioned homes in air-conditioned cars to go to air-conditioned offices and air-conditioned shopping malls rather than walk from shop to shop in the old town. The historic centers of Dubai and Sharjah have been transformed by merchants from other parts of the Islamic world who are used to living without the luxury of air-conditioning and their own mode of transportation. New outlets have sprung up to cater to the Indian and Pakistani

population and to the growing number of Western tourists who are eager to see the romantic Orientalist image of the Arabian city with its exotic souks selling gold, spices and carpets from around the region. These areas of the city are dirty, congested and very hard to drive to, let alone find a parking space. Most people are much more attracted by the sanitized, air-conditioned modern shopping malls where convenience wins out over tradition. You still see many locals using the city center to take care of specific business needs. The shopping malls have become more of a leisure activity and social space.

In Dubai, time has been compressed. Because the ruling families are instrumental in both the government and the economic and business development, the process of designing and building is streamlined. While the transformation of the American city from a pre-modern city to the present has developed over a roughly 100-year period, Dubai has experienced this transformation in only 30 years. Mario Gandelsonas, in his book *X-urbanism*, has described the development of the American city through seven urban scenes. These scenes trace the development from the Renaissance city, the Baroque, the gridded, the city of skyscrapers, the modernist, to the suburban city with the final scene being the development of the X-urban city. In many ways, the multi-centered X-urban city is an American phenomenon. Yet Dubai, which is almost unrecognizable from how it appeared just 10 years ago, is being created or re-created as an X-urban city. The modernist city and the development of the suburban city that played out in American over a 40-year period have been compressed into a 15-year period--from the mid-1970s to the beginning of the 1990s in Dubai. The historical part of Dubai has been dwarfed by a modern, clean city of the future. The city's monumental architecture has changed from traditional windtowers to the glass and steel Emirates Towers (presently the tallest buildings in Europe and the Middle East) and the Burj al Arab, the tallest freestanding hotel in the world. The continual march to build a modern, world-class city of skyscrapers exacerbates a latent typology characteristic of the American city. (Gondalsonas p.23)



Emirates Towers on Sheik Zayed Road



The Burj al Arab

If there were one city that Dubai mostly closely resembles, it would have to be Las Vegas. Except for the gambling, these two desert cities share much in common. First, the economic growth of both cities is affected considerably by the tourist industry. Dubai, which was once a stopover for European flights en route to Asia, is now being developed as a major tourist destination for both leisure and business travel. Second, both are very artificial environments. The developments that cater to the tourist and expatriate population present an idealized Arabian image and lifestyle. New luxury hotels and conference centers are being built at a staggering rate to attract tourists and business travelers from other parts of the Middle East and Europe. Like Las Vegas hotels, these new "theme" hotels are self-contained environments offering restaurants, bars, nightclubs, shopping and leisure activities. In developments like these, the architecture and urban planning reinforces the fragmentation of the city fabric with buildings designed to stand on their own and be self-sufficient. These buildings are designed

and marketed to appeal to the tourist and appear unconcerned with the physical connections to the rest of the city. If there is a single building that typifies the new image of Dubai, it is the Burj al Arab. Besides being the tallest freestanding hotel in the world, it is also the world's first seven star hotel. Built on its own man-made island 200 meters offshore, the Burj is designed in the image of a billowing sail yet is very high tech and modern. Opened in 1999, the hotel has become an icon. For example, it is pictured on Dubai license plates, and souvenir shops at competing hotels feature miniature crystal versions of the Burj in all sizes.

The strong design influence that Dubai takes from North America is represented in many forms. The preferred neighborhood form is the residential development designed, in many ways, like upscale North America models. The design of residential units at Dubai Creek Country Club mixes an American influenced driveway and garage at the front of the house with Arabian architecture. Although UAE crime levels certainly do not warrant it, many of these new developments are gated or at least have a security officer at the neighborhood's only entrance. The local Arab population, who has traditionally separated public life from private life, embraces this type of development. In addition to gates at the neighborhood entrance, a high wall with a large gate surrounds many freestanding houses. These walls provide privacy for the women of the house (some of whom choose to wear the veil or *hijab* when in public) away from the public view of the street. Additionally, these residential developments, like the theme hotels, are separate and distinct from the fabric of the city. Like suburban America, these neighborhoods are designed with all the conveniences of shopping and restaurants so that residents no longer have to rely on the city center to for day-to-day needs. The peace and quite and leisure lifestyle of the suburban neighborhood is an appealing alternative to the congested and dense neighborhoods of the city center. Like the cities of North America, Dubai is made up of multiple cities within cities, each catering to a different segment of the population.



Houses at the Dubai Creek Country Club

As with new hotels of Dubai, these suburban residential communities are designed around a "theme." Perhaps one of the more ironic communities is that of the Andalusia Villas at Emirates Hills. The houses incorporate design motifs taken from Andalusian architecture and thereby "re-import" that which was exported to Spain from the Middle East centuries ago. Another notable residential community is Arabian Ranches. This new self-contained community being built on the very edge of the desert incorporates 5000 "desert inspired homes" with an equestrian center, riding trails and polo fields to complete the ranch theme. It also includes a golf course, spa and a town center with retail shops. Like their American counterparts, some of the most sought-after residential developments are designed around golf courses and incorporate water features. However, this is not because the Arab population plays a lot of golf; it is primarily a symbol of wealth to have a lot of water and green space surrounding one's house. Additionally, the golf course, as a recreational outlet, is there to attract the Western expatriate population.

Shopping Malls as Community Center

In Dubai, visiting the shopping mall is a favorite pastime for both locals and visitors. Historically a trading city, Dubai is famous for its duty-free shopping and the lowest prices for gold jewelry anywhere in the world. A website describing the benefits of living in Dubai notes that “family shopping and selected entertainment and entertainers from around the world are



Pyramids at Wafi City Shopping Mall



Entrance to Wafi City

transforming the city of Dubai into one big shopping mall.” (Andaluciadubai.com) The shopping mall has replaced the *souk* as the preferred place for leisure shopping. The shopping mall provides air-conditioning, western clothing stores, restaurants and parking convenience that the traditional *souks* of the city center cannot provide. Most new developments incorporate at least some form of shopping mall. In spite of its artificiality, the shopping mall is the most public and social space in the city and so a great deal of care goes into the design and theme of each mall to attract the preferred clientele. The population of Dubai is incredibly diverse in ethnic, social and economic background. The shopping mall, like no other space in the city, brings this diverse population together. Borrowing design ideas out of a Las Vegas guide to architecture, the “theme” shopping centers incorporate motifs as diverse as the Pyramids at Wafi City, designed as an Egyptian stage set; Mercato, designed as an Italian city block; the new Madinat Jumeirah, designed as a traditional *souk* complex complete with traditional wind-towers; and the new Ibn Battuta Mall with with themed courts comprising architectural imagery of Andalusia, Tunisia, Egypt, Persia, India and China.



Andalusian Court at Ibn Battuta Mall



Tunisia at Ibn Battuta Mall

Shopping in Dubai has become a major tourist attraction. Since the terrorist attacks of September 11, 2001, residents of the Middle East have been less likely to travel to North America for shopping. Instead, they have flocked to Dubai, which has provided an almost equal alternative in quality and variety. Once a year, Dubai hosts the month-long Dubai Shopping Festival with citywide sales discounts and a Global Village with merchants from all over Asia, Africa and Middle East. It is a truly consumerist event with all the novelty of a world's fair. The new Mall of the Emirates, planning to open in 2005, promises to be the largest shopping mall outside North America with 350 shops and spread over 2.4 million square feet. (ameinfo.com) It will also include a 400-meter-long indoor ski run using real snow. Peter Walichnowski, the chief executive officer of the project, stated that he "hopes the Middle East will choose Dubai over traditional destinations such as Europe and America for their special shopping and leisure needs." In addition to this, the shopping mall is as much of a hang out for the youth as it is in the states. In Dubai, the mall is even more intense as a social space since traditional families do not allow their children the same independent roaming as those families in the West. The shopping mall provides just enough freedom of movement to be acceptable.



Mercato Shopping Center



Madinat Jumeirah

The supermarket is another vestige of American design that has penetrated the market in the Middle East. The giant supermarket chains present in the UAE look and function like any supermarket in America and include many of the same (or similar) products as well. However, these supermarkets have not shut down the independent grocers, which has unfortunately happened in some cases in America. Many of the small independent grocers have a very

specific customer base, such as Subcontinent laborers who live nearby and walk to shops. The large supermarkets cater to the middle and upper income local and expatriate population, who have their own transportation, and provide a variety of items from all over the world to appeal to the diverse populations that live in Dubai. Along with the shopping malls, these supermarkets are where the diverse populations of locals and expatriates mingle.

While there may not be a drive through at every intersection, American fast-food chains seem to be popular with all members of the population. Small towns across America share this now global cuisine of Hardee's, Burger King, McDonald's, Dunkin Donuts, Pizza Hut and Kentucky Fried Chicken with Dubai and Sharjah. It is perhaps this vestige of America that stands out the most in the cities of the UAE. Some menu items have been introduced to cater to more local tastes, such as the McArabia (a chicken sandwich served on Arabian bread), but the ubiquitous burgers and fries have become synonymous with the American lifestyle that penetrates these other cultures. In the shopping malls, these chains greatly outnumber those outlets that feature Middle Eastern food. Starbucks has numerous locations in Dubai.

Conquering the Desert

The development and growth of most American cities relied on the boundless space of the American landscape. This was characterized by the soft edge of the suburbs that was always free to expand as populations grew and as economic and market forces permitted. Dubai, with its placement at the edge of the desert, is not so different. With the introduction of the technology to produce drinking water from desalination plants, the unimpeded expansion of the city into the desert is now possible. In Dubai most development is taking place parallel to the beach along a stretch of highway known as Sheikh Zayed Road, named after the founding and current president of the UAE. Yet, other developments are taking place far out into the desert where the land is very inexpensive with the expectation that in a few years' time the city will grow out to meet them. Some of these residential developments are literally surrounded on four sides by rolling dunes where camels graze. What is perhaps more striking is the number of developments that have not relied on the inexpensive, unoccupied land surrounding Dubai to build new multi-use developments. Instead, some developers have created islands offshore in the Arabian Gulf. Two such developments, the Palm Jumeirah (nearing completion) and the Palm Jebel Ali, are massive palm-tree shaped islands so large that they supposedly will be visible from the moon. What makes these developments attractive is that they add beachfront property. The Palm Jumeirah, which extends 5 kilometers into the Gulf, will add 120 kilometers of beaches and include 2,000 villas and 40 luxury hotels. The Palm Jebel Ali will be even larger.

Cultural Identity and the Arab City

The cultural identity of the Arab, as well as the Arab city, is undergoing an incredible transformation. The local population is trying to shape its modern global aspirations as a world presence without losing its history. However, history in this part of the world is more about family, religion and business rather than the built environment. The architectural and urban identities have always been very fluid in this part of the world. Islamic design has generally favored the decorative aspect over the spatial, the two-dimensional over the three-dimensional. The Islamic architecture seen in the UAE has been borrowed from images of Mogul India, Pakistan, Iran and other parts of the Muslim world. The origins of even the most iconic of gulf architecture such as the wind towers of the Trucial Coast and the forts of the Ottoman Empire were established outside the gulf before being introduced to this region. This aspect has given the UAE a very limited repertoire of architectural and urban vocabulary. Before the introduction of oil, the coastal areas and interior of the Arabian Peninsula were occupied by merchants and traders. These merchants were greatly influenced by the other cultures with which they traded. Today, it is the same; the only difference is that the trade is global and so too is the architecture and urbanism. Despite the artificiality that characterizes much of the city, Dubai is an incredibly vibrant, diverse and cosmopolitan environment. The traditional elements that make a city a good place to live are not so apparent here. There is a lack of cohesion that characterizes almost every aspect of the city. There is a lack of public infrastructure. It is a city very much dependent

on the automobile. Each new project, whether it is a mall, hotel, office tower or residential development, has the objective to stand on its own, to create its own identity. The city is fragmented into architectural and urban stage sets designed to appeal to an incredibly diverse population. In some way, Dubai is in the midst of inventing another form of authenticity, one that does not reflect a cohesive indigenous society with the city and architecture as a remnant or artifact of the culture. Dubai's authenticity and identity come out of the fact that this is a city designed by foreigners, built with foreign labor, maintained by foreign labor, and bankrolled and governed by members of the local Emirati population. It is a city designed around consumption and mass appeal and to maximize financial opportunities and the lifestyle this affords. Its lack of urban and architectural unity comes from the extreme diversity of its population and the diversification of its business development. Its authenticity comes from the fact that Dubai and its Arab and expatriate population are engaged in a struggle to recreate their identity within a new global context.

BIBLIOGRAPHY

Brown, Denise Scott, "Invention and Tradition in the Making of American Place." Harvard Architecture Review, volume 5, Rizzoli International Publications, 1986.

1. "Dubai Shopping," <http://www.andaluciadubai.com/shopping.htm>, 2002, accessed April 30, 2005.
2. "Dubai population growth fuels GDP expansion," <http://www.ameinfo.com/16342.html>, 2001. accessed April 30, 2005.
3. Gandelsonas, Mario, X-Urbanism: Architecture and the American City. Princeton Architectural Press, 1999.
4. Grist, Pamela, (editor), Dubai Explorer. Explorer Publishing & Distribution, 2002.
5. "Mall of the Emirates contractor announced," <http://www.ameinfo.com/29036.html>, 2003, accessed April 30, 2005.
6. Mapelli, Elisabetta, (editor) *AD Urban Environments*. Wiley-Academy, John Wiley & Sons Ltd. 2001.
7. Sorkin, Michael, *Some Assembly Required*. University of Minnesota Press, 2001.

URBAN PLANNING IN HERMOUPOLIS - A NEW VIEW ON THE CONSERVATION AND ENHANCEMENT OF HISTORIC SETTLEMENTS

J. STEFANO

Professor at National Technical University of Athens (N.T.U.A)

R. MITOULA

Lecturer at Harokopio University of Athens (H.U.A.)

ABSTRACT: Hermoupolis, capital city of the Cyclades, is a small but particularly important Greek City which was developed as a principal Greek urban centre in the 19th century, as part of the country's struggle for independence after 400 years of Ottoman Empire rule. A thorough research on the city of Hermoupolis determined with precision the content of terms such as "Historical city", "Historical Centre", "Traditional settlement"; it redefined the meaning of the terms "tradition, traditional", and even the terms "urban, urbanism", and clarified approaches to planning or other kinds of intervention in these contexts. Nowadays, it is generally considered that the protection of a place's architectural heritage mainly aims at the preservation and elevation of the place's physiognomy. This is arguably because, according to recent research on the physiognomy of cities, the various architectural and urban planning shells are a foundation for all the elements that constitute and present the physiognomy and character of a place.

Keywords: Hermoupolis, Urban Planning, Conservation, Historic Settlements

INTRODUCTION

The subject of protection and elevation of cultural – and particularly architectural and urban – heritage in Greece has a history of about 30-35 years. Greeks realized much later from other Europeans the value of architectural heritage that all previous centuries, and not just the Classical times, bequeathed to the country. And it was even later that we first arrived at systematic efforts for the protection and enhancement of this heritage.

VIEWS AND PRACTICES ON PROTECTION UP TO THE PRESENT

Museum Protection

The relations of Greece with Europe during the last quarter of the 20th century allowed, or in some cases even imposed, a relative concordance between Greece and Europe regarding methods of architectural heritage protection. This concordance, however, was essentially limited to the shaping of common views about the subject, rather than to any direct action. Consequently, significant protection-related projects, including those of protected sectors, were not applied in Greece.¹ The rest of Europe, including the Eastern European countries, thus proceeded in large organized interventions in several historical centres and settlements, besides the traditional "museum type" protection, undertaken by archaeological services, the Administrations of historical monuments (France: Direction des Monuments Historiques) or the Administrations of Fine Arts (Italy: Belle Arti) etc.² In Greece, however we continue to base the protection of architectural heritage on the Archaeological Administration or on characterizations of settlements as traditional, without, however, having planned any systematically organized intervention as yet. Several specialized studies of protection have been undertaken since the

1970's, but most of them only appeared on paper³ and, with a few exceptions such as the Athenian neighbourhood of Plaka⁴, the old city of Rhodes⁵, or the recent case of Rethimno, no special institutional body was constituted for the application and management of any form of intervention. In other cases, like the old city of Thessalonica, a lack of relevant experience and specialist knowledge combined with wrong estimations and choices produced rather negative results.

Hotelization

From all the known forms of protection⁶ only that of "tourismisation" or "hotelisation" could be considered as an organized effort with very positive results. Indeed, by systematically promoting the utilization of particularly important traditional settlements, such as the Vathia in Mani, the Ia in Santorini, or the Makrinitza in Pilion, the Greek Tourist Organization restored to a limited scale significant compounds in the above mentioned regions by converting them to specially designed hotels.⁷ The success of the undertaking (award by the Europa Nostra) does not mean, however, that this form of protection was or is the best or only choice regarding an organized policy of protection of architectural heritage. Of course, the fact that the only alternative to this economically efficient form of protection in Greece was that of "imposed protection"⁸ – in most cases, enforced via stiff and unskilled government services has, understandably, created a negative public attitude towards the subject.

This opposition has often been expressed through violent protests and clashes (as in the case of Hermoupolis during the 1970s) and with the circumvention of legal directions or even with an immediate resort to illegal building activity. The reasons of this opposition by the public outside the cumbersome strategies and unjustifiable delays of Administration authorities can be traced in the lack of public awareness and the fact that government institutions, such as the Church, the Army Services, or Public Welfare Agencies appeared to be excluded from those protection directives, making the laws effectively applicable only to the private sector. Thus, while this protection system has greatly succeeded in other European countries where the state and the public institutions set an example and shaped the models of protection, only in recent years has it become a common conviction in Greece that notable historical and traditional architectural shells or greater traditional urban areas should be protected. Even today, if one excludes small groups of well-informed citizens, most Greeks tend to link the protection of the country's architectural and general cultural heritage with tourist exploitation. However, even when the best of intentions have been adopted, viewpoints and expertise on the character and physiognomy of cultural heritage have up to now been limited and vague even among academic circles, and even more so in the area of everyday practice and control organisations. Thus, poor imitations, attempts to copy materials and the repetition of morphemes that are considered as tradition-enhancing in appearance and necessitate the adoption of a common so-called traditional style (as in the case of Mykonos), lead to a scenographic effect that is often deflationary and scarcely does justice to the value of any genuine elements.

Organised Sections of Protection

In this point we must reach certain decisions concerning the views that can be adopted on the issue. Between (a) complete and precise imitation (pastiche), (b) tolerance of the existing notable shells and (c) their complete depreciation, there is also the choice of (d) a creative incorporation, i.e. the truly difficult but creative architectural quest for new forms of architectural expression, which will meet the eternal and contemporary needs of the space with equal integrity and sincerity. Such architectural constructions, identifiable as "right" and "good" can be defined as "beautiful". Understandably, this point of view also entails great dangers. Every experience or inexperienced engineer who is legally deemed capable or licensed to carry out an architectural study, regardless of his training, his knowledge of the location, his sensitivity or talent, can use any forms he believes to correspond with the abovementioned conditions. Here, one could say that the basic key and only guarantee to this effort is the Architectural Control Committee. Indeed, this is the role of such a committee: to check, guide, and assist in the architectural design of a place with regard to the preservation and enhancement of its physiognomy and character. However, this presupposes a very high level of expertise among

the members of these committees, who would have to be of recognized prestige, with an appropriate cognitive background and experience and with a particular affinity towards the architectural values of each place. It is obvious that even with such scientists the recycling of knowledge, the attendance of relative seminars and conferences are also essential both to themselves and to the transmission of experience to their successors.

To the above mentioned points of reflection we will have to add some further thoughts. Nowadays, it is generally considered that the protection of a place's architectural heritage mainly aims at the preservation and elevation of the place's physiognomy. This is arguably because, according to recent research on the physiognomy of cities⁹, the various architectural and urban planning shells are a foundation for all the elements that constitute and present the physiognomy and character of a place¹⁰. The uniqueness of a city's physiognomy is based on the particularity of its landscape, i.e. its image. By "image" we imply the appearance of the city in a sense far broader than the merely visual. We refer to a landscape, which is related to all the senses: touch, scent, hearing and even taste, as a particularity of pleasures connected with our senses of hearing, smell, or taste that characterize a place. This notion thus concerns not only the senses, but also the various sentiments that a place offers us, as well as the opinion that we form and which finally composes our view of a place as a landscape (knowledge, sentiments and senses).

Today, through the effects of globalization, this particularity and uniqueness tends to be altered.¹¹ Local peculiarities are blunted and domestic elements tend towards uniformity. From the utmost northern to the utmost southern spot of Greece the same manmade tourist landscape is predominant, with objects that one can buy from the Athens tourist market. The same visual, auditory, olfactory and other stimuli are everywhere and generally an identical element of folklore prevails in most areas, arguably demonstrating a kind of mediocrity. The image that the modern man creates for his city is that of a modern way of life, that presents the same morphemes for the supermarkets, as for the gas stations, banks or fast-food restaurants (Goody's or Mc Donalds).¹² Even graffiti-covered walls make someone wonder about their purported international character. In their majority, people everywhere eat the same food, dress in the same clothes, have fun in the same ways, and this takes place in all Greek cities and of course everywhere in the world. Everything changes at a faster or slower pace, but by overwhelmingly destroying or irreversibly altering values and particularities that are precious and should be preserved not just for our sake but for future generations too.¹³

Active Protection

Efforts to deal with the above phenomenon were originally restricted to the safeguarding of shells in buildings that had been characterized as important in the history, architectural development and the cultural expression of a place. This interest predictably led to a kind of protection that, up to that time, was used by the archaeologists, the only individuals committed to the rescue and restoration of historical monuments: the museum-style protection. As known, a period followed where it became understood that apart from the shells, a significant role in what we define as architectural heritage and its contribution to the physiognomy of a place, belongs to the guarantee of continued use of these shells. This new phase focuses mainly on the tactics of protected sectors, i.e. on the organized and systematic restoration of entire historical centres and settlements.¹⁴ As the currently used terminology indicates¹⁵, the interest is divided between the shells and their use.

Finally, this recognition of a solution in the form of active protection and creative rehabilitation of urban and architectural heritage in the every day life and continuity of the city has brought to surface our interest on the user. Thus, the current ways of confrontation with the issue are based upon a triadic model of shell–use–user, which even allows for the disappearance of the chronic polarization and subsequent fanaticism generated between the ideas of maintenance and development, between the partisans of protection and those of renewal.

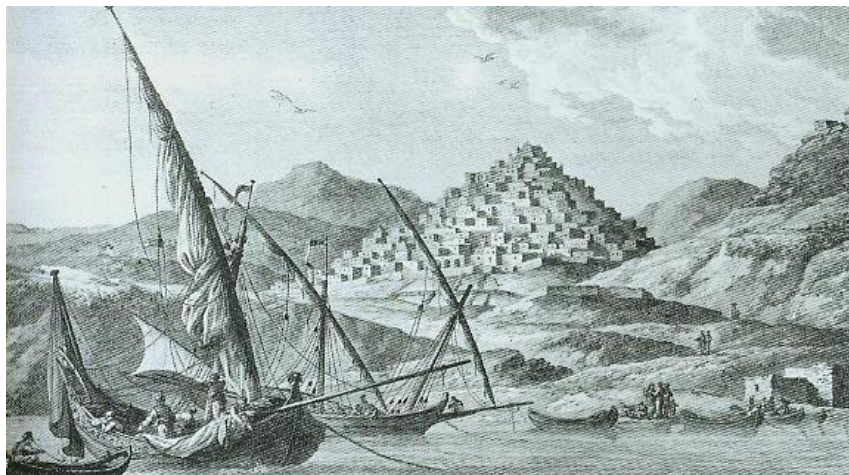
Holistic Protection through the Protection of the Physiognomy of the city

The experience of dealing with the issues of architectural heritage over the past 50 years has taught us a lot¹⁶. Most importantly, it has led us to reconnect of material exteriors of forms with spatial and temporal qualities or corresponding attitudes. This re-attachment of architectural heritage to the totality of our sensuous qualities – to all the elements of hearing, scent, taste or touch – brings about the actualized physiognomy of a city.

Therefore, any contemporary form of dealing with the protection of architectural heritage requires a total approach combining all aforementioned qualities. In itself, this presupposes a redefinition of a significant amount of data, since it is imperative that we avoid the generalizations that we had been forced to accept in the first phases previously described. Today, a specialized case-by-case approach to each place, so that all the separate qualities that express and bring forward its physiognomy are made noticeable, is considered essential. For example, it cannot be acceptable for cities of the caliber and historical significance of Hermoupolis to be defined by the same legislative status which defines traditional settlements¹⁷ of a minor scale such as Folegandros, Sikinos, Anafi, Irakleia etc. simply because they all fall within the same administrative and cultural complex, that of the Cyclades.

THE EXAMPLE OF HERMOUPOLIS

A thorough research on the city of Hermoupolis determined with precision the content of terms such as “Historical city”, “Historical Centre”, “Traditional settlement”; it redefined the meaning of the terms “tradition, traditional”, and even the terms “urban, urbanism”, and clarified approaches to planning or other kinds of intervention in these contexts. The orientation of the legislative framework, not in generalized terms of protection but towards specialized handling methods for each subgroup which falls under one of the aforementioned classifications, is considered essential.¹⁸ Indeed, something like that solves the problems presented above and allows for the protection and promotion not only of the general character of urban regions but also of their particular physiognomy. As mentioned above, this problem is simply technical and despite its difficulties, can be solved.



Picture 1: The Hermoupolis of Siros. The existing Middle Aged settlement was protected by France because of the catholic monasteries that were there. In the foothills of this settlement came the refugees and the persecuted of the revolted islands (Hios, Psara etc.) to establish the first city of the contemporary Greece.



Picture 2:

In 1822 came at Hermoupolis 40.000 refugees hunted from Turks. In 1823 they decided to settle down permanent. In 1825, the residents named the New City by the name of the Greek God of Trade. The city of Hermis. In 1830, just five years after, Hermoupolis became the first urban-industrial and shipping center of after-revolted Greece.

However, there is a more serious and more deeply-rooted problem, whose potential resolution appears extremely difficult and time-consuming: it is a problem of moral attitude and mentality, an ideological problem that keeps in pace with the wider ideology of the devastating globalization phenomenon. At this moment, the city of Hermoupolis has undeniably become more beautiful and is trying by all means necessary to become a striking city, attempting to attract visitors who will be interested in its beauties.



Picture 3:

The city as a phenomenon of rapid development and urbanism, developed a high civilization, which characterize Hermoupolis today and is impressed in its physiognomy. At the photo we can see the town hall of the city, a work of grate Vavarism architect Ziller.

Having rejected more familiar productive activities it has turned either towards parasitic activities (the Casino is a classic example), or ephemeral and dubious activities which depend on unreliable factors such as tourism. This is the city that first introduced the industrial revolution to

It is a fact that, in terms of public opinion, there are two motives behind the protection of the character and the promotion of the physiognomy of a certain place. The first, which concerns the greater public, is the expectation of economic gain from a widely recognized pseudo-traditional form, marketed as the perfect tourist commodity. The second, relevant to a small cultured elite, refers to what could be named as “tradition-chasing”. That is the constant hunt of fossilized imitations of traditional forms, with no interest in the truth that created them and gave them their paradigmatic value, but simply on the basis of their ability to look real; their ability to look old – since the ‘old’ as a product of the ‘good old days’ is by definition better than the modern.²¹



Pictures 5: The physiognomy of urban-industrial Hermoupolis can't be protected from an official order relative to the traditional settlements of Cyclades, because as traditional settlements are determined these which are “products” of popular unnamed architecture. In the photo we can see the Hermoupolis of Siros and the Marpisa of Paros.

As one clearly understands neither of these motives can support a genuine form of protection and promotion of the character and, most crucially, of the authentic physiognomy of a place. It is also understandable that every serious and sincere effort to deal with this problem will be contradicted by the reactions of both groups mentioned above, while it may be supported by the fans of modernization and evolution – the very enemies of protection. With today's standards and with the experience that has been gained through the last forty years of systematic research on this and cognate subjects, we believe that it is time for a revision of both the ideology and the practice which should be adopted for the protection and promotion of architectural heritage. A more specialized approach to each kind of space (historical city, traditional settlement, etc.) but mainly a more specialized confrontation of issues on a city- or settlement-level basis, which will reconnect the material shells of given forms with their temporal qualities, is now considered essential.²²



Picture 6: The building provisions and the uses of land of Hermoupolis have to serve the general aim of protection and elevation of its unique physiognomy.

The reconnection between the elements of architectural heritage and the whole of sensory qualities (noises, smells, flavours or elements of touch), promotes the actualized physiognomy of a place. However, such an attempt can be concentrated on the notion of *use* and, in particular, not so much the *type* of use but what recent Research of the Laboratory of Urban Design has defined as "*form of use*". For example, the Market of Hermoupolis, renowned for its particularly vivid local colour (*couleur local*) traditionally gathered local groceries, greengrocer's shops, butcher shops, fish shops and was the place of production of an intricate and especially interesting sensory landscape which is nowadays rapidly fading away. The area continues to be described as a place of commerce but the form of use has been completely altered.²³

The groceries, fruit stores, butcheries and other shops are rapidly being replaced by jewellery shops, women's accessories stores, tourist shops etc. The Market has been spruced up and revamped; through this process, however, it is no longer "the Market", but a typical commercial street with tourist character. At the same time, the above-mentioned sensory landscapes are disappearing, since the last remaining fish-shop will soon be considered as a bothersome sensory source, and will be removed from the tidied up commercial street. Of course, life evolves: the Super Markets located at the edge of the city offer everything in standardized form, with everything under one roof and the important advantage of parking space and easy access.

The Market, by contrast, with its known vehicle access problems and its overwhelming lack of space, not simply in terms of parking, can no longer serve the whole of the island or even the greater city of Hermoupolis, and is limited only to the few pedestrian locals. At this point, however, it is worth mentioning the example of the Saint Joseph market in the historical center of Barcelona. With its characteristic facade, decorating the most central, busy and world-renowned street of the Catalonian capital, the wonderful Ramblas, it has maintained its traditional character intact, offering its residents and visitors the ideal archetype picture of the central market of a city with its special auditory, olfactory and gustatory landscape.

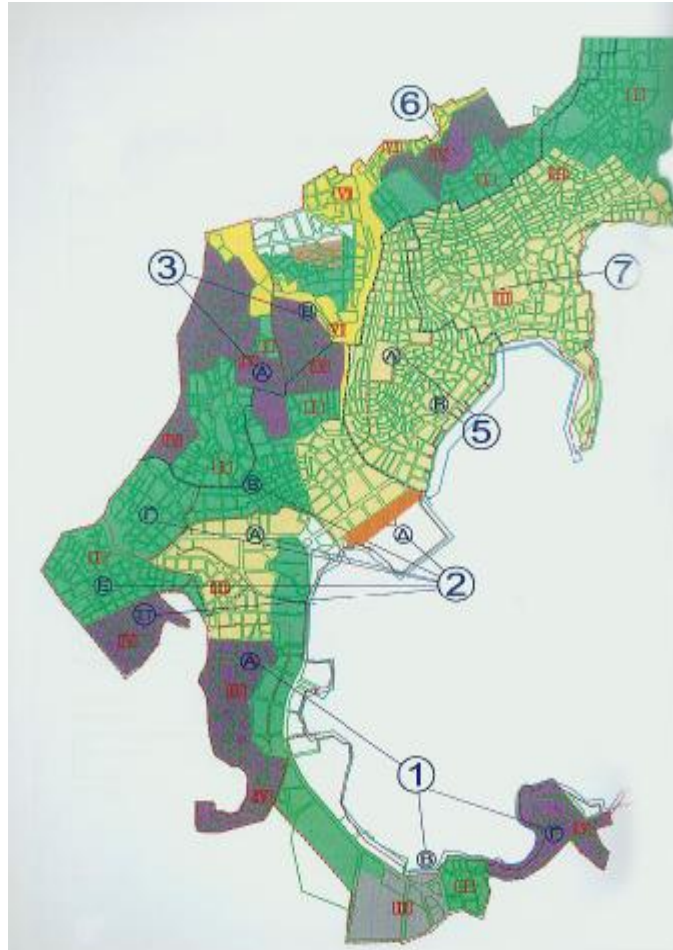


Photo 7: The building provisions. The numbers are showing the districts of Hermoupolis: 1) Lazareta, 2) The shipyard of Agios Konstantinos, 3) Neapoli, 4) Ano Siros, 5) Metamorfofi, 6) Anastasi, 7) The center of the city.



Photo 8: The Sky line of city. One after the other, the colors are showing the different skylines of Hermoupolis. The light blue shows the skyline of Ano Siros. The deep blue shows the skyline of the hill of Anastasis and the rest city. The deep red shows the church of San Nicolas and the coast regions.

CONCLUSIONS

From the abovementioned examples it becomes clear that the proposed multilevel approach may at first seem particularly difficult and inaccessible, but is not entirely infeasible. In fact, it is all but necessary if we honestly wish to maintain architectural heritage alive as opposed to merely presenting exhibits of fossilized shells or their poor imitations. Architectural heritage constitutes a part of the much broader concept of cultural heritage, and only through processes of respect, promotion and evolution of that cultural heritage can an occupation with the architectural elements of a place be justified and understood.

REFERENCES

1. Xatzopoulou A., Stefanou J., Nikolaidou S., "Urban Reshaping", ed. Technical Chamber of Greece, Athens 1995.
2. Stefanou J., "Views and practices of the nowadays protection", Proceedings of the Conference "History and Conservation Problems", Rhodes 1992.
3. Stefanou J., "The protection of the Architectural Heritage", ZIGOS, Athens 1976, Vol. 22-23.
4. Zivas D., Travlos I., Xatzopoulou A., Lambiri et al, "The study of old city of Athens." Regulatory Design of Athens.
5. Manousou D.K., Papavasiliou, "Middle aged city of Rhodes", Proceedings of the Conference "New Cities up to the Old", Rhodes 27-30 September 1993.
6. Stefanou J., «Eléments Spatiaux Spécifiques des Villes Historiques», Université Paris VIII Thèse de doct., Paris 1980.
7. Greek Tourist Organization (GTO), "Work Exhibition of the Traditional Settlements", 1975-1990, Athens 24 May 1990.
8. Stefanou J., "Ideology and views of the nowadays protection", Notes of the Postgraduate Lessons for the Protection of the Monuments, ed. National Technical University of Athens, Athens 2003.
9. Stefanou J. & Partners, "The Physiognomy of the Greek City", ed. Urban Design Laboratory, National Technical University of Athens, Athens 2000.
10. Stefanou J. & Partners, "The Physiognomy of a Landscape: The character of a Greek city on 21st century", ed. Urban Design Laboratory, National Technical University of Athens , Athens 2001.
11. Stefanou J., Mitoula R., "The Globalization, the European Unification and the physiognomy of a Greek City", ed. PAPAIZISI, Athens 2003.
12. Mitoula R., "The protection of the architectural heritage as a factor for the conservation of the physiognomy of cities", ARCHEOLOGIA, Vol. 72, Athens, September 1999, p.61-71.
13. Wilcheim J., "Urbanization and Globalization," Courier of UNESCO, February 1991.
14. Stefanou J., "The regaining of a historical center. Development and comparative appreciation of the possible choices today", Proceedings of the Conference "New Cities on the Old", Rhodes September 20-23, 1993.
15. See 1
16. Contract of Granada, Contract for the protection of the European Architectural Heritage, ratification April 1992, Official Journal of the Hellenic Republic Vol. 1, No. 61, 1992.
17. About traditional Settlements, Presidential Decree, Official Journal of the Hellenic Republic/345, 1969.
18. Research "Model urban planning confrontation of a historical city – Urban planning of Hermoupolis", ed. Laboratory of Urban Design, National Technical University of Athens, June 2001.
19. Drakaki A., "The history of the settlement of Hermoupolis", Volume B, 1983, Athens 1983.
20. Stefanou J., "The physiognomy of a Greek city and the globalization," Ili & Ktirio, Athens, March 2000, Vol. 47.
21. Stefanou J., "About Physiognomy of a City. The Physiognomy of a Landscape", Urban Design Laboratory, National Technical University of Athens, Athens 2001.
22. See 10
23. See 10

EVALUATION OF COOLING SYSTEM'S DESIGN FOR RURAL DEVELOPMENT IN UPPER EGYPT

A. M. FAHIM

*HVAC Consultant & Researcher, Housing & Building National Research Center,
P.O. Box 1770 Cairo, Egypt, Email: a.medhat@hbrc.edu.eg & medhet@egyptwww.com*

ABSTRACT

This paper focuses on the practical investigation and field experimental analysis of in-service cooling systems. The main goals are evaluating and optimizing energy consumption of the expected commonly used cooling systems in Upper Egypt. Based on field experimental results, an extensive analysis was executed to evaluate the impact of energy consumptions of different cooling systems especially indirect and direct evaporative systems against traditional water and/or air-cooled direct expansion systems, and chilled water systems and simple multi-bank evaporative systems. Investigations in Upper Egypt showed that the use of air-cooled cooling systems leads to a very low energy efficiency ratio, EER, and poor coefficient of performances. While water-cooled cooling systems ranged from 25KW to 175KW in cooling capacity showed good practices but have higher initial and running costs, which are not anticipated for residential projects. Evaporative systems, which have over 92% effectiveness's could be used in limited situations, While, utilizing indirect evaporative system combined with direct enclosed fog system, IEDEF, could be more efficient and durable in Upper Egypt Climates. The paper outspreads the detailed design of typical IEDEF cooling system based on pre-defined architectural approach for common buildings designs that meet both of culture and life styles of residential applications in Upper Egypt.

KEYWORDS: Hot and Dry Climates, HVAC-Systems, and Evaporative Cooling Systems.

INTRODUCTION

Upper Egypt citizen's cultures and life styles are reflected on their designs and types of housing as most of designs have the same construction concept, circulation, and feeling approaches [1]. Figure.1 shows one of commonly used building designs including ground, and first floors, and patio in the middle of house. Families for meetings use patios continuously; while some of owners leave it open to sky and others closed it by operable glazed skylights [2]. Generally Upper Egypt is considered as hot and dry climate as per the following conditions:

Latitude	From 22.50-to-23.00 Deg. North								
Elevation.	From 80 m-to-160 m Over Sea Level								
Average Daily Range	Ranged From 16°C -to-17°C.								
Summer Design DBT	Ranged From 40°C -to-47°C								
Summer Avg. RH%	Ranged From 10%-to-20 %								
Winter Design DBT	Ranged From 17°C -to-22°C								
Winter Avg. RH%	Ranged From 20%-to-50 %.								
Exposures	NE	E	SE	S	SW	W	NW	N	HOR
Min. SHG W/m ²	98.1	574.4	360.0	134.3	360.0	574.4	97.6	82.4	648.7
Max. SHG W/m ²	569.3	741.3	799.2	735.6	799.2	741.3	558.7	179.3	896.8

DBT = Dry Bulb Temperature, RH% = Relative Humidity, SHG = Solar Heat Gain
Min. = Minimum, Max. = Maximum, Avg. = Average

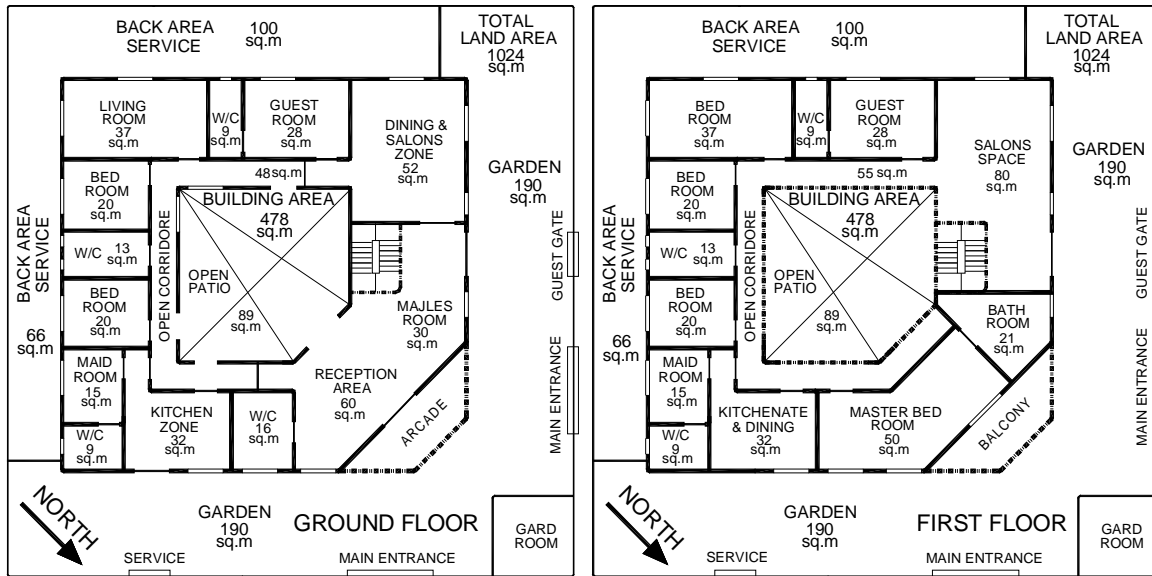


Fig.1: Conceptual Design Layout of Under Study Residential Building

Human biological and physiological impacts were studied to evaluate and justify the acceptable comfort conditions limits [3]. Outdoors design conditions, prevailing sandy-storms, comfort requirements, building pressurization, and estimated thermal loads, affect the economical operations of cooling systems [4].

PROPOSED COOLING SYSTEMS

Building envelopes and their characteristics play a vital role in controlling and protecting buildings from external extreme conditions [1, 5], this was implemented by local codes to reduce and limit the overall heat transfer coefficients of all used materials and treat exposures to limit solar heat gains, while cooling systems will adjust and produce acceptable Indoor Air Quality IAQ for occupants according to thermal acclimatization of citizens [6].

The main Thermal Factors that directly affect indoor air quality for acclimated peoples in Upper Egypt are indoor air dry bulb temperature, $DBT^{\circ}C$, air relative humidifies, $RH\%$, mean radiant temperatures, $MRT^{\circ}C$, and local air speed, AV m/s, over occupants [7]. Previous researches show that from $28^{\circ}C$ -to- $30^{\circ}C$ DBT , 45% -to- 60% $RH\%$, and $30^{\circ}C$ -to- $35^{\circ}C$ MRT , and 0.20 m/s – to- 0.3 m/s AV could be well accepted for occupants in residential applications [8].

Table 1 shows the estimated thermal cooling loads summary of four different case studies related to the understudy family house presented in Fig. 1 including the presence of open and closed patio and also incase of using full outside air scavenging strategies. The latter strategies are used in many situations to help and protect occupants from the feeling of staying in enclosures and enjoying with clean and fresh air, as pollutions and air contaminations are minimal in Upper Egypt [8].

Estimated cooling loads calculations are based on net floor level height 3.00m, window-wall ratio, WWR , 13% -to- 17% , indoor conditions are $28^{\circ}C$ DBT , 50% $RH\%$, $35^{\circ}C$ MRT , 0.25 m/s, AV , are accepted for occupants in residential applications [3, 5], weighted average overall heat transfer coefficient 1.119 $W/m^2^{\circ}C$ to 1.4310 $W/m^2^{\circ}C$, total lighting and power intensities are 22.5 W/m^2 and the maximum occupancy rate is one person per $50m^2$ of the built-up footprint area.

Table 1: Estimated Thermal Cooling Loads Summary for Four Building Cases Study

Case	Description	I II III	G.S.H G.T.H G.SHF	R.S.H R.T.H R.SHF	S.A. Qty. F.A. % Overall-U	Area, m ² (l/s)/kW Coil ADP	In-Coil °C Off-Coil °C DBT/WBT
1	Ground & First Floors at Open Patio	I	120.74	98.41	7551	778.00	29.8 / 19.9
		II	122.99	101.29	6.5%–8.0%	61.39	16.1 / 15.2
		III	0.9800	0.9700	1.1190	58.30	°C / °C
2	Ground & First Floors at Closed Patio, Skylight	I	177.13	150.62	11321	956.11	29.2 / 19.7
		II	179.31	155.41	4.5%–7.5%	63.17	16.1 / 15.2
		III	0.9880	0.9690	1.4310	58.40	°C / °C
3	Ground & First Floors at Open Patio & 100% Fresh Air	I	271.01	98.41	7551	778.00	47.0 / 24.4
		II	288.91	101.29	100%	26.14	16.1 / 14.1
		III	0.9381	0.9700	1.1190	54.80	°C / °C
4	Ground & First Floors at Closed Patio 100% F.A.	I	419.42	150.62	11321	956.11	47.0 / 24.4
		II	447.13	155.41	100%	25.33	16.1 / 14.1
		III	0.9380	0.9690	1.4310	54.80	°C / °C
G.S.H , Grand, Coil, Sensible Heat, kW G.T.H , Grand, Coil, Total Heat, kW G.SHF , Grand Sensible Heat Factor R.S.H , Room Sensible Heat, kW R.T.H , Room Total Heat, kW R.SHF , Room Sensible Heat Factor. SHF = Sensible Heat / Total Heat				S.A.Qty , Supply Air Quantity, l/s ADP , Coil, Apparatus Dew-Point, °C Overall-U , Weighted Average Overall Heat Transfer Coefficients (Building Elements), W/m ² °C DBT , Dry Bulb Temperature, °C WBT , Wet Bulb Temperature, °C F.A.% , Fresh Air Percentage.			

These four case studies focus on the matched equipment cooling capacities and on the anticipated systems that could be utilized in hot and dry climate to achieve comparable indoor comfort conditions, with optimum EER, and that could be also considered and implemented in the Egyptian Energy Efficiency Codes EEEEC.

Table 2 shows different cooling system selection summary of mentioned four cases including air-cooled and water-cooled direct expansion systems or liquid water chillers. Cooling capacities are presented in metric and imperial units as, till now in Egypt, tons of refrigeration, T.R, is more sense and value for the local engineers and also for EER's that based on both the cooling unit and the global cooling system, i.e. cooling unit, air handling units, pumps, cooling tower, sand filters...etc., and finally the ratings KW/T.R.

T.R = 12000 Btu/hr = 3.51597 KW,

EER = (Btu/hr) / (watts), (Cooling capacity) / (Power Consumption)

Add. = Additional Power for air handling units, cooling tower, chilled & condenser pumps.

Table 2: EER, Power Ratings, and Power/Capacity Ratios of the Suggested Five Cooling Systems Alternatives Based on the Four Case Studies

Case	Capacity		Units + Add.	Unit	System	Unit	System	System
	kW	T.R	Power kW	EER	EER	kW/T.R	kW	kW/T.R
1A	2*63.15	35.92	55.00+00.00	7.84	7.84	1.531	55.00	1.531
1B	2*62.54	35.57	64.00+5.00	6.67	6.19	1.799	69.00	1.940
1C	2*66.35	37.74	33.20+10.00	12.72	12.05	0.879	43.20	1.146
1D	128.33	36.50	58.73+15.00	7.50	6.64	1.609	73.73	2.020
1E	123.86	35.23	31.00+25.00	13.60	10.46	0.880	56.00	1.589
2A	2*90.22	51.32	82.00+00.00	7.50	7.51	1.598	82.00	1.598
2B	2*93.17	52.99	86.00+7.50	7.39	6.99	1.623	93.50	1.767
2C	2*96.37	54.82	50.96+15.00	12.91	11.88	0.929	65.96	1.204
2D	186.35	53.00	84.80+22.50	7.50	6.91	1.594	107.30	2.025
2E	258.78	73.60	53.85+32.50	16.4	13.83	0.733	86.35	1.173

Table 2 (Continue): EER, Power Ratings, and Power/Capacity Ratios of the Suggested Five Cooling Systems Alternatives Based on the Four Case Studies

Case	Capacity kW T.R		Units + Add. Power kW	Unit EER	System EER	Unit kW/T.R	System kW	System kW/T.R
3A	47°C DBT Is Not Accepted For Inlet Cooling Coil Conditions Of Packaged Units							
3B	4*62.54	71.15	128.00+15.00	6.67	6.19	1.799	143.00	2.010
3C	47°C DBT Is Not Accepted For Inlet Cooling Coil Conditions Of Packaged Units							
3D	297.80	84.70	139.23+20.00	7.30	6.63	1.647	159.23	1.880
3E	289.72	82.40	61.42+25.00	16.10	12.45	0.747	86.42	1.049
4A	47°C DBT Is Not Accepted For Inlet Cooling Coil Conditions Of Packaged Units							
4B	4*116.06	132.04	208.00+20.00	7.62	7.27	1.575	228.00	1.727
4C	47°C DBT Is Not Accepted For Inlet Cooling Coil Conditions Of Packaged Units							
4D	474.66	135.00	225.00+25.00	7.20	6.60	1.670	250.00	1.852
4E	482.39	137.20	101.63+30.00	16.2	13.00	0.742	131.63	0.959

Cases 1,2,3, & 4 Represent Cooling Loads Selection of HVAC System of Building
A, Air-Cooled Packaged Units, Self-Contained or Split Type.
B, Air-Cooled Direct Expansion Units, Air handling Units & Condensing Units.
C, Water-Cooled Packaged Units, Self-Contained Only.
D, Air-Cooled Liquid Water Chiller.
E, Water-Cooled Liquid Water Chiller.

Table 2 Describes the real selections of cooling systems based on international manufacturers available in the Egyptian market, use of standard units, lower initial cost, reasonable EER, common practices, maintenance and spare parts availability, In this table cases assigned with characters C & E show that water-cooled packaged and chillers units which maintain and minimize the losses in cooling capacities as its operation principles are based on cooling towers “evaporative cooling” that is affected by wet bulb temperature only. Generally the wet bulb temperatures are almost stable and ranged from (21.00°C-to-24.00°C). Also water-cooled cooling systems have good sustainability in hot and dry climate as they consume low energy up to 0.959 kW / T.R compared with air-cooled system that have high power demands reaching 2.020 kW / T.R.

SUGGESTED COOLING SYSTEMS

Because of this work is devoted to the design and construction of low initial and running cost cooling system that could be utilized to serve residential and some public-use commercial applications in Upper Egypt. Fig.2 shows the schematic flow diagram of the suggested system based on calculations of Case-4 in Table 1.

Suggested system has high EER based on combinations of indirect evaporative cooling systems, and direct evaporative cooling system based on enclosed flash evaporation process (micro-mist or fog system).

Flash evaporation concept is basically depends on water evaporates only from the surface, so, the faster the water evaporates, the faster the ambient conditions change. The latter could be enhanced when the surface area of the droplets in relation to the volume of water is greatly increased, and the action of a small water droplets will stay airborne for a longer period before falling.

These could be accomplished by increasing the water pressure to over 70 bars using positive displacement plunger pump and at this pressure the water is atomized into micron size droplets (droplet size is less than 50micro-meter) when using nozzle orifice diameter that ranged from 0.110 mm to 0.380 mm which can flash water and produce droplet sizes less than 50 micro-meter in diameter at number of droplets more than 7500 times the low pressure nozzles.

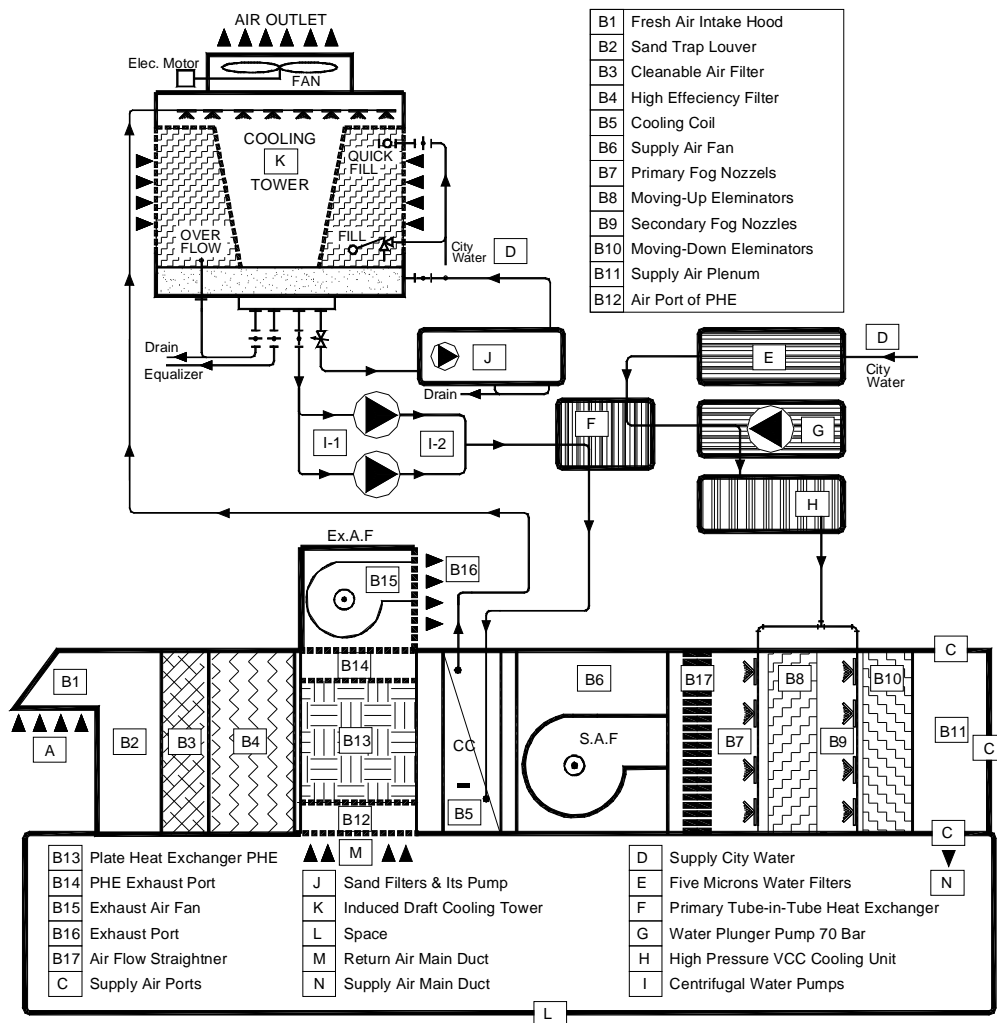


Fig.2: Suggested Evaporative Cooling System Using Indirect Cooling Tower System , Air-to-Air Plate Heat Exchanger and Flashing, Fog, Chamber

This approach leads to surface area to volume ratio over 400 compared with normal spraying nozzles in air washers. These micro droplets have evaporation period ranged from 0.190 sec to 0.075 sec. Flash evaporation is better in use when dealing with occupied spaces supply air as it generates better indoor air quality and due to there are no water recirculation in spraying process, there are no possibility for micro-organisms generations in water, moreover fog chambers have high effectiveness and saves water as no need for blow down.

Figures, 2 and 3 show the schematic flow diagrams of suggested IEDEF cooling systems showing the main components and their related psychrometric process respectively. The flow diagram in Fig.2 shows an open type cooling system where circulated water is cooled via cooling tower. Fresh air will be filtered in three stages starting from sand trap louver and end up with high efficiency bag filter and then, Exhausted air from space will exchange heat sensibly with filtered fresh air via air-to air plate heat exchanger as a pre-cooling process, while cold water from cooling tower will be utilized by water-to-air cooling coils “Pure sensible cooling heat exchangers” that reduce treated fresh air dry bulb temperature sensibly, On the other hand the treated air with new low DBT and WBT will enter high efficiency flashing or fog chamber based on adiabatic cooling and then deliver air to the required spaces.

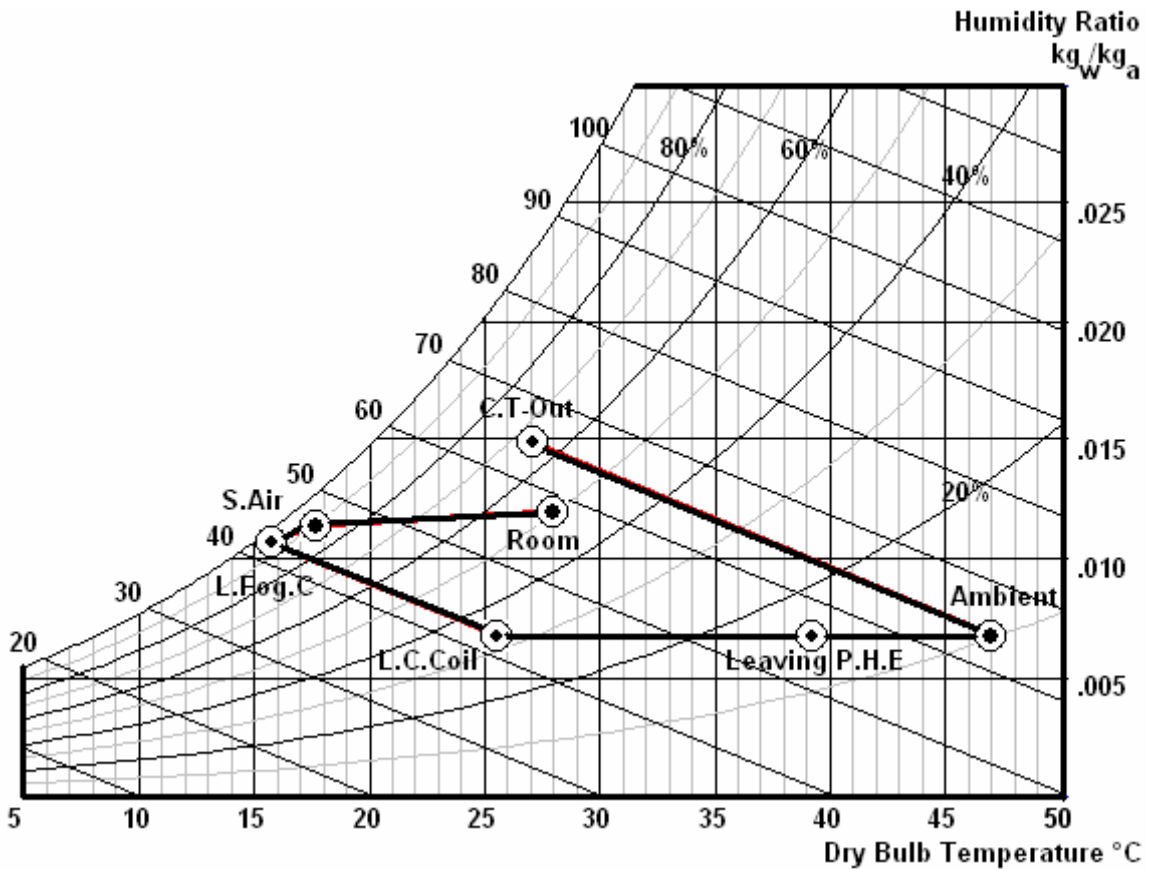


Fig.3: Psychrometric Process of the Suggested IEDEF Cooling System

As indicated in Fig.3 psychrometric process shows that supply air temperature can reach 18.20°C supply air temperature leading to indoor condition about 29.50°C DBT at 47% R.H with total power consumption rate up to 0.42 kW/T.R.

This process is valid for room sensible heat factor, RSHF, 85% to 97% and it has the ability to accommodate room conditions 27.0°C to 30.0°C DBT, dry bulb temperature, at 48% to 55% relative humidity with indoor pressurizations to avoid infiltrations that is acceptable for acclimated people in Upper Egypt.

Cooling Tower

Total Heat Rejected	300.00 kW	Water Flow Rate, Max.	10.50 l/s
Inlet Water Temperature.	35.00°C	Circulated Water Flow.	9.820 l/s
Outlet Water Temperature.	24.40°C	Evaporation Loss.	00125 l/s
Design Wet Bulb Temperature.	22.22°C	Drift Loss.	0.021 l/s
Air Flow Discharge.	6250 l/s	Fan Motor Power.	3.75 kW
Tower Dimension L x W x H	(2.5x1.4x2.4) m	Operating Weight.	1150 Kg

Cooling Tower Circulating Centrifugal Pump

Water Flow Rate.	9.82 l/s	Pump Head.	225 k.Pa
Pump Motor Power	3.44 kW	Pump Static Efficiency.	80%

Supply Air Fan

Air Flow.	11321 l/s	Fan Motor Power.	11.50 kW
Fan Type.	F.C.F *	Fan Total Pressure.	300 Pa
Fan Efficiency.	57%	Fan Power.	9.60 kW

* F.C.F, Forward Curved Fans

Exhaust Air Fan

Air Flow.	10377	Fan Motor Power.	10 kW
Fan Type.	F.C.F	Fan Total Pressure.	250 Pa
Fan Efficiency.	50%	Fan Power.	8.30 kW

Air-to-Air Plate Heat Exchanger (For System Enhancing), (Option)

Primary Inlet Conditions. Flow / DBT / RH%	10377 l/s 28°C / 55%	Secondary Inlet Conditions. Flow / DBT / RH%	11321 l/s 47°C / 10%
Primary Outlet Conditions. Flow / DBT / RH%	10377 l/s 98°C / 34%	Secondary Outlet Conditions. Flow / DBT / RH%	11321 l/s 39°C / 15%
Primary Face Air Velocity.	3.516 m/s	Secondary Face Air Velocity.	4.078 m/s
P.H.E. DIM. L x W x H	(1.5x2x1.6) m	Exchanger Effectiveness.	42%

Indirect Cooling Coil

Total Heat Load.	296 kW	Total Sensible Load.	296 kW
Inlet Water Temperature.	24.50°C	Circulated Water Flow.	9.82 l/s
Outlet Water Temperature.	31.64°C	Inlet Air Temperature DBT.	47.00°C
Outlet Air Temperature DBT.	25.56°C	Inlet Air Temperature WBT.	22.22°C
Outlet Air Flow Rate.	11321 l/s	Air Face Velocity.	2.478 m/s
Coil Dimension L x W x H	(0.45x2.75x1.5) m	Water Flow Velocity.	1.432 m/s
Coil # Rows, Fins/mm, Circuits	10 / 0.56 / Full	Outlet Air Temperature DBT.	15.30°C

Flashing, Fog, Chamber

Air Sensible Load Removed.	134.20 kW	Air Latent Load Added.	135.30 kW
Inlet Fogged Water Temperature.	15.30°C	Fog Flow Rate.	0.15 l/s
Number of Nozzles / Bank.	60	Nozzle Spacing	450 mm
Nozzle Orifice Diameter.	0.2032 mm	Step Down Eliminators	60 mm
Water Pressure.	70 bar	Step Up Eliminators	60 mm
Chamber Dimension L x W x H	1.8x3.0x1.5	Air Flow Velocity.	2.500 m/s
Number of Nozzles Banks.	2-Counter	Field Test Effectiveness	About 90%

High Pressure Plunger Water Pump

Total Flow Rate.	0.15 l/s	Pump Head.	70 bar
Pump Motor Power	1.80 kW	Pump Static Efficiency.	85%

Vapor Compression Cycle VCC Cooling Unit

Total Cooling Capacity.	18.39 kW	Total Heat Rejected.	26.76 kW
Inlet Water Temperature.	44.75°C	Circulated Water Flow.	0.15 l/s
Outlet Water Temperature.	15.00°C	Storage Tank Capacity	20 lit
Operation Period	12-Hours	Power Consumption.	8.37 kW

Tube-In-Tube Heat Exchanger (Option)

Total Heat Transfer Load.	4.104 kW	Sec. Inlet Water Temperature.	24.4°C
Primary Inlet Water Temperature.	49.66°C	Sec. Outlet Water Temperature.	24.50°C
Primary Outlet Water Temperature.	44.75°C	Heat Exchanger Effectiveness	75%

From previous quick selections of the required equipment for IEDEF cooling system, it could be concluded that the maximum total power consumption will be 38.86 kW, that around 40 kW while the cooling system was able to handle 447.13 kW cooling capacity at the same supply and room air parameters listed for other traditional systems in Table-2. This means that the EER of the whole system could range from 38-to-40 at best outdoor conditions, while power consumption ratings could reach 0.315 kW/T.R. Incorporating these combinations techniques among water-cooling systems, air-to-air heat exchangers and "micro-mist" fog evaporation chambers, will ensure that HVAC systems will have comparable initial and running costs and life time up to 20-years which is adequate in Egypt and also for small and medium public zones projects ranged from 400.00 kW to 1800 kW cooling capacities.

CONCLUSIONS

This work outlined many conclusions, which were arrived at, from field studies, collected statistical data for installed projects; the important conclusions can be summarized as:

- 1- The use of water evaporative systems, which have effectiveness's more than 92%, could be used in limited situations at hot and dry climates especially in residential buildings.
- 2- In Upper Egypt, it is impractical to utilize air-cooled direct expansion systems, or water chillers that have higher power consumptions with very low coefficient of performances and consequently low energy efficiency ratio.
- 3- Proposed IEDEF system shows good agreements with the HVAC designers' wishes in tropical climatic zones especially for power consumptions.
- 4- All HVAC systems that exceed 1000 kW in cooling capacity and utilize **VCC** shall be water-cooled base when used in Upper Egypt zone and shall be implemented in the Egyptian Energy Efficiency Code, EEEEC.
- 5- Electrical requirements for air-cooled cooling systems are around 1.96 kW per T.R., while water-cooled units are around 0.99 kW per T.R.
- 6- On the Egyptian consumer level, air-cooled plants are distinctly more economical than water-cooled plants even for large capacity installations. While, on the International level, the situation is reversed, though water-cooled plants become only marginally more economical than air-cooled plants.
- 7- Till now there is a water restriction with the use of fog chambers, this problem arise from presence of high level of total dissolved solids, TDS, and the resulting nozzles blocking maintenance.
- 8- Design and construction of fog chambers, shall, need more researches and investigations to enhance the performance as up-till-now it reach 92% in laboratory tests.

REFERENCES

1. Al-Emara Wa Al-Bia'a Fi Al-Manatiq Al-Sahrawia, Prof.Dr. Khaled Sliem Fajal, Egypt, ISBN: 977-339-052-7. Architectural And Urban In Hot Desert Regions.
2. Egyptian Climatic Authorities, The Classifications of Climatic Regions In Egypt Based on CIBSE, England, Adopted @ 1999, Averaged Printed Data for Upper Egypt Climatic Regions, 1997
3. The Data Book For Upper Egypt, Toshka Report, Presented for The National Housing And Building Research Center, HBRC, International Conference on Future Vision and Challenges For Urban Development, 20-22 December 2004, Cairo, Egypt.
4. Climatic and Energy For Rural Development in Upper Egypt " Basic Site Analysis", by Dr. Ahmed A. Medhat Fahim and Prof. Essam E. Khalil, At Cairo International Conference On Energy & Environment, Sharm El-Sheikh 15-19 March, 2005.
5. Optimizing Energy Efficiencies of Cooling Systems at [HOT and DRY] Climates, by Dr. Ahmed. A. Medhat Fahim, International Conference for Future Challenges, Egypt-2004.
6. Man, Climates and Architecture, Second Edition, B. GIVONI, 1976.
7. ASHRAE Standard 55-1999 "Thermal Environmental Conditions For Human Occupancy ", Atlanta. And ASHRAE Handbook Applications, 2003, (Tulle Circle), N.E., Atlanta.
8. Improving Energy Efficiency of Air Conditioned Buildings through Summer Elusive Climate, Dr. Ahmed A. Medhat Fahim and Prof. Essam E. Khalil, @ 2-nd International Energy Conversion Engineering Conference 16-19 August 2004, Rhode Island, USA, AIAA, American Institute of Aeronautics and Astronautics.
9. International Companies Catalogues for the selection of Direct Expansion, Chilled Water, Air Washers, Pumps, Fans, Heat Exchangers, Nozzles, and Fog Systems.

COMPUTATION OF CONCRETE MIX INGREDIENTS ON AN INTERNET PLATFORM

A. M. Ghaly

Civil Engineering Department, Union College, Schenectady, NY 12308

L. G. Almstead

Computer Science Department, Union College, Schenectady, NY 12308

ABSTRACT

Design of concrete mixtures is a task that can be accomplished using the standard method outlined in the specifications of the American Concrete Institute (ACI). The weight method or the absolute volume method can be used to design a concrete mixture. The ACI method involves the use of parameters related to the properties of the ingredients used in the design. It also involves making simple calculations to proportion the mix to meet the desired design criteria. The ACI procedure of concrete mix design has been simulated to make it possible to accomplish on an Internet platform. The JavaScript programming language is used to perform the required computations. A website has been constructed where the designer can enter the values required in the design in cells especially prepared to receive input parameters. Having entered these parameters, the designer can get the results of the design by clicking special buttons to perform the necessary computations. The results are displayed in output cells. The design procedure concludes with a summary of the input parameters and the output ingredients. This concrete mix design website accommodates all design scenarios given in ACI's method. The highlight of this site is that it allows users to alter the design input values at any stage of the design, thus adding to the interactive nature of the technique and enhancing the design experience.

KEYWORDS: Aggregate, Batching, Concrete Mix Design, Internet, Mix Proportioning, Water-Cement Ratio.

INTRODUCTION

The design of concrete mixtures is a systematic task that is outlined in the specifications of the American Concrete Institute (ACI). The steps followed in designing a concrete mix have been structured using the JavaScript programming language, which is used to conduct the required computations. This program uses the Internet as computing platform. A website (Ghaly and Almstead 1997-2005) has been developed and constructed where the procedure of concrete mix design is outlined in a logical form. The user can navigate through the process in an orderly fashion and may return to review any step at any time. All major factors related to concrete mix design as detailed by ACI are incorporated in this website. Tables of data related to mix design are given. Included also are pages which allow users to enter data, and to calculate the weights and/or volumes of the ingredients of concrete mixtures. For wet aggregates with or without a degree of absorption, water contents can be taken into consideration and included in the computations of the water quantity to be added to the mix. The site also includes provisions to incorporate pozzolanic materials and/or water reducers in the design. The procedure concludes with a list of the weights and/or volumes of the different components of a concrete mixture. The entire procedure can be done using different systems of units. The highlight of this approach is the interactive nature of the technique, in addition to the convenience due to its accessibility from any computer.

LITERATURE REVIEW

There have been several early attempts to use computers in concrete mix design. Day (1984) described a computer method to proportion concrete mixtures based on the specific surface of aggregates. Shilstone and Shilstone (1985) outlined a program for the potential use of microcomputers in concrete technology. Peyfuss (1990) presented a spreadsheet that can be used to calculate the quantities of concrete mix ingredients. Hover (1995) introduced a graphical approach to concrete mix proportioning based on ACI 211.1-91. In 1996, Ganju described what he referred to as "spread sheeting" mix designs. In this procedure, a method for concrete mix design was presented taking into account the variability in the characteristics of aggregates and the process of arriving at the proper combination of ingredients. In 1996 too, DeLarrard and Sedran framed a computer-aided mix design in which the proportioning involved writing a series of specifications in terms of strength, workability, and water-cement ratio. The first version of the program presented in this paper was made available on the Internet in 1997. To the knowledge of the authors, there had been no previous attempt to use the Internet as a computing platform to proportion concrete mixtures. Presently, an Internet search using various search engines confirms this finding.

PROCEDURE

Concrete mixtures are made of four basic ingredients: cement, water, coarse aggregate (such as gravel or crushed stone), and fine aggregate (such as sand). These ingredients may be mixed with other components as the need be to attain certain characteristics of the mix. A concrete mix has properties that are described in ACI (211.1-96 Reapproved 2002). According to ACI, concrete proportions of normal, heavyweight, or mass concrete must be selected to provide workability, consistency, density, strength, and durability for the particular application under consideration. These properties are defined in the following:

- **Workability:** The property of the concrete that determines its capacity to be placed and consolidated properly and be finished without harmful segregation.
- **Consistency:** It is the relative mobility of the concrete mixture, and measured in terms of the slump; the greater the slump value the more mobile the mixture.
- **Strength:** The capacity of the concrete to resist compression at the age of 28 days.
- **Water-cement (w/c) or water-cementitious [w/(c+p)] ratio:** Defined as the ratio of weight of water (w) to the weight of cement, or the ratio of weight of water to the weight of cement (c) plus added pozzolan (p). Either of these ratios is used in mix design and considerably controls concrete strength.
- **Durability:** Concrete must be able to endure severe weather conditions such as freezing and thawing, wetting and drying, heating and cooling, chemicals, deicing agents, and the like. An increase of concrete durability will enhance concrete resistance to severe weather conditions.
- **Density:** For certain applications concrete may be used primarily for its weight characteristics. Examples are counterweights, weights for sinking pipelines under water, shielding from radiation, and insulation from sound.
- **Generation of heat:** If the temperature rise of the concrete mass is not held to a minimum and the heat is allowed to dissipate at a reasonable rate, or if the concrete is subjected to severe differential or thermal gradient, cracking is likely to occur.

The user can learn more about the design procedure by navigating through a menu (Fig. 1) with links describing, for instance, the advantage of using chemical admixtures as an additive in the concrete mix.

DEVELOPMENT

The flow chart shown in Fig. 2 outlines the steps used in the concrete mix design. Proportioning of concrete mixtures using the ACI method requires making decisions and selecting the proper design parameters. The selection of slump is the first step in this procedure. Slump is a representation of the degree of workability of concrete. The maximum size of coarse aggregate should then be selected. The size of the aggregate should be the largest possible but it also should be smaller than the clear distance between the reinforcement in the structural section to ensure that the concrete will not form a honeycomb. To determine the water amount in the mix, it is imperative to determine whether or not the concrete will be subjected to severe weather conditions. Severe exposure requires the use of air-entrained concrete, and mild exposure requires non air-entrained concrete. For non air-entrained concrete, there will always be a given amount of unintended entrapped air in the mix. The amount of water and air in the mix are then determined. For the required concrete strength and the type of concrete used, the water/cement ratio (w/c) is determined. Using this w/c ratio, the amount of cement can be calculated. This step is followed by the determination of the amount of coarse aggregate in the mix. At this point in the design, the user should decide whether to use the weight method or the absolute volume method.

If the weight method is the desired one, the total weight of the fresh concrete mix can be determined from an ACI table. Having determined the weights of water, cement, and coarse aggregate, the weight of fine aggregate constitutes the difference between the total weight of the mix and the sum of other ingredients.

In the absolute volume method, a similar procedure for the design is used but all quantities are considered in terms of volumes rather than weights. Additional parameters are needed in order for the program to achieve the task of converting weights to volumes. These parameters are the specific gravities of ingredients and the unit weight of water. The mix proportions resulting from the volume method are slightly different from those obtained using the weight method. The reason for that difference is that air content is taken into consideration as one of the ingredients in the design using the absolute volume method, whereas the presence of air exerts no impact on the design using the weight method because, for all practical purposes, air can be considered weightless. The difference between the results of the weight and the volume methods becomes more appreciable with the increase of the amount of air in the mix.

Since this site was intended for the engineering community worldwide, both the SI system of units, and the US customary system of units were made available to users. The design procedure is initiated as the user clicks the "Start the Design Process" button shown in Fig. 3. Input design parameters are picked from ACI design tables and entered in specially prepared cells. In steps where calculations need to be made, the user is directed to click preprogrammed buttons marked "Compute". These buttons achieve certain calculations and display the results in special cells programmed to receive and display the output. An example of input and output cells, and of "Compute" buttons is shown in Fig. 4.

ADDITIONAL FEATURES

Although the design of concrete mix requires the proportioning of the four basic ingredients (water, cement, coarse aggregate, and fine aggregate), other materials may be added to enhance some specific qualities of the mix, or to impart certain characteristics. The program has been provided with additional features that enable the user to introduce other materials in the mix design. If, for example, a pozzolanic material such as fly ash, silica fumes, or ground granulated blast-furnace slag (GGBFS) is used in the mix, the weight of the cement will be affected. This can be accounted for by using the weight equivalency method or the volume equivalency method as shown in Fig. 4. The designer needs to enter the percent of pozzolanic material in the mix in the proper cell and the specific gravity of that material in the box below the Table in Fig. 4. Upon clicking the "Compute" button the adjusted water-cementitious materials

ratio, weight of pozzolanic materials, and weight of cement in the mix will be displayed in the corresponding cells.

The aggregates that should be used in concrete mixtures are calculated considering that they are in the dry conditions. In many cases, the aggregates stored in mixing plants may not be totally dry. Wet aggregates can greatly affect the design strength of the concrete because the free water in the aggregate will increase the water/cement ratio, thus reducing the concrete strength. It becomes apparent that the free water in the aggregate should be accounted for. If coarse and/or fine aggregates contain free water, and/or have some degree of water absorption, this requires adjustment of moisture content. This adjustment is made by directing the user to enter the percentage of free water and the degree of water absorption in special input cells. Clicking the "Compute" button that follows these cells results in displaying the adjusted amount of water in output cells, in addition to the adjusted weights of wet coarse and fine aggregates.

Furthermore, the program allows for the addition of water reducer chemicals in the mix. Water reducers affect the weight of water used in the mix and reduce the water-cement ratio, thus increasing the concrete strength. Whether the water reducer is added to the mix as a percentage of cement or as a percentage of cementitious materials, that percentage should be entered in the proper input cell. The designer should also enter the percent of reduction of water as given by the manufacturer. Upon clicking a "Compute" button that follows the entered data, the adjusted mix water and the weight of water reducer will be displayed in their corresponding cells.

DEBUGGING

The coding of the program was considered complete after all cells have been named, functions have been written, and buttons have been declared. This signaled the beginning of the debugging phase. Numerical design examples that cover all possible scenarios of concrete mix design have been made by hand. The input parameters used in these design scenarios were used in the actual program to verify the correctness and the accuracy of the program. In some cases there were syntax errors that the computer detected and had to be corrected for the proper functioning of the program. Error messages displayed by the computer were always helpful in finding and correcting these errors. In other cases there were programming errors. These errors were detected when the computer-calculated results that did not match those calculated by hand. This required a review of the functions, input cell designations, and other input parameters that could have resulted in the error. These programming errors were less frequent but correcting them was more laborious.

MIX AND BATCH INGREDIENTS

In the end of every design page, tables are structured to display the outcome of the entire design procedure including the weights of individual ingredients (Fig. 5). These are the weights that a mixing plant measures in order to produce concrete with the specified quality and strength. If a small batch is required for testing purposes, an added feature allows the user to enter the desired amount as a percentage of the total mix, and the results would be displayed in a specially designated table (Fig. 5).

DESIGN EXAMPLE

For demonstration purposes, the following is a design example where the weight method and SI system of units are used to design a cubic meter of non air-entrained concrete. The algorithm of this method is shown in an attached Appendix. The concrete is assumed to serve in a mild environment. For simplicity, no pozzolanic material or water reducer chemical will be used.

1. Slump = 100 mm maximum, and 25 mm minimum.
2. Nominal maximum size of coarse aggregate = 25 mm.
3. Water weight for non-air-entrained concrete = 193 kg/m^3 of concrete.
4. Amount of entrapped air = 1.5%.
5. Compressive strength at 28 days = 35 MPa.
6. Water-cement (or water-cementitious materials) ratio = 0.47.
7. Weight of cement = 410.64 kg/m^3 of concrete.
8. Unit weight of coarse aggregate = 1700 kg/m^3 .
9. Fineness modulus of fine aggregate = 2.6.
10. Volume of coarse aggregate per unit volume of concrete = 0.69.
11. Weight of coarse aggregate = 1173 kg/m^3 of concrete.
12. First estimate of concrete weight = 2380 kg/m^3 .
13. Weight of fine aggregate = 603.36 kg/m^3 of concrete.
14. Free water in coarse aggregate = 4%.
15. Free water in fine aggregate = 6%.
16. Degree of absorption of coarse aggregate = 1.5%.
17. Degree of absorption of fine aggregate = 2.6%.
18. Net mix water = 143.16 kg/m^3 of concrete.
19. Wet weight of coarse aggregate = 1219.92 kg/m^3 of concrete.
20. Wet weight of fine aggregate = 639.56 kg/m^3 of concrete.
21. Summary of design: Weight of cement = 410.64 kg/m^3 of concrete, Net mix water = 143.16 kg/m^3 of concrete, Wet weight of coarse aggregate = 1219.92 kg/m^3 of concrete, Wet weight of fine aggregate = 639.56 kg/m^3 of concrete.

CONCLUSIONS

An approach to the design of concrete mixture using the Internet as a computing platform is developed and presented. This approach uses the capabilities of the JavaScript programming language to make the calculations needed to accomplish the design task. The standard specifications of the American Concrete Institute (ACI) are used as a basis for the design. A website containing the ACI's design tables, together with cells for data entry and preprogrammed buttons to initiate the computations has been constructed and presented. The design steps in this website are listed in an orderly fashion where the designer is able to navigate through an orderly outlined design procedure. Calculations of different mix ingredients are made using built-in JavaScript functions that facilitate the design even further. The values entered as input parameters can be altered at any time during the design process, and this subsequently affects all dependent parameters, thus adding an extra layer of convenience in the design.

NOTE

This concrete mix design site was first developed and posted on the web in 1997. It has gone through a number of revisions and additions to look the way it is currently structured. Annual revisions are made to incorporate new additions or enhancements introduced to the design procedure. The site has been accessed thousands of times by users from all over the world. The first author received hundreds of email messages from users asking questions, making suggestions or recommendations, or just expressing their appreciation for the practical and free tool the site provides. Several messages have also been received from professors at colleges

and universities requesting permission to use the program in their teaching. All requests were granted.

REFERENCES

1. American Concrete Institute (ACI), "Standard Practice for Selecting Proportions for Normal, Heavyweight, and Mass Concrete," (*ACI 211.1-91 Reapproved 2002*).
2. Day, K.W., "Computer Mix Design," *Concrete International*, ACI, 6(9), 1984, 26-31.
3. DeLarrard, F. and Sedran, T., "Computer-Aided Mix Design: Predicting Final Result," *Concrete International*, ACI, 18(12), 1996, 39-41.
4. Ganju, T.N. (1996). "Spreadsheets Mix Designs," *Concrete International*, ACI, 18(12), 35-38.
5. Ghaly, A.M. and Almstead, L.G., "<http://concrete.union.edu>", (1997-2005).
6. Hover, K., "Graphical Approach to Mixture Proportioning by ACI 211.1-91," *Concrete International*, ACI, 17(9), 1995, 49-53.
7. Peyfuss, K.F., "Simplifying Concrete Mix Design With the PC," *Concrete International*, ACI, 12(12), 1990, 47-49.
8. Shilstone, J.M. and Shilstone, J.M., "Concrete Field Applications of Microcomputers," *Concrete International*, ACI, 7(6), 1985, 43-48.

APPENDIX

Sample algorithm of concrete mix design for non air-entrained concrete using the weight method and SI system of units.

```
// Rounds a number to 2 places
function Round2( number )
{
    return Math.round(number * 100) / 100
}
// Rounds a number to three decimal places
function Round3( number )
{
    return Math.round(number * 1000) / 1000
}
function ComputeWaterReducer(theForm)
{
    // Compute water reducer
    if (theForm.OptWaterReducer[0].checked)
    {
        if (theForm.WeightPoz2.value > 0)
        {
            theForm.WtWR.value = Round3(theForm.WeightPoz2.value *
theForm.WRPercent1.value / 100.)
        }
        else
        {
            theForm.WtWR.value = Round3(theForm.WeightCement.value *
theForm.WRPercent1.value / 100.)
        }
    }
    else if (theForm.OptWaterReducer[1].checked)
    {
```

```

        theForm.WtWR.value = Round3((parseFloat(theForm.WeightPoz1.value) +
parseFloat(theForm.WeightPoz2.value))*theForm.WRPercent2.value/100.)
    }
// Compute net mix water
    if (theForm.OptWaterReducer[0].checked || theForm.OptWaterReducer[1].checked)
        theForm.NetMixWR.value = Round3(theForm.NetMixWater.value -
theForm.WRPercent3.value * theForm.WaterWt.value / 100.)
}
function ComputePoz(theForm)
{
    var WW = theForm.WaterWt.value
    var WC = theForm.WtrContent.value
    var WtCem = theForm.WeightCement.value
    var SG = 3.15
    var PSG = theForm.PozSG.value
// Compute weight of pozzolanic materials
    if (theForm.OptPoz[0].checked) // Weight Equivalency Method - percent by weight
    {
        theForm.PozRatio.value = theForm.WtrContent.value
        theForm.WeightPoz1.value = Round2( WtCem *
theForm.WEMPozWt.value/100)
    }
    else if (theForm.OptPoz[1].checked) // Weight Equivalency Method - percent by volume
    {
        theForm.PozRatio.value = theForm.WtrContent.value
        var Denom = 1 + SG/PSG * (100/theForm.WEMPozVol.value - 1)
        theForm.WeightPoz1.value = Round2( WtCem / Denom )
    }
    else if (theForm.OptPoz[2].checked) // Volume Equivalency Method - percent by weight
    {
        var PW = theForm.VEMPozWt.value / 100
        theForm.PozRatio.value = Round3( SG*WC / ( SG*(1-PW) + PSG*PW ) )
        theForm.WeightPoz1.value = Round2( (WW / theForm.PozRatio.value) * PW )
    }
    else if (theForm.OptPoz[3].checked) // Volume Equivalency Method - percent by volume
    {
        Term1 = 1. / ( 1. + (PSG / SG) * (100 / theForm.VEMPozVol.value - 1) )
        Term2 = SG * WC / ( ( SG * ( 1 - Term1) ) + PSG * Term1 )
        theForm.PozRatio.value = Round3( Term2 )
        theForm.WeightPoz1.value = Round2( (WW / Term2) * Term1 )
    }
}
// Compute weight of cement
    if (theForm.OptPoz[0].checked || theForm.OptPoz[1].checked)
    {
        theForm.WeightPoz2.value = Round2( WtCem - theForm.WeightPoz1.value )
    }
    else if (theForm.OptPoz[2].checked || theForm.OptPoz[3].checked)
    {
        theForm.WeightPoz2.value = Round2( WW / theForm.PozRatio.value -
theForm.WeightPoz1.value )
    }
}
function ComputeWeight(theForm)
{
    theForm.WeightCement.value = Round2(theForm.WaterWt.value /
theForm.WtrContent.value)
}

```

```

function DisplayMaxSize(theForm)
{
    theForm.MaxSize2.value = theForm.MaxSize.value
}
function CAVolWt(theForm)
{
    theForm.CAWeight.value = Round2(theForm.CAUnitWeight.value *
theForm.CAUnitVolume.value)
}
function AdjustAM(theForm)
{
    theForm.NetMixWater.value = Round2(theForm.WaterWt.value -
theForm.CAWeight.value*(theForm.FWCA.value/100-theForm.DofACA.value/100) -
theForm.FAWt.value*(theForm.FWFA.value/100-theForm.DofAFA.value/100))
    theForm.WetCAWt.value = Round2(theForm.CAWeight.value*(1 +
theForm.FWCA.value/100))
    theForm.WetFAWt.value = Round2(theForm.FAWt.value * (1 +
theForm.FWFA.value/100))
}
function DisplayMaxSizeCA(theForm)
{
    theForm.MaxSize3.value = theForm.MaxSize.value
}
function FAWeight(theForm)
{
    if (    theForm.OptPoz[0].checked || theForm.OptPoz[1].checked ||
theForm.OptPoz[2].checked || theForm.OptPoz[3].checked )
        theForm.FAWt.value = Round2(theForm.FEConWt.value -
theForm.CAWeight.value - theForm.WeightPoz1.value - theForm.WeightPoz2.value -
theForm.WaterWt.value)
    else
        theForm.FAWt.value = Round2(theForm.FEConWt.value -
theForm.CAWeight.value - theForm.WeightCement.value - theForm.WaterWt.value)
}
function DisplayMixWater(theForm)
{
    theForm.WaterWt2.value = theForm.WaterWt.value
}
function Summarize(theForm)
{
    ComputeWeight(theForm)
    ComputePoz(theForm)
    DisplayMaxSize(theForm)
    CAVolWt(theForm)
    DisplayMaxSizeCA(theForm)
    FAWeight(theForm)
    DisplayMixWater(theForm)
    AdjustAM(theForm)
    ComputeWaterReducer(theForm)
    theForm.CompStrength2.value = theForm.CompStrgth.value
    theForm.MaxSlump2.value = theForm.MaxSlump.value
    theForm.MinSlump2.value = theForm.MinSlump.value
    theForm.MaxSize4.value = theForm.MaxSize.value
    if (theForm.OptPoz[2].checked || theForm.OptPoz[3].checked)
        theForm.WtrContent2.value = theForm.PozRatio.value
    else
        theForm.WtrContent2.value = theForm.WtrContent.value
}

```

```
theForm.Entrainment.value = "Non-air-entrained"
theForm.TrapAir2.value = theForm.TrapAir.value
theForm.CAUnitWeight2.value = theForm.CAUnitWeight.value
if (theForm.NetMixWR.value > 0)
    theForm.NetMixWater2.value = theForm.NetMixWR.value
else
    theForm.NetMixWater2.value = theForm.NetMixWater.value
if (theForm.WeightPoz2.value > 0)
    theForm.WeightCement2.value = theForm.WeightPoz2.value
else
    theForm.WeightCement2.value = theForm.WeightCement.value
theForm.WetCAWt2.value = theForm.WetCAWt.value
theForm.WetFAWt2.value = theForm.WetFAWt.value
theForm.PM2.value = theForm.WeightPoz1.value
theForm.WR2.value = theForm.WtWR.value
theForm.BatchPercent2.value = theForm.BatchPercent.value
theForm.Water.value = Round2(theForm.NetMixWater2.value *
theForm.BatchPercent.value/100)
theForm.Cement.value = Round2(theForm.WeightCement2.value *
theForm.BatchPercent.value/100)
theForm.CA.value = Round2(theForm.WetCAWt.value *
theForm.BatchPercent.value/100)
theForm.FA.value = Round2(theForm.WetFAWt.value *
theForm.BatchPercent.value/100)
theForm.PM.value = Round3(theForm.PM2.value * theForm.BatchPercent.value/100)
theForm.WR.value = Round3(theForm.WR2.value * theForm.BatchPercent.value/100)
}
```

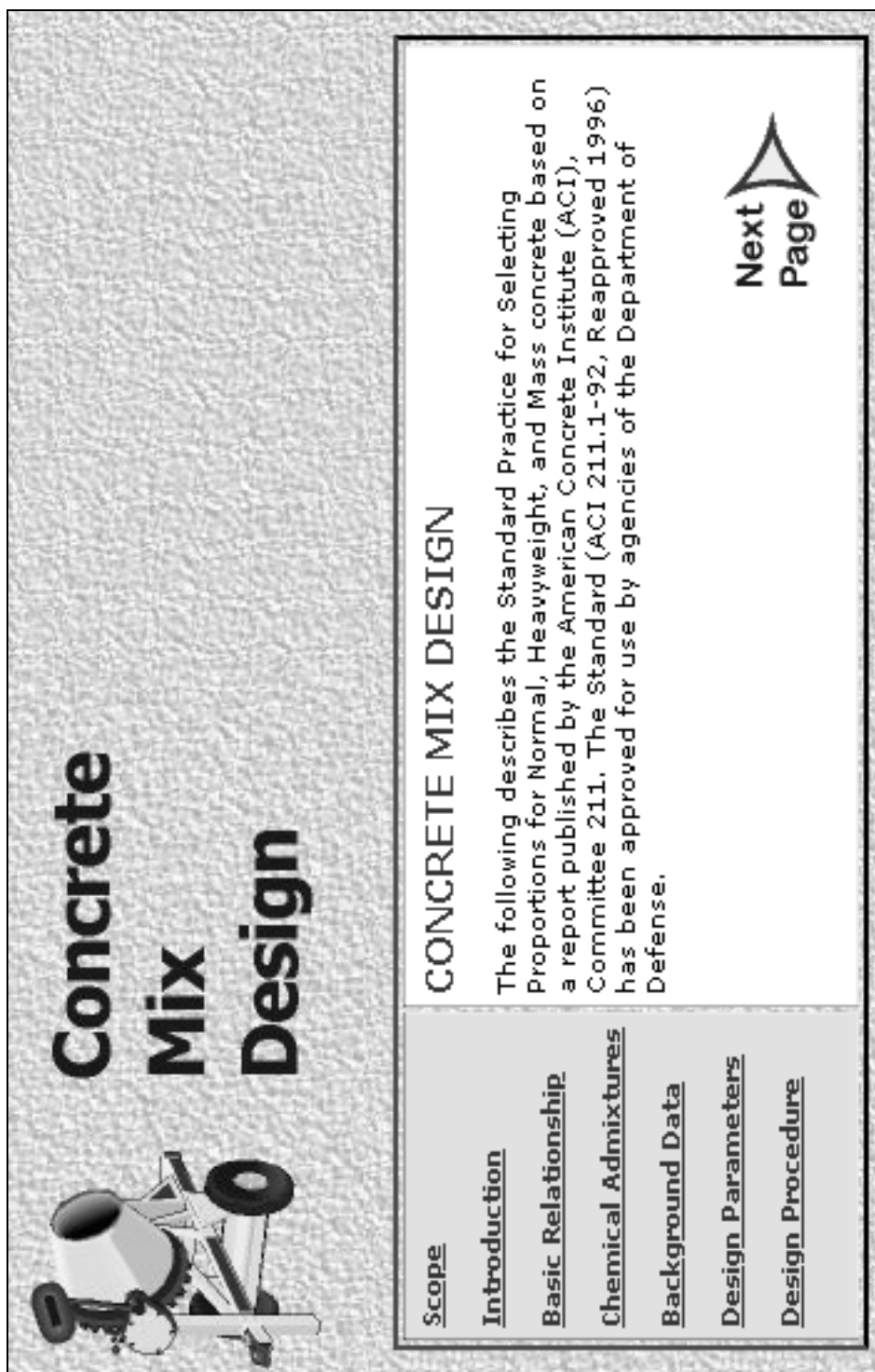


Fig. 1: Main Menu in Concrete Mix Design Site.

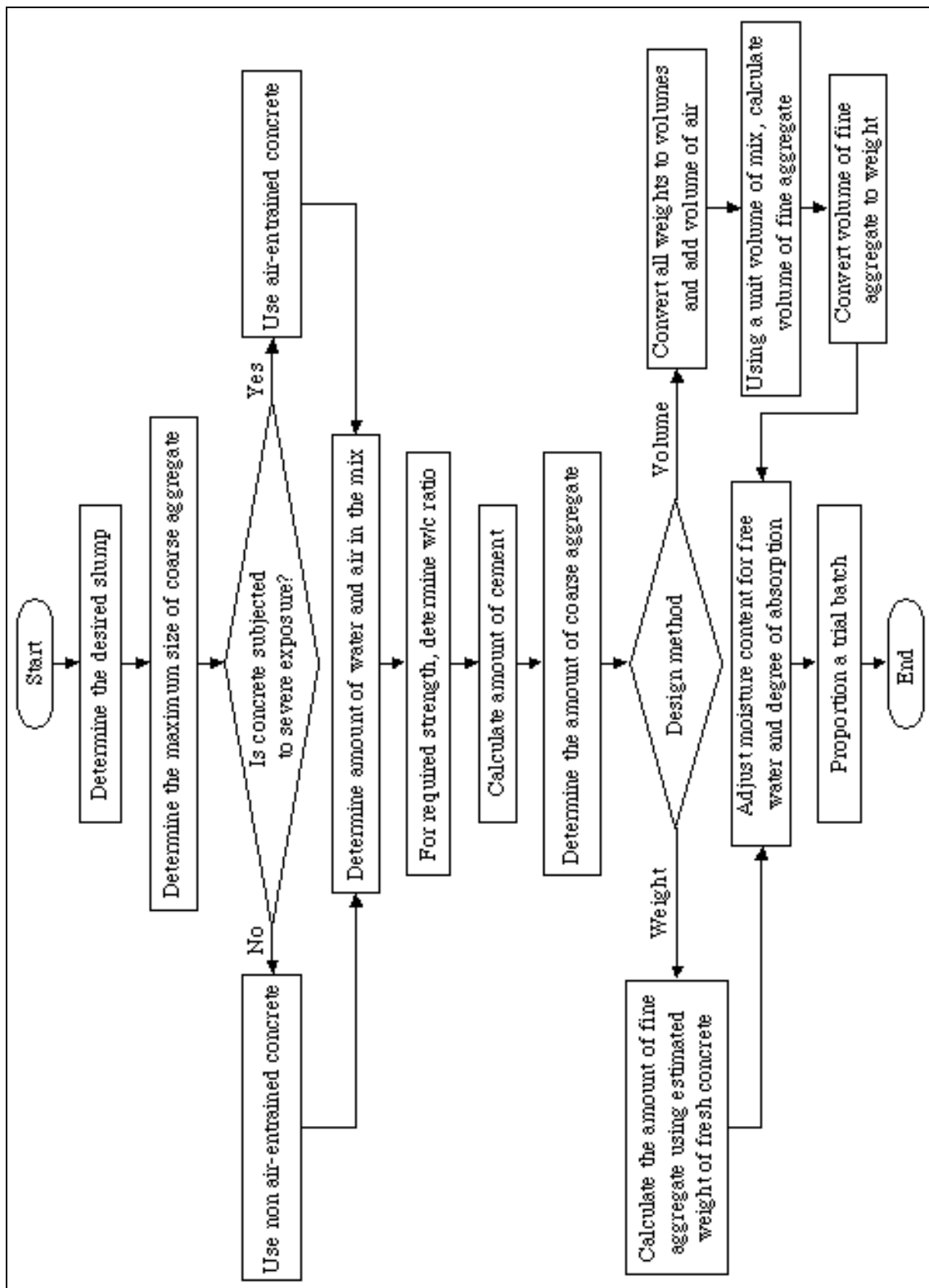


Fig. 2. Flow Chart Used in Developing the Concrete Mix Design Site.

DESIGN PROCEDURE

Select a design method	<input checked="" type="radio"/> WEIGHT <input type="radio"/> ABSOLUTE VOLUME
Select a system of units	<input checked="" type="radio"/> SI <input type="radio"/> US
Select type of concrete	<input checked="" type="radio"/> NON-AIR-ENTRAINED <input type="radio"/> AIR-ENTRAINED



**Previous
Page**



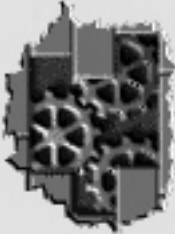


Fig. 3: Page for Selection of Design Method, System of Units, and Type of Concrete.

Are pozzolanic materials [such as Fly Ash, Silica Fumes, Ground Granulated Blast-Furnace Slag (GGBFS)] used in the mix?

* NO, [click here to proceed with regular mix design.](#)

* YES, select desired calculation method, and make input in one of the Tables below:

Weight Equivalency Method	Volume Equivalency Method
If pozzolanic materials percentage by weight of cementitious material is known, click here <input type="radio"/> , and Enter this percentage <input type="text"/> %	If pozzolanic materials percentage by weight of cementitious material is known, click here <input type="radio"/> , and Enter this percentage <input type="text"/> %
If pozzolanic materials percentage by volume of cementitious material is known, click here <input type="radio"/> , and Enter this percentage <input type="text"/> %	If pozzolanic materials percentage by volume of cementitious material is known, click here <input type="radio"/> , and Enter this percentage <input type="text"/> %

Enter specific gravity of pozzolanic material (if unknown, use 2.4) =

Adjusted water-cementitious materials ratio (only for volume equivalency method) =

Weight of pozzolanic materials = kg/m³

Weight of cement = kg/m³

Fig. 4: Computation of Adjusted Water-Cementitious Materials Ratio, Weights of Pozzolanic Materials and Cement.

Ingredients of Concrete Mixture					
Water <i>kg/m³</i>	Cement <i>kg/m³</i>	Coarse Aggregate <i>kg/m³</i>	Fine Aggregate <i>kg/m³</i>	Pozzolanics Materials <i>kg/m³</i>	Water Reducer <i>kg/m³</i>
<input type="text"/>	<input type="text"/>	<input type="text"/>	<input type="text"/>	<input type="text"/>	<input type="text"/>
Ingredients of <input type="text"/> % Concrete Batch					
Water <i>kg</i>	Cement <i>kg</i>	Coarse Aggregate <i>kg</i>	Fine Aggregate <i>kg</i>	Pozzolanics Materials <i>kg</i>	Water Reducer <i>kg</i>
<input type="text"/>	<input type="text"/>	<input type="text"/>	<input type="text"/>	<input type="text"/>	<input type="text"/>

Fig. 5: Weight of Ingredients In a Cubic Meter of Concrete, and In a Given Percentage of Batch.